PB90-126038

EPA/IFP (Environmental Protection Agency/Institute Francais du Petrole) European Workshop on the Emission of Nitrous Oxide from Fossil Fuel Combustion (Rueil-Malmaison, France, June 1-2, 1988)

Acurex Corp., Research Triangle Park, NC

Prepared for:

Environmental Protection Agency, Research Triangle Park, NC

Oct 89

U.S. Department of Commerce
National Technical Information Service
NTIS

TECHNICAL REPORT DATA

(Please read Instructions on the reverse before completing)

1. REPORT NO.
EPA-600/9-89-089

2.

3. RECIPIENT'S ACCESSION NO.
PB90 126038/AS

4. TITLE AND SUBTITLE
EPA/IFP European Workshop on the Emission of Nitrous Oxide from Fossil Fuel Combustion

5. REPORT DATE
October 1989

6. PERFORMING ORGANIZATION CODE

7. AUTHOR(S)
Jeffrey V. Ryan and Ravi K. Srivastava

8. PERFORMING ORGANIZATION REPORT NO.

9. PERFORMING ORGANIZATION NAME AND ADDRESS
Acurex Corporation
P.O. Box 13109
Research Triangle Park, North Carolina 27709

10. PROGRAM ELEMENT NO.

11. CONTRACT/GRANT NO.
68-02-4701

12. SPONSORING AGENCY NAME AND ADDRESS
EPA, Office of Research and Development
Air and Energy Engineering Research Laboratory
Research Triangle Park, NC 27711

13. TYPE OF REPORT AND PERIOD COVERED
Proceedings; 6/88-9/89

14. SPONSORING AGENCY CODE
EPA/600/13

15. SUPPLEMENTARY NOTES AEERL project officer is Joseph A. McSorley, Mail Drop 65, 919/541-2920. EPA-600/8-88-079 and EPA-600/8-86-035 relate to earlier workshops in this series.

16. ABSTRACT The report summarizes the proceedings of an EPA/Institut Francais du Petrole (IFP) cosponsored workshop addressing direct nitrous oxide (N2O) emission from fossil fuel combustion. The third in a series, it was held at the IFP in Rueil-Malmaison, France, on June 1-2, 1988. Increasing atmospheric N2O concentrations have been linked to depletion of stratospheric ozone (O3) and to global climate warming. The combustion of fossil fuels has been identified as a potential major anthropogenic source of N2O. The workshop had two goals: (1) to exchange information among various international research and industrial groups that are involved in N2O chemistry, modeling, and measurement; and (2) to develop a network for coordinating future related efforts. The five technical sessions addressed: stratospheric O3 depletion and global climate change, mechanisms of N2O formation and destruction during combustion, N2O measurement techniques, full-scale field data, and practical conclusions based on general discussion. A sampling artifact discovered during an EPRI funded research study revealed that N2O can be generated in a sample container in the presence of NOx, SO2, and H2O. This artifact potentially discredits much of the N2O emissions data collected from samples containing the above compounds when stored for some time prior to analysis.

17. KEY WORDS AND DOCUMENT ANALYSIS

a. DESCRIPTORS		b. IDENTIFIERS/OPEN ENDED TERMS	c. COSATI Field/Group	
Pollution	Chemistry	Pollution Control	13B	07
Nitrogen Oxide (N2O)	Mathematical Models	Stationary Sources	07B	
Fossil Fuels		Global Warming	21D	12A
Combustion	Measurement		21B	14G
Ozone	Sampling			14B
Climatic Change			04B	

18. DISTRIBUTION STATEMENT
Release to Public

19. SECURITY CLASS *(This Report)*
Unclassified

20. SECURITY CLASS *(This page)*
Unclassified

21. NO. OF PAGES

22. PRICE

EPA Form 2220-1 (9-73)

PB90-126038

EPA-600/9-89-089
October 1989

EPA/IFP EUROPEAN WORKSHOP ON THE EMISSION OF NITROUS OXIDE FROM FOSSIL FUEL COMBUSTION

(Rueil-Malmaison, France, June 1-2, 1988)

Prepared by:

Jeffrey V. Ryan

and

Ravi K. Srivastava

Acurex Corporation
Environmental Systems Division
Post Office Box 13109
Research Triangle Park, North Carolina 27709

EPA Contract No. 68-02-4701

EPA Task Officer:

Joseph A. McSorley
Air and Energy Engineering Research Laboratory
Research Triangle Park, North Carolina 27711

AIR AND ENERGY ENGINEERING RESEARCH LABORATORY
OFFICE OF RESEARCH AND DEVELOPMENT
U.S. ENVIRONMENTAL PROTECTION AGENCY
RESEARCH TRIANGLE PARK, NC 27711

REPRODUCED BY
U.S. DEPARTMENT OF COMMERCE
NATIONAL TECHNICAL INFORMATION SERVICE
SPRINGFIELD, VA. 22161

RESEARCH REPORTING SERIES

Research reports of the Office of Research and Development, U.S. Environmental Protection Agency, have been grouped into nine series. These nine broad categories were established to facilitate further development and application of environmental technology. Elimination of traditional grouping was consciously planned to foster technology transfer and a maximum interface in related fields. The nine series are:

1. Environmental Health Effects Research
2. Environmental Protection Technology
3. Ecological Research
4. Environmental Monitoring
5. Socioeconomic Environmental Studies
6. Scientific and Technical Assessment Reports (STAR)
7. Interagency Energy-Environment Research and Development
8. "Special" Reports
9. Miscellaneous Reports

This report has been assigned to the MISCELLANEOUS REPORTS series. This series is reserved for reports whose content does not fit into one of the other specific series. Conference proceedings, annual reports, and bibliographies are examples of miscellaneous reports.

EPA REVIEW NOTICE

This report has been reviewed by the U.S. Environmental Protection Agency, and approved for publication. Approval does not signify that the contents necessarily reflect the views and policy of the Agency, nor does mention of trade names or commercial products constitute endorsement or recommendation for use.

This document is available to the public through the National Technical Information Service, Springfield, Virginia 22161.

ABSTRACT

This report summarizes the proceedings of an Environmental Protection Agency (EPA)/Institut Francais du Petrole (IFP) cosponsored workshop addressing direct nitrous oxide (N_2O) emission from fossil-fuel combustion. The third in a series, the workshop was held at the IFP in Rueil-Malmaison, France, on June 1-2, 1988.

Increasing atmospheric N_2O concentrations have been linked to depletion of stratospheric ozone (O_3) and to global climatic warming. The combustion of fossil fuels has been identified as a potential major anthropogenic source of N_2O. This workshop was organized to accomplish two goals. The first goal was to exchange information among various international research and industrial groups that are involved in N_2O chemistry and modeling as well as N_2O measurement. The second goal was to develop a network for coordinating future efforts.

The 5 technical sessions at this workshop addressed the following issues:

1. Stratospheric O_3 depletion and global climate change
2. Mechanisms of N_2O formation and destruction during combustion
3. N_2O measurement techniques
4. Full-scale field data
5. Practical conclusions based on general discussion

A sampling artifact discovered in the course of an EPRI/EPA sponsored research study revealed that N_2O can be generated in a sample container in the presence of nitrogen oxides (NO_x), sulfur dioxide (SO_2), and water. This artifact potentially discredits much of the N_2O emissions data collected from bomb samples containing the above compounds. Recent sampling techniques that minimize the artifact have produced data from stationary sources that indicate that the direct emission of N_2O from fossil-fuel combustion may not be as great as previously believed. However, limited data indicate that some specific sources (e.g., fluidized bed combustors) may be high N_2O emitters. A standardized sampling protocol needs to be designed and implemented to validate or supercede current data.

TABLE OF CONTENTS

Section Page

Abstract ii
Acknowledgement ix

1 Introduction 1

2 Opening Session 2
  2.1 Stratospheric Ozone Depletion and Global Climate Change (S. Seidel, EPA) 2
  2.2 OECD Perspective (P. Stolpman, OECD) 4
  2.3 Discussion 5
  2.4 Impacts of N_2O and Other Trace Gases in Stratospheric Ozone (J. Levine, NASA) 6
  2.5 Modeling the Effects of N_2O and Other Trace Gases on Climate and Ozone Distribution (C. Brühl, Max Planck Institut) 11

3 Session 1: The Mechanisms of N_2O Formation and Destruction During Combustion 13
  3.1 Basic Kinetics (N. Brown, Lawrence Berkeley Laboratory) 13
    3.1.1 Gas Phase Kinetics (J. Kramlich, EERC) 24
    3.1.2 Heterogeneous Reactions (G. de Soete, IFP) 33
  3.2 Overall Chemical Information From Laboratory Combustor Experiments 44

4 Session 2: N_2O Measurement Techniques 59
  4.1 Operating Procedure for In-House Research 60
  4.2 Water Sorbents Used in N_2O Measurement 60
  4.3 Interferences From Sulfur Dioxide 62
  4.4 Continuous Infrared Analyzer for On-Line N_2O Measurement 66
  4.5 Optical Interferometry 70

5 Session 3: Full-Scale Field Data 71
  5.1 Flue Gas Exhaust Data From Stationary Sources 71
    5.1.1 N_2O Emission Data From Test Rigs and Full Scale Units 71
    5.1.2 German Power Plants 74
    5.1.3 Italian Power Plants 74
    5.1.4 Emissions of N_2O From British Power Stations 80
    5.1.5 Emission Data from Swedish Stationary Combustion Sources 80
    5.1.6 Excess Air Variation in a Circulating FBC 87
    5.1.7 N_2O Emissions From Power Plants in Finland 87
    5.1.8 Data from Dutch Power Stations 87
    5.1.9 Data From U.S. Power Plants 95
  5.2 Exhaust Data From Mobile Sources 95
    5.2.1 Comparison of Vehicles With and With Out Catalytic Converters 95
    5.2.2 Comparison of N_2O Emissions from City and Suburban Driving 101

(continued)

TABLE OF CONTENTS (concluded)

Section Page

6 Session 4: General Discussion to Arrive at Practical Conclusions . . . 104

7 Summary and Conclusions . . . 108

8 References . . . 114

Appendix A: European Workshop on N_2O Emissions Agenda . . . 115

Appendix B: European Workshop on N_2O Emissions List of Participants . . . 118

LIST OF FIGURES

Figure Page

3-1 N_2O formation in methane and hydrogen flames. 14
3-2 N_2O formation versus equivalence ratio. 15
3-3 N_2O formation versus dopant concentration. 16
3-4 N_2O formation versus nitrogen dopant. 17
3-5 Edge effects on N_2O formation. 19
3-6 Comparison of modeling and experimental results with NH_3-doped flame. 20
3-7 Comparison of modeling and experimental results with NO-doped flame. 21
3-8 Comparison of modeling and experimental results with N_2O-doped flame. 22
3-9 Comparison of modeling and experimental results with NH_3-doped flame. 23
3-10 Kinetics used in model calculations. 25
3-11 Post-flame modeling results. 27
3-12 Post-flame modeling results (artificial HCN introduction). 28
3-13 Post-flame experiment. 29
3-14 Mechanism overview. 30
3-15 Reaction mechanisms. 32
3-16 NO and CO over metal (JPB 93) catalyst. 35
3-17 Heterogeneous formation and destruction of N_2O on metal catalyst. 36
3-18 Heterogeneous reduction of N_2O on char bound carbon. 38
3-19 Reaction rates for Eschweiler char. 39
3-20 Cedar Grove char conversion of nitrogen. 40
3-21 O_2 + HCN on graphite. 41
3-22 Formation of N_2O from bound nitrogen during heterogeneous char oxidation. 42
3-23 Main reaction paths of N_2O formation during char combustion. 43
3-24 Reburn condition using natural gas. 46
3-25 NO/N_2O for Utah bituminous (N_2O measured from sample containers). 47
3-26 NO/N_2O for Montana sub-bituminous (N_2O measured from sample containers). 48
3-27 On-line data in relation to other reported data. 49
3-28 Fluid bed modeling. 51
3-29 Predictions under varied conditions. 52
3-30 Reburning predictions. 53
3-31 NO_x and N_2O formation from coal. 56
3-32 Schematic of experimental flame measurements. 58
4-1 Losses of N_2O on different absorbents. 61
4-2 N_2O sampling system. 63
4-3 Effect of SO_2 on N_2O. 64
4-4 Synthetic gas mixtures in glass sample flask. 65
4-5 Effect of SO_2 level on N_2O. 67
4-6 Effect of NO_x level on N_2O formation. 68
4-7 Hypothetical chemistry. 69

(continued)

LIST OF FIGURES (concluded)

Figure Page

5-1 Comparison with previous results. 76
5-2 Extractive flue gas sampling system. 82
5-3 N_2O and NO_x concentrations from all plants and combined combustion techniques. 92
5-4 N_2O versus NO_x emissions. 96
5-5 N_2O versus NO_x emissions compared with Boulder Workshop data. 97
5-6 EPRI N_2O measurements with repeat condition. 98
5-7 City versus suburban driving. 102
5-8 Gasoline versus diesel vehicles. 103

LIST OF TABLES

Table — Page

2-1 Atmospheric Nitrogen Species 10

3-1 Experimental Measurements 54

5-1 N_2O Data: PFBC Test Rig 72
5-2 N_2O Data: SCR Test/Pilot-Scale 73
5-3 N_2O Data: Brown Coal Full-Scale RWE 75
5-4 N_2O Emissions From German Power Plants 77
5-5 Data From Facility Burning #6 Fuel Oil 78
5-6 Data From Facility Burning Coal 79
5-7 Summary of N_2O and Total NO_x Emissions 81
5-8 Measurement of N_2O Under Varied Conditions 83
5-9 Combustion Methods and Fuels in Swedish Combustors 84
5-10 Emissions From Various Combustors 85
5-11 FBC Emissions 86
5-12 Excess Air Variation Data 88
5-13 N_2O Field Test Data From Various Combustion Plant Sources Using an FBC 89
5-14 N_2O Field Test Data From Various Combustion Plant Sources Using a Conventional Burner . . 90
5-15 N_2O Field Test Data From Various Combustion Plant Sources Using Grate Combustion 91
5-16 N_2O Concentrations in Stack Gas From Electricity Power Stations 93
5-17 Catalytic $DeNO_x$ (SCR) 94
5-18 Catalyst Vehicle Versus Carburetor Vehicle 99
5-19 Catalyst Vehicle Data 100

7-1 N_2O Emissions Data Summary 110

ACKNOWLEDGMENT

Many people are responsible for the success of the Rueil-Malmaison workshop. Dr. G. de Soete of the Institut Francais du Petrole (IFP) deserves special praise for locating and contacting participants worldwide and for soliciting international interest in characterizing N_2O emissions from combustion sources. The authors would like to acknowledge IFP for hosting the workshop and the U.S. Environmental Protection Agency (EPA) for being the leading organizer and co-sponsor. Special thanks are extended to Mr. J. McSorley of EPA for his efforts in organizing the workshop.

SECTION 1

INTRODUCTION

This report summarizes the European workshop on direct nitrous oxide (N_2O) emissions from fossil-fuel combustion that was held at the Institut Francais du Petrole (IFP), Rueil-Malmaison, France, on June 1-2, 1988. The workshop was the third in a series on N_2O emissions and was co-sponsored by the U.S. Environmental Protection Agency (EPA) and the Institut Francais du Petrole (IFP). Its primary focus was to assess and evaluate the role that combustion of fossil fuels plays in directly emitting N_2O into the atmosphere. This subject is significant because the ambient levels of N_2O have been reported to be increasing and because N_2O has been linked to stratospheric ozone (O_3) depletion and global climatic warming. Another focus was to establish an international network for exchanging information related to N_2O emissions.

The workshop brought together a complementary group of experts involved in the various aspects of N_2O research. Specifically discussed were the role of N_2O in stratospheric O_3 depletion and global climate change, the mechanisms of N_2O formation/destruction (involving both homogeneous and heterogeneous reactions), and the status of N_2O measurement techniques. Presentations were also made on emissions data collected from a variety of stationary, sub- and full-scale facilities, as well as on data from mobile sources. After these presentations/discussions, conclusions were reached regarding the current status and future direction of N_2O research.

This report documents both the formal and informal material presented at the workshop, and it includes vigorous discussion periods that followed formal presentations. It is an account of the proceedings and summarizes the workshop's content chronologically.

SECTION 2

OPENING SESSION

2.1 STRATOSPHERIC OZONE DEPLETION AND GLOBAL CLIMATE CHANGE (S. SEIDEL, EPA)

Mr. S. Seidel presented an overview of projected stratospheric O_3 depletion and global climate change. He suggests that human activities are responsible for increases in atmospheric gases' concentrations in recent times. These changes are causing global warming (a result of the greenhouse effect) and stratospheric O_3 depletion.

Carbon dioxide (CO_2) is considered to be one of the major contributors to climatic warming. From 1950 to 1985, the ambient concentration of CO_2 has increased from 315-345 ppm. This increase in CO_2 concentration of approximately 0.5 percent annually may be mostly attributed to burning fossil fuels [1].

Chlorofluorocarbons (CFCs) are known to participate in stratospheric reactions that destroy O_3. Used primarily in aerosol spray cans, solvents, refrigerants, and foam blowing, the concentration of CFCs in the atmosphere has increased 5-7 percent annually since 1975 [2].

Methane (CH_4) also plays a major role in O_3 depletion and global climate change. Rice paddies, fermentation, and natural gas leaks resulting from mining and transportation of natural gas are the possible major sources of CH_4 emissions. Over the past 10 years, CH_4 emissions are estimated to be increasing at the rate of 1.0 percent per year [3].

Nitrous oxide (N_2O) is another trace gas that contributes to the depletion of O_3 in the stratosphere. Ice core data show steady levels of N_2O until the start of the industrial revolution, [4] but currently ambient concentrations of N_2O are increasing at an annual rate of about 0.2 percent.

N_2O, CFCs, CH_4, and CO_2 are essentially transparent to solar radiation, but they trap the earth's infrared radiation, resulting in the greenhouse effect. Increases in the concentrations of these gases lead to increased global warming. There is a need to characterize this phenomenon. Various climate change models that take into account the greenhouse effect of these gases are able to predict the temperatures on earth and other planets reliably, which supports the view that these gases are contributors to the greenhouse effect.

The modeled predictions of global temperature, using recorded data, suggest that temperatures may rise as much as 5 °C worldwide by the year 2030. Moreover, by the year 2025, temperatures will reach their highest point in the past 100,000 years. Global temperatures have already increased 0.63 °C since 1880, and the 4 hottest years on record have occurred during the 1980s.

Many global features are expected to be adversely affected by greenhouse climatic changes. For example, the ecosystem will be thrown off balance as organisms attempt, over a relatively short span, to adapt to environmental changes that would normally occur over thousands of years. Global warming will melt the polar ice caps, causing the seas to rise and to change coastlines. Warmer temperatures will tax human health and society; infrastructure decisions, such as resource management and distribution, will become significantly more difficult, owing to an inability to predict supplies.

Whe comparing a sector analysis of proposed sources of N_2O, natural sources are thought to comprise over 50 percent of total emissions, while combustion of fossil fuels and biomass burning are considered to be major anthropogenic contributors. A breakdown of combustion by sector shows utilities and industry as being the major sources. Projections of contributions to N_2O emissions suggest a greater rate of increase as economies and populations grow; the relative contribution by the United States will decrease, while that of the rest of the world will increase with continued development [5].

EPA was designated by the U.S. Congress to conduct 2 studies related to climate change. The first was to study the impact of global environment change, and the second was to investigate possible ways to stabilize atmospheric concentrations of greenhouse gases. The stabilizing report had the following goals: (1) to develop an analytical framework for the study of N_2O; (2) to provide information on the relative effectiveness of control options that may be available; and (3) to highlight future research issues for analysis.

Currently, the N_2O data base is insufficient. Moreover, there is a critical need to foster research aimed at developing a better inventory of N_2O emissions sources and contributions, to obtain an improved understanding of the combustion process related to N_2O emissions, and to improve understanding of control options. Accelerated N_2O research is vital, because critical decisions are being made to control nitrogen oxides, new combustion devices are being designed and built, and developing nations are growing and contributing to the N_2O problem—all with insufficient information.

An international cooperation is essential if nations are to respond effectively to global environmental threats. Until recently, such cooperation has been nonexistent. For example, the first international meeting to address the potential environmental impact of CFCs was the Vienna Convention of 1985. The Montreal Protocol of 1987 was the first cooperative, international accord designed to regulate anthropogenic emissions.

Mr. Seidel summarized the lessons of the Montreal Protocol as follows:

1. A scientific consensus is necessary among all nations that recognizes the seriousness of O_3 depletion.
2. Scientists must focus on emission trends throughout the world.
3. Solutions (i.e., control technologies) must be found, and all nations seeking solutions must have a common direction.
4. Incremental steps must be followed, because O_3 depletion involves long-term problems.
5. Active international programs must be developed because the effects of O_3 depletion are international. Before any agreement can be reached, however, research must be standardized for a common understanding on emission-control options.

2.2 OECD PERSPECTIVE (P. STOLPMAN, OECD)

Dr. P. Stolpman stated that at this time Organization for European Countries Development (OECD) is only involved in the issue of global climate change. OECD's involvement in this area is relatively new and has evolved from a meeting in Washington, DC, among 8 OECD countries, the World Meteorological Organization (WMO), the Commission of European Communities, OECD, and representatives of EPA. At this meeting, the participants proposed a program to assess the effects of worldwide climate changes and to examine preventive policy options.

OECD intends to work closely with UNEP, WMO, and the International Energy Agency in implementing the program over the next 3 years, focusing on the following tasks:

1. Review the assessment projects being undertaken throughout the world.
2. Develop a computer data base. The United States currently employs AP42, a major emissions data base. Similarly, OECD hopes to develop a data base like AP42 for greenhouse gases.
3. Develop alternative emission scenarios.
4. Project environmental and socioeconomic changes.
5. Examine policy options that will address the consequences of atmospheric changes and prevent further changes.

2.3 DISCUSSION

A brief discussion of Mr. Seidel's and Dr. Stolpman's presentations followed. Professor A. Williams from University of Leeds asked about the accuracy of the climate change models in view of feedback mechanisms and pointed out that EPA models differ in the range of global temperature increases predicted. He asked Mr. Seidel to comment on the accuracy of his predictions.

Mr. Seidel responded that feedback mechanisms, such as clouds, changes in the earth's albedo, and changes in the oceans, were too complex to be included in the simple climate change models. These models, however, did include the greenhouse effect associated with CO_2 and other relevant gases. Mr. Seidel further stated that the models seem to agree that a global temperature increase of 4 °C was imminent for doubled CO_2 concentration. The 5 °C increase predicted by the models was based on increases of CO_2 and other trace gases.

Mr. S. Jansson of ASEA PFBC asked how the measurements and temperatures were calculated for the models.

Mr. Seidel responded that the original estimates were based on measurements over land. Recent improvements include measurements over the seas thus producing a better average.

Dr. S. Lanier asked if the models described by Mr. Seidel assume a 2.7 percent annual growth rate of CFCs as projected above their current base over the next 100 years, or if they assume a constant influx.

Mr. Seidel responded that his experience in analyzing future trends in CFC emissions in the United States and other countries showed that in the past 5-6 years, the growth has been 6-7 percent globally and 10-13 percent in the United States. The 2.7 percent growth rate used in the models is an approximation that includes about a 4 percent growth rate in the developing world and a somewhat lower growth rate in the developed world.

2.4 IMPACTS OF N_2O AND OTHER TRACE GASES IN STRATOSPHERIC OZONE (J. LEVINE, NASA)

Dr. J. Levine of Langley Research Center, NASA, began his presentation by expressing NASA's interest over the last 15 years in the relationship between the origin, evolution, and future of the earth's atmosphere. NASA has developed theoretical computer models to study this relationship, some of which are used to predict climate changes in the coming decades. NASA's three major areas of environmental concern are: the ozone layer depletion, global climate change, and increasing N_2O emissions.

Levine believes that in the last 100 years the trace gas composition of the atmosphere has changed faster than in the past 4.5 billion years, owing to increased human activity. Measurements from NASA's Nimbus 7 Satellite on October 3, 1979, using TOMS (Total O_3 Measurement System) depicting O_3 distribution in Dobson Units (DUs), shows the O_3 distribution to be between 250-350 DUs at the South Pole. Dr. Levine also presented measurements of the same view of the earth taken 4 years after the first set of measurements. The second measurement set revealed a 50 percent decrease in O_3 (to 150 DUs) over the center of the South Pole, which dramatically represents the Antarctic ozone hole.

The phenomenon shown in Dr. Levine's second measurement set only exists for 4-6 weeks, during which time the O_3 starts to disappear from the South Pole stratosphere as spring begins in the Southern hemisphere. Dr. Levine suggested that the O_3 disappearance probably represents the largest geophysical perturbation ever measured over so short a period. NASA's studies have also shown that the total column of O_3 in the atmosphere has been depleted by 60 percent and, at certain altitudes, by 95 percent from a decade earlier.

Ozone may be second only to oxygen as the earth's most important gas, because O_3 has made possible the evolution and survival of life on the earth's surface. NASA believes that ozone, the only gas that absorbs ultraviolet radiation, developed some 600 million years ago, about the same time that life evolved from the ocean to land. Ninety percent of the earth's O_3 is found in the stratosphere, and 10 percent is found in the troposphere. If the total mass of the atmosphere were brought to the earth's surface at standard temperature and pressure, the gas layer would be 8 km thick, while the ozone layer would be only 2.1 mm thick. However, O_3 is actually distributed in a layer located between 15 and 50 km. When the total column of O_3 is reduced by 10 percent, the UV radiation reaching the earth increases by 20 percent. Therefore, the rule of thumb is that the percent increase of ultraviolet radiation reaching the earth increases by twice the percent decrease of O_3.

Dr. Levine also discussed the causes of the Antarctic ozone hole phenomenon. A unique meteorological situation occurs over the South Pole every spring called the South Polar Vortex. For 4-6 weeks, a mass of air is isolated from the rest of the atmosphere and does not physically interact with it. Because of its low temperature, some interesting atmospheric chemistry takes place that has been only recently understood.

In the stratosphere, where 90 percent of the O_3 resides, the following equations characterize the production of O_3.

$$O_2 + h\upsilon \rightarrow O + O (\leq 242\ \text{nm}) \tag{1}$$

$$O_2 + O + M \rightarrow O_3 + M \tag{2}$$

In 1929, Dr. Sydney Chapman from the University of Alaska stated that O_3 may be destroyed in two ways. The first is by undergoing photolysis by solar radiation.

$$O_3 + h\upsilon \rightarrow O_2 + O\ (\leq 1100\ \text{nm}) \tag{3}$$

The second is to react with atomic oxygen and become molecular oxygen, as shown in the following reaction:

$$O_3 + O \rightarrow 2O_2 \qquad (4)$$

The reactions (1), (2), (3), and (4) are called the Chapman Reactions.

The first satellite measurements of O_3 were made in the early 1970s; however, the O_3 level was found to be much lower than predicted by the Chapman reactions.

Beginning in the early 1970s, three O_3 destruction mechanisms were found that involve oxides of nitrogen (N), hydrogen (H), and chlorine (Cl).

The NO_x catalytic loss mechanism is:

$$\begin{array}{l} NO + O_3 \rightarrow NO_2 + O_2 \\ NO_2 + O \rightarrow NO + O_2 \\ \hline \text{net: } O_3 + O \rightarrow 2O_2 \end{array}$$

The only source of NO in the stratosphere is the following reaction:

$$N_2O + O\,(^1D) \rightarrow 2NO$$

Thus the only source of NO in the stratosphere originates with N_2O.

The HO_x catalytic loss mechanism is:

$$\begin{array}{l} OH + O_3 \rightarrow HO_2 + O_2 \\ HO_2 + O_3 \rightarrow OH + 2O_2 \\ \hline \text{net: } 2O_3 \rightarrow 3O_2 \end{array}$$

The major source of OH in the stratosphere is CH_4. Very little water vapor diffuses from the troposphere into the stratosphere. Methane, however, diffuses up and is chemically transformed to water vapor.

The ClO_x catalytic loss mechanism is:

$$\begin{array}{l} Cl + O_3 \rightarrow ClO + O_2 \\ Cl + O \rightarrow Cl + O_2 \\ \hline \text{net: } O_3 + O \rightarrow 2O_2 \end{array}$$

When asked why there is such concern about CFCs, Dr. Levine responded that there are no natural sources of Cl in the stratosphere, but there are two sources of Cl in the troposphere: volcanos and sea salt spray. However, neither of these sources penetrate into the stratosphere. Scientists are interested in CFCs because they are virtually the only sources of Cl in the stratosphere and atmospheric CFC concentrations are increasing at a very rapid rate.

The catalytic cycle that destroys O_3 may vary with altitude. World Meteorological Report #16 states that integrated over all altitudes and all seasons, 60-70 percent of the global O_3 destruction is caused by NO_x, and that the ultimate source of NO in the stratosphere is N_2O.

Certain gases in the atmosphere have the ability to trap infrared (IR) radiation, thereby producing the greenhouse effect. Dr. Levine suggested that the major greenhouse gas is water vapor, which may cause 90 percent of the natural greenhouse effect. The next major gas is CO_2. These two gases absorb and trap IR radiation, which is then reradiated and directed toward the earth's surface. In this context, Dr. Levine referred to two EPA reports, "Can We Delay a Greenhouse Warming?" and "Projecting Future Sea Level Rise." The latter report suggests that an increase in the earth's temperature of 4 °C is amplified at the North and South Poles to 8-12 °C because of feedback caused by melting ice. The increased temperature at the poles may cause a significant increase in ice-cap melting.

Dr. Levine noted that the atmospheric window is a wavelength band in 8-12 µm and is so named because very little IR absorption occurs within it by the 2 major greenhouse gases (water vapor and CO_2). Any gas that has IR absorption between 8-12 µm can greatly influence the climate. CFCs and N_2O have IR absorption in this band.

After molecular nitrogen at 78 percent by volume, N_2O is the second most abundant nitrogen species in the earth's atmosphere at 330 ppbv (see Table 2-1). Major sources of N_2O are soil, biomass burning, and fossil fuel combustion. Fertilization of agricultural fields is a major source of N_2O. Soil

TABLE 2-1. ATMOSPHERIC NITROGEN SPECIES (LEVINE)

SPECIES	SURFACE CONCENTRATION OR RANGE (BY VOLUME)[1]
MOLECULAR NITROGEN (N_2)	78.08%
NITROUS OXIDE (N_2O)	330 ppbv
AMMONIA (NH_3)	0.1 - 1.0 ppbv
NITRIC ACID (HNO_3)	50 - 1000 pptv
HYDROGEN CYANIDE (HCN)	~200 pptv
NITROGEN DIOXIDE (NO_2)	10 - 300 pptv
NITRIC OXIDE (NO)	5 - 100 pptv[2]
NITROGEN TRIOXIDE (NO_3)	100 pptv[3]
PAN ($CH_3CO_3NO_2$)	50 pptv
DINITROGEN PENTOXIDE (N_2O_5)	1 pptv[3]
PERNITRIC ACID (HO_2NO_2)	0.5 pptv[2]
NITROUS ACID (HNO_2)	0.1 pptv
NITROGEN AEROSOLS:	
AMMONIUM NITRATE (NH_4NO_3)	10 pptv
AMMONIUM CHLORIDE (NH_4Cl)	0.1 pptv

[1] ppbv = PART PER BILLION BY VOLUME = 10^{-9}; pptv = PART PER TRILLION BY VOLUME = 10^{-12}; THE TOTAL ATMOSPHERIC NUMBER DENSITY AT THE SURFACE = 2.55×10^{19} MOLECULES cm^{-3}.

[2] EXHIBITS STRONG DIURNAL VARIATION WITH MAXIMUM CONCENTRATION DURING THE DAY.

[3] EXHIBITS STRONG DIURNAL VARIATION WITH MAXIMUM CONCENTRATION DURING THE NIGHT.

undergoes denitrification, during which nitrate is converted to N_2O, and nitrification, in which ammonia eventually forms N_2O.

Dr. Levine felt that biomass burning is currently underestimated as a major source of N_2O. Analysis of Defense Meteorological Society Project (DMSP) satellite measurements of the earth at night, suggests that as much as 1-5 percent of the land area of our planet may be burned every year, primarily in developing countries. Measurements made by NASA of N_2O levels from biomass burning yielded concentrations of several ppm.

Laboratory and field measurements suggest that lightning is not a major source of N_2O. Currently, its importance is believed to be 3 orders of magnitude less important than other sources. Atmospheric sinks, or loss mechanisms, destroy approximately 10.5×10^{12} g of N_2O. Assuming an annual N_2O increase of 0.2-0.3 percent, the amount of N_2O in the atmosphere would increase by 3.5×10^{12} g. The total of the sinks and the increase (14×10^{12} g) equals the total annual source. Dr. McElroy and Dr. Wofsy from Harvard University and Dr. Seiler and Dr. Conrad from the Max Planck Institut have estimated sources that generally agree with the numbers reported by Dr. Levine. [6,7]

In conclusion, N_2O affects the stratosphere by chemical conversion to NO and subsequent destruction of O_3. Nitrous oxide affects the troposphere by contributing to the greenhouse effect. Further research investigating N_2O in the stratosphere and troposphere is needed. At this point, the key task is determining exactly the sources of the measured increase in concentration of N_2O in the earth's atmosphere.

2.5 MODELING THE EFFECTS OF N_2O AND OTHER TRACE GASES ON CLIMATE AND OZONE DISTRIBUTION (C. BRÜHL, MAX PLANCK INSTITUT)

Dr. C. Brühl of the Max Planck Institut for Chemistry in Mainz, Germany, discussed a one-dimensional photochemical climate model [8]. The model is used to examine variations in globally and hemispherically averaged vertical profiles of temperature and chemical constituents from preindustrial times up to the present, and for 4 future scenarios.

The model considers the growing concentrations of CO_2, CH, N_2O, CFCs, halons, CO, and NO_x owing to anthropogenic causes. One case assumes that emissions of CFCs and halons will be affected by adherence to the Montreal Protocol with no exceptions or delays (about 7 ppbv total Cl in 2070 in the upper stratosphere). The other case assumes only a 15 percent reduction in the rate of emissions (about 9 ppbv total Cl in 2070 in the upper stratosphere). Each case then studies increased emissions of N_2O from combustion (13.7 x 10^{12} g N/yr for the year 2050, [5]) for one scenario and constant N_2O emissions on the 1985 value (3.5 x 10^{12} g N/yr) for the other scenario. The natural other sources of N_2O are estimated to be 6.5 x 10^{12} g N/yr. Preindustrial concentrations are deduced from ice core data.

In the case of moderate total Cl concentrations (effective Montreal Protocol adherence), below about 5 ppbv in the upper stratosphere, the depletion of O_3 is dominated by the NO_x catalytic O_3 destruction cycle in the middle stratosphere. For the case of higher total Cl concentrations (a reduction in the emission rates of CFCs and Halons by only 15 percent), the dominant effect of transforming active chlorine into reservoirs, such as $ClONO_2$ and HCl by NO_x, formed in the stratosphere from N_2O results in less depletion of total O_3 through increasing N_2O emissions. However, the increase in N_2O concentration contributes significantly to the greenhouse effect, resulting in higher global temperatures, as predicted by the model. The global temperature increase by the year 2075 will be about 2.2 K, of which 0.12 K will be due to the increase in N_2O emissions, while an increase in CO_2 alone to 590 ppmv by that year will cause a 1.4 K rise in global temperature, compared to preindustrial times. This model takes into account heat fluxes into the oceans, but does not include ice albedo or cloud feedback which is considered in some global climate models. The heating by N_2O is largest in the tropopause region.

SECTION 3

SESSION 1: THE MECHANISMS OF N_2O FORMATION AND DESTRUCTION DURING COMBUSTION

3.1 BASIC KINETICS (N. BROWN, LAWRENCE BERKELEY LABORATORY)

Dr. N. Brown of Lawrence Berkeley Laboratory was the discussion moderator of the first session. She described her ongoing investigation, assisted by R. Martin, examining the formation/destruction chemistry of N_2O in premixed, laminar, lean, atmospheric-pressure flames. The study involves both experimental and modeling efforts. For the experimental work, CH_4/air/nitrogen compound flames and H_2/O_2/argon/nitrogen compound flames were chosen. The H_2 flames were chosen to provide results without the complexities of carbon chemistry and to allow a comparison of results to model predictions. These flames were lean to simulate power plant operating conditions. Experimental variables were bulk flow rate (28-40 lpm), to include the effects of heat transfer to the burner, equivalence ratio (0.75-0.9), and nitrogen additive (NH_3, NO, N_2O, and N_2). Ammonia (NH_3) was chosen because it simulates typical nitrogen compounds found in oil flames; NO was chosen to provide information about NO destruction/N_2O formation; N_2O was chosen to provide information about N_2O destruction; and N_2 was chosen to provide information for an emissions inventory. The N atom concentration for each additive was varied between 2,100 and 3,300 ppm. Thermochemistry, probe, and quenching effects were also studied.

Very little difference was found in the amounts of N_2O formation in the CH_4 and H_2 flames (Figure 3-1). N_2O occurred as an early flame intermediate in concentrations less than 20 ppm but was minimal (<1 ppm) in post-flame regions. N_2O formation increased with decreasing flame temperature, decreasing equivalence ratio (Figure 3-2), and increasing dopant concentration (Figure 3-3). N_2O concentration for a dopant varied in the order $NH_3 > NO > N_2$ (Figure 3-4). Nitrous oxide concentrations were found to be highest at the burner edge, possibly because of an interaction with cool surroundings

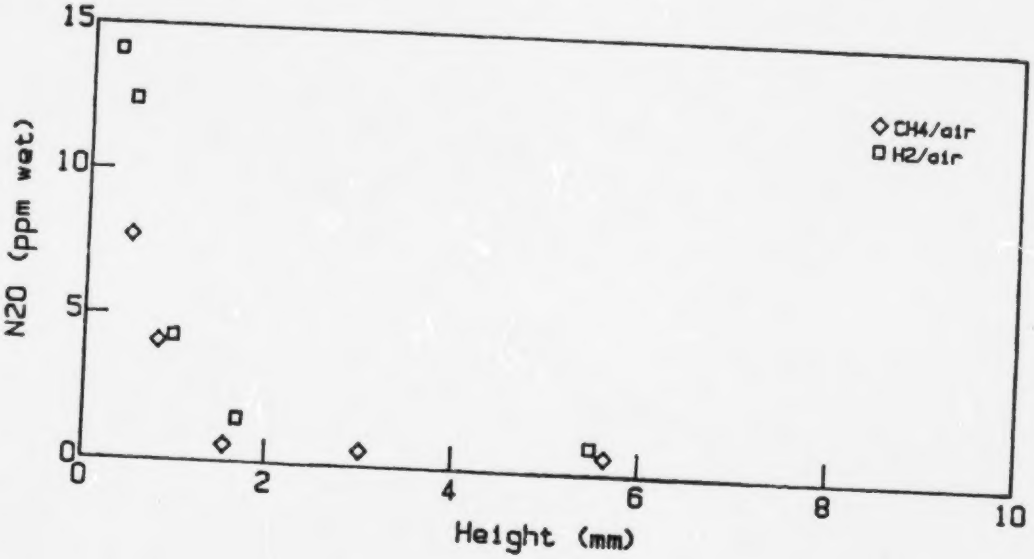

Figure 3-1. N_2O formation in methane and hydrogen flames. (Brown)

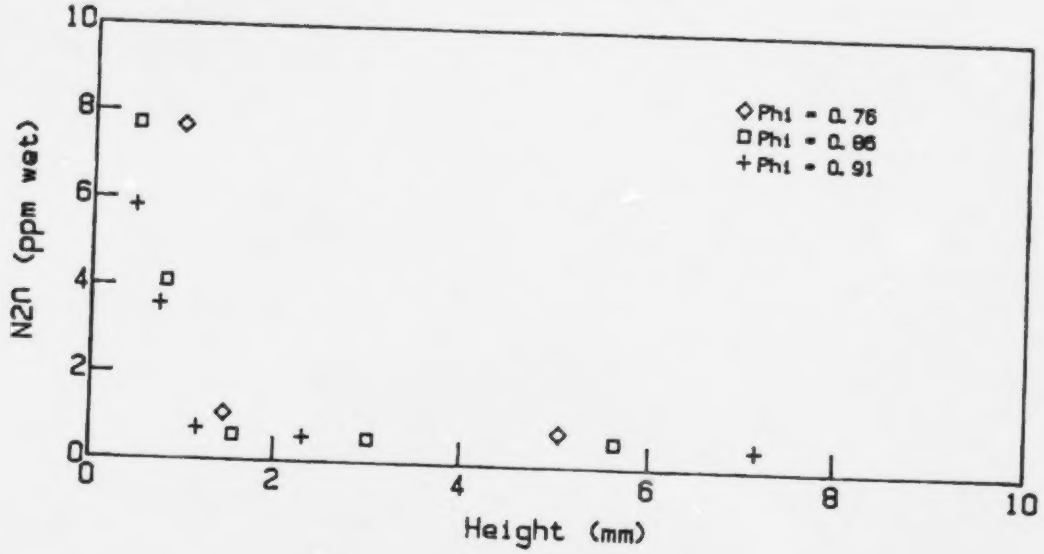

Figure 3-2. N_2O formation versus equivalence ratio. (Brown)

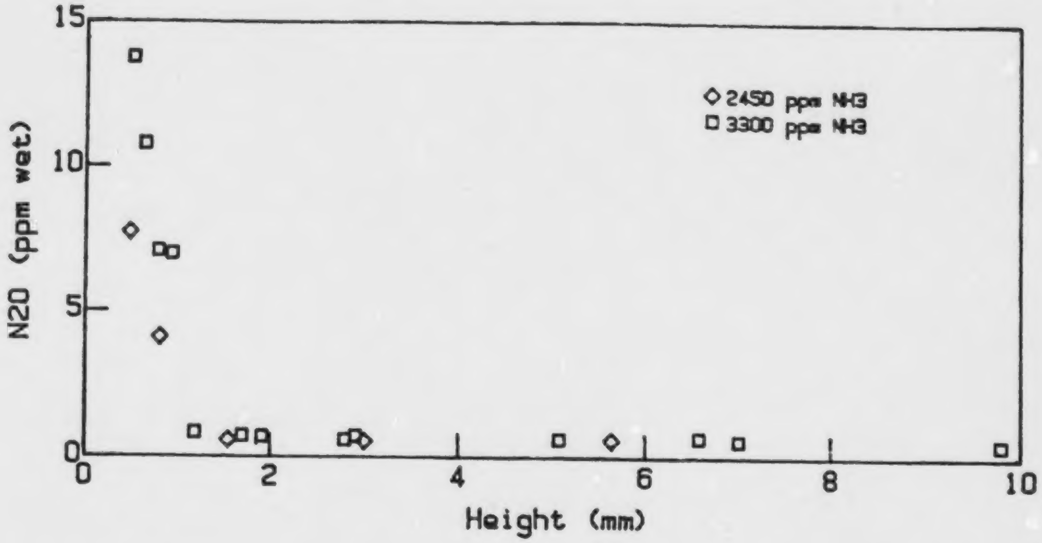

Figure 3-3. N_2O formation versus dopant concentration. (Brown)

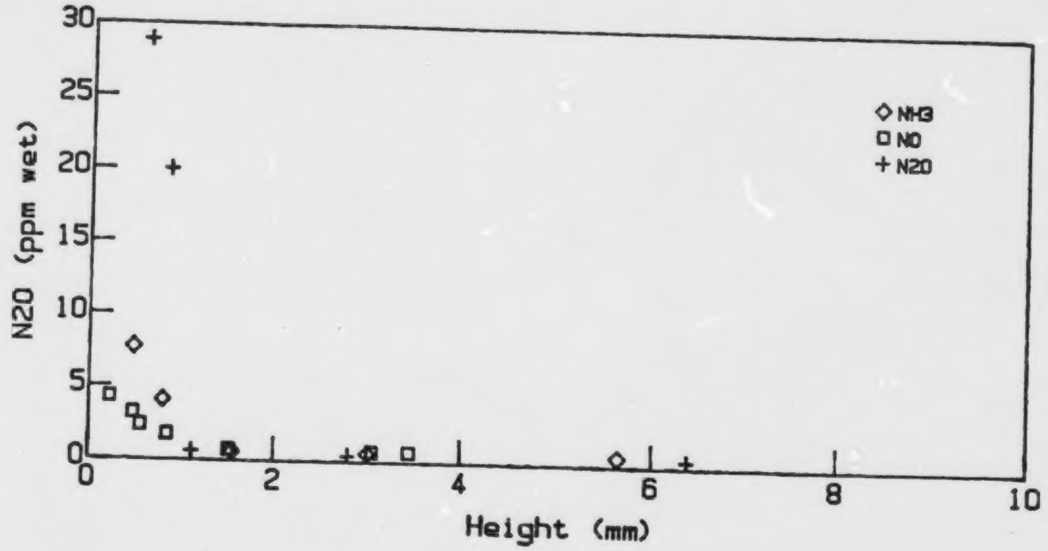

Figure 3-4. N_2O formation versus nitrogen dopant. (Brown)

leading to quenching (Figure 3-5). Conversion of N_2O to NO was less than 8 percent, and the ratio N_2O/NO was less than 2 percent.

For modeling efforts, Dr. Brown used Sandia codes Premix with full chemistry and transport, Chemkin with full chemistry, and Thermochemistry—1987 Chemkin release. Dr. Brown stressed the importance of a thermodynamic data base on model predictions. The results of her model predictions and H_2 flame experiments are shown in Figures 3-6 to 3-9. For modeling purposes, actual measured temperature profiles were used rather than solutions of the energy equation.

Figure 3-6 depicts an NH_3 doped flame at temperature of 1,750 K. There is an excellent agreement (within 2 percent) between model predictions and experimental measurements. Figure 3-7 shows an NO doped flame at about 1,750 K; the agreement between model and experiments is not quite as good. NO agrees within 6 percent, while measurements of N_2 are scattered, possibly because of measurement errors of the order of 25 ppm over measured N_2 values of the order of 75 ppm. Figure 3-8 depicts a N_2O doped flame at about 1,750 K; the model overpredicts NO and underpredicts N_2. Figure 3-9 shows results from a cooler NH_3 flame at about 1,250 K. Changes in flame chemistry at lower temperatures cause a decrease in modeling ability. Thus the agreement between model and experiments is lacking for N_2O and NO. Also noticeable is a slower decay of N_2O with height as opposed to a faster decay observed in higher temperature flames. Ongoing work by Dr. Brown has shown large chemistry changes between 1,100 and 1,250 K. Thus temperature is an extremely important parameter in modeling efforts.

In N_2O formation chemistry, the dominant reaction in H_2 flames is $NH + NO \rightarrow N_2O + H$ and is 3,000-6,000 times more dominant than $NH_2 + NO \rightarrow N_2O + H_2$ reaction. In hydrocarbon flames, $NCO + NO \rightarrow N_2O + CO$ seemed dominant. In both types of flames, the destruction mechanism of $N_2O + H \rightarrow N_2 + OH$ seemed most likely, although $N_2O + H \rightarrow NH + NO$ is another path. The branching ratio of above two destruction paths is temperature dependent and is not well understood.

Dr. Brown concluded that agreement between the experiment and modeling was satisfactory near 1,700 K, but the chemistry at temperatures less than 1,100 K needs more clarification. Other conclusions of Dr. Brown's research are:

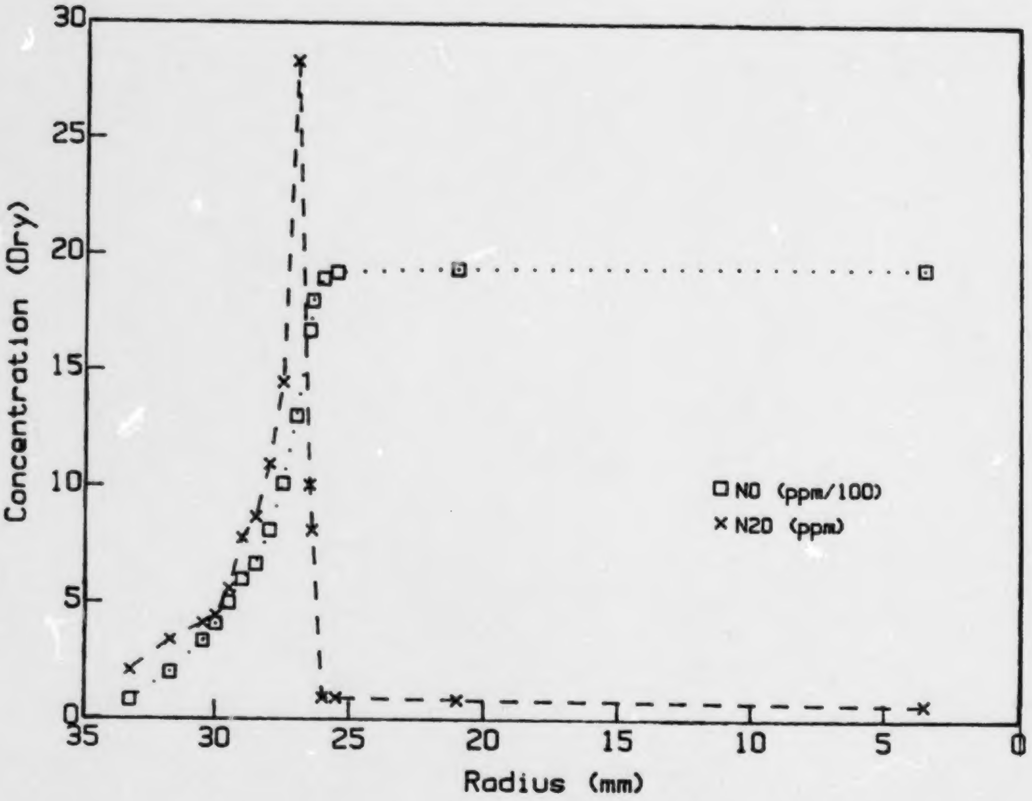

Figure 3-5. Edge effects on N_2O formation. (Brown)

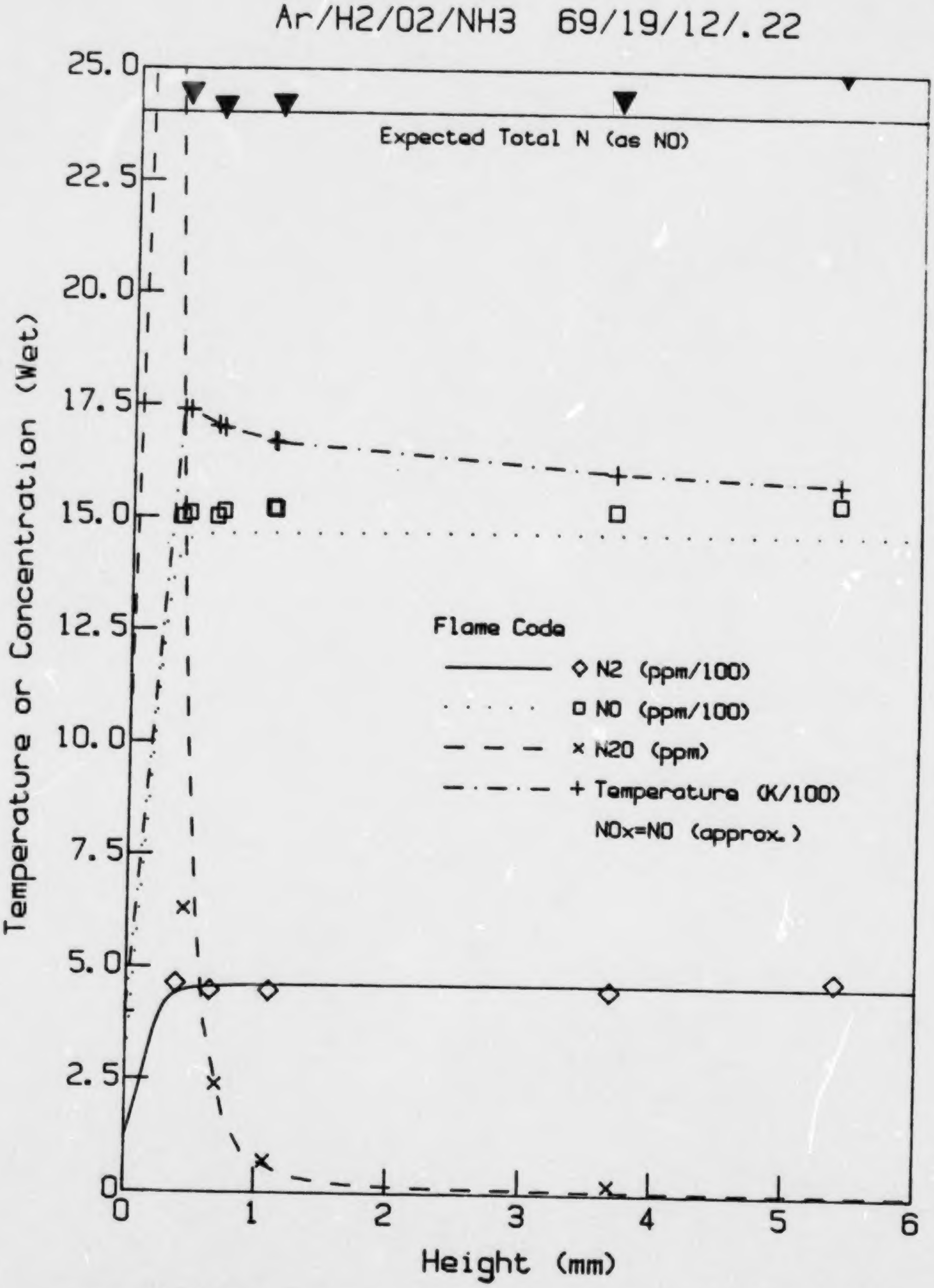

Figure 3-6. Comparison of modeling and experimental results with NH_3-doped flame. (Brown)

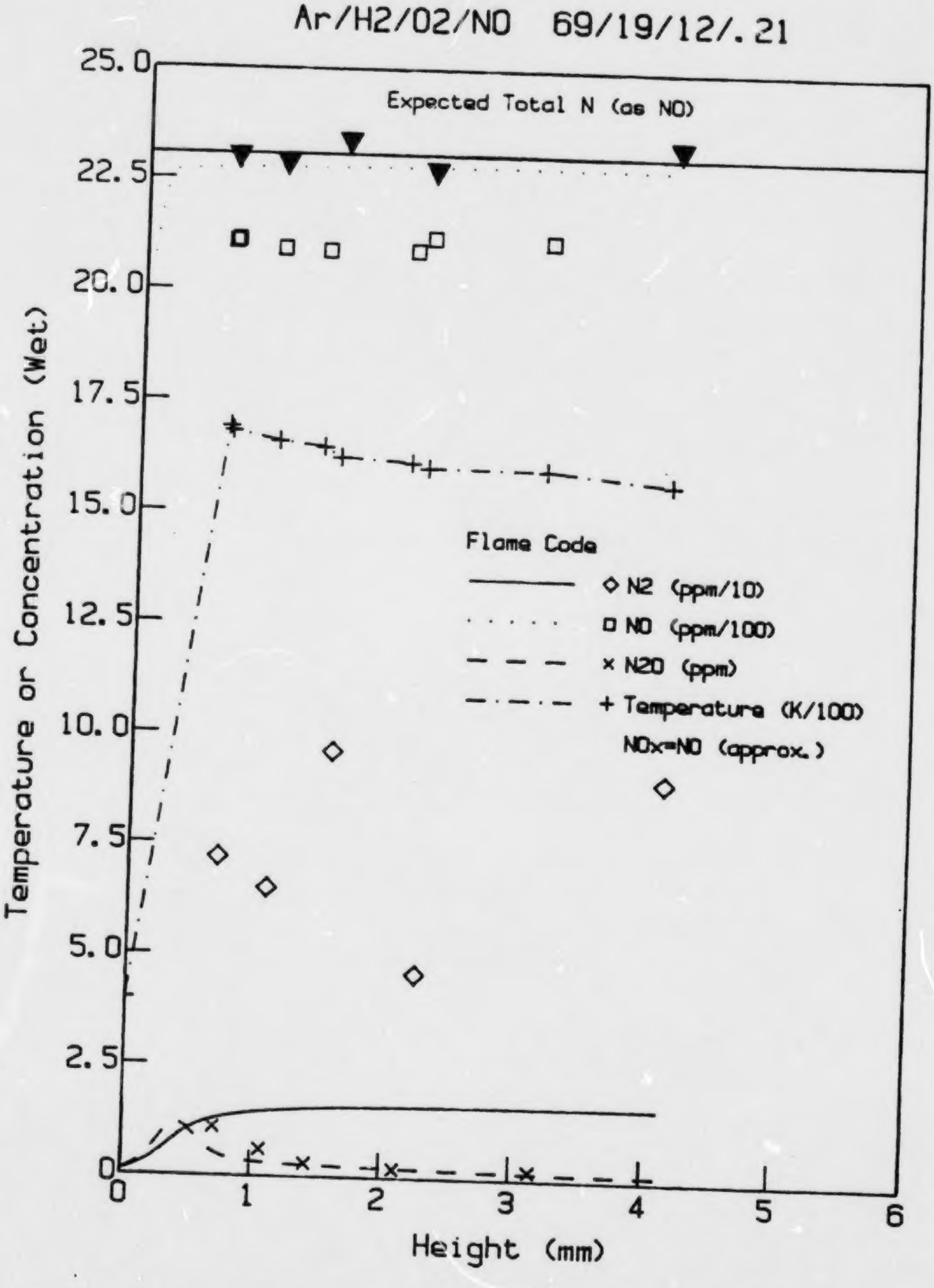

Figure 3-7. Comparison of modeling and experimental results with NO-doped flame. (Brown)

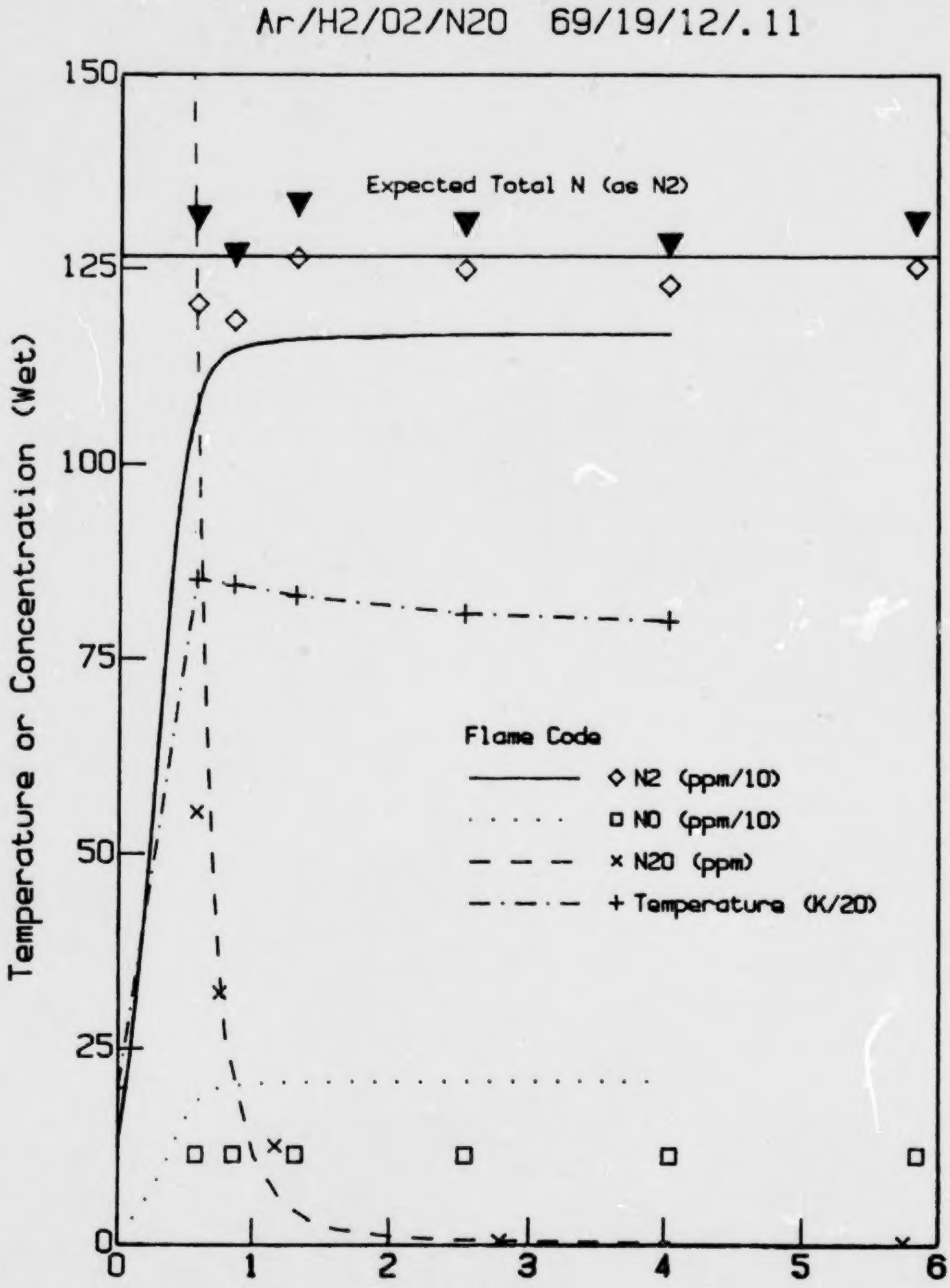

Figure 3-8. Comparison of modeling and experimental results with N_2O-doped flame. (Brown)

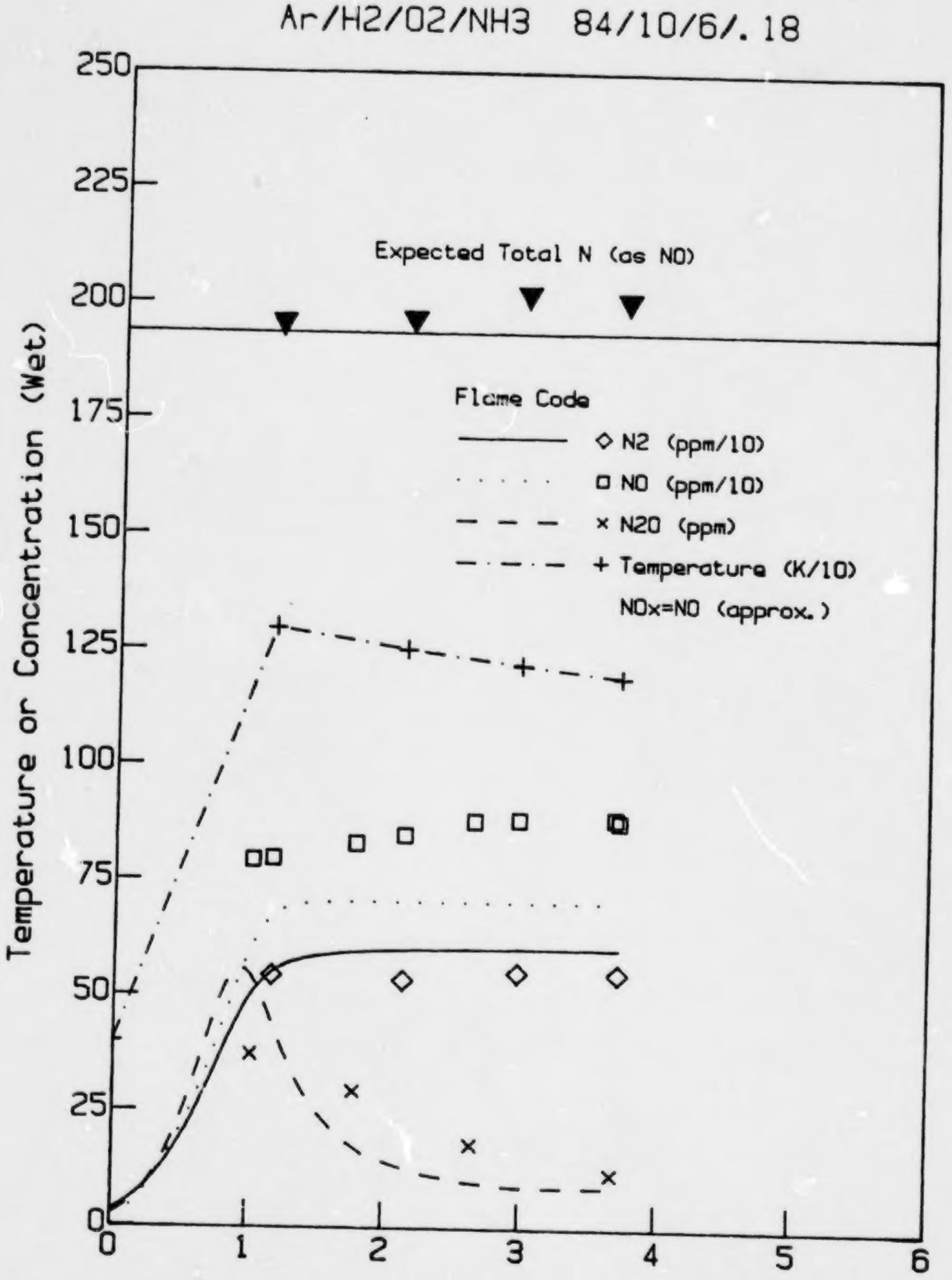

Figure 3-9. Comparison of modeling and experimental results with NH3-doped flame. (Brown)

- N_2O destruction results in N_2 production.
- Destruction reactions need to be determined over a wide range of temperatures and product yields.
- More information on N_2O production reactions is needed.
- Probe effects need to be eliminated because they could have a significant effect on N_2O measurements.

3.1.1 Gas Phase Kinetics (J. Kramlich, EERC)

Dr. J. Kramlich, of Energy and Environmental Research Corporation (EERC), focused on the emissions of N_2O from industrial flames. Specifically discussed were the issues of N_2O formation and emission in coal and oil flames and the effects of firing configuration and pollution control strategies on these emissions. This study has involved both experimental work and modeling.

A significant amount of N_2O, well over the 10 ppm level, is emitted from many industrial coal and oil flames. However, little N_2O is emitted from gas flames; the highest level measured so far from industrial gas flames is 11 ppm, with levels of 2-3 ppm being typical.

A down-fired tunnel furnace, with a realistic quench environment, was used to establish baseline N_2O concentrations from natural gas/air and coal/air flames. About 70 ppm of NO and an unmeasurable amount of N_2O were measured from the gas flame, and about 1,100 ppm of NO and about 80 ppm of N_2O were measured from the coal flame. The N_2O measurements were made using GC/ECD analysis. A possible hypothesis at this point was that fuel nitrogen present in coal caused an increase in N_2O emissions. To verify this hypothesis, fuel N was added to the gas flame in the form of HCN and NH_3. These doped gas flames emitted about 900 ppm of NO but still almost no N_2O (<0.5 ppm). The experiments described revealed that there was something special about the coal flame that caused it to emit higher concentrations of N_2O.

Kinetic calculations using a 5 ms well stirred reactor (to simulate ignition zone) and a 200 ms plug-flow reactor (to simulate burnout zone) were performed to investigate NO and N_2O emissions from gas flames. The kinetic set used is shown in Figure 3-10. A realistic temperature profile was imposed on the plug-flow reactor for these simulations. The results indicate that for the two gas flames (with and

KINETICS

$NH + NO$ ->	$N_2O + H$ $N_2 + OH$
$NH_2 + NO$ ->	$N_2H + OH$ $N_2 + H_2O$ $N_2O + H_2$
$NCO + NO$ ->	$N_2O + CO$ $N_2 + CO_2$
$N_2 + O + M$ ->	$N_2O + M$
$N_2O + H$ ->	$NO + NH$ $N_2 + OH$

Figure 3-10. Kinetics used in model calculations. (Kramlich)

without fuel nitrogen) N_2O was formed in the flame zone, with maximum concentrations of about 6-7 ppm, but decayed rapidly to insignificant levels. The rapid decay is due possibly to the N_2O destruction reaction, involving a H atom, being sufficiently rapid in the high temperature flame zone. These results verified earlier experimental findings and further indicated that, given rapid N_2O destruction in the flame zone, the key to N_2O emissions from coal and oil flames was in the post-flame chemistry.

Subsequently, post-flame generation of N_2O from coal flames was modeled. Taken into account were heterogeneous effects of char oxidation, char-NO reduction, and volatiles chemistry. Generally, the combustion of volatiles is fairly complete in the flame zone. However, depending on the firing configuration, fuel type, and stoichiometry, some volatile combustion may take place in the post-flame regions. The N_2O destruction reaction involving a H atom slows down in the post-flame zone because of lower temperatures and the paucity of H atoms. The results of this modeling effort, shown in Figure 3-11, indicate that char oxidation and char-NO reduction cannot form sufficient N_2O. NH_3 volatiles give low N_2O yields (maximum of about 2.5 ppm), but HCN volatiles react to produce N_2O levels of about 100 ppm at the exit of the reactor. Production of HCN volatiles in the post-flame zone may be linked to the N carried by char beyond the flame zone. Model results, shown in Figure 3-12, also indicate that if HCN is artificially introduced into the system, it will convert to N_2O between 1,100-1,400 K and that maximum N_2O yields will be about 700 ppm and 250 ppm for 100 percent and 40 percent conversion, respectively.

Experiments were then carried out on a down-fired laboratory furnace with a CH_4/Air/NO flame where HCN, NH_3, and acetonitrile were injected into the furnace at various locations (temperatures) along the combustor. The results, shown in Figure 3-13, are congruent with the model predictions obtained earlier and further indicate that other cyano species such as acetonitrile will also yield N_2O in post-flame regions.

Figure 3-14 summarizes the study with a mechanism overview and shows that predominant generation of N_2O occurs in the post-flame zone from conversion of HCN to N_2O. Presence of HCN in the post flame can be credited to devolatilization of char-N and to free HCN transported from the edge of

POST-FLAME

- USE FCR–III MECHANISM

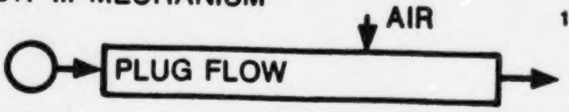

- HCN AT STAGING POINT OXIDIZED
- CHAR OXIDATON + CHAR–NO REDUCTION CANNOT FORM SUFFICIENT N_20
- NH_3 VOLATILES SHOW LOW CONVERSION
- HCN VOLATILES REACT TO N_20

CONCLUSION:

- N_20 FORMED IF HCN APPEARS IN POST–FLAME
- CHAR MAY BE VEHICLE FOR CARRYING N BEYOND FLAME ZONE

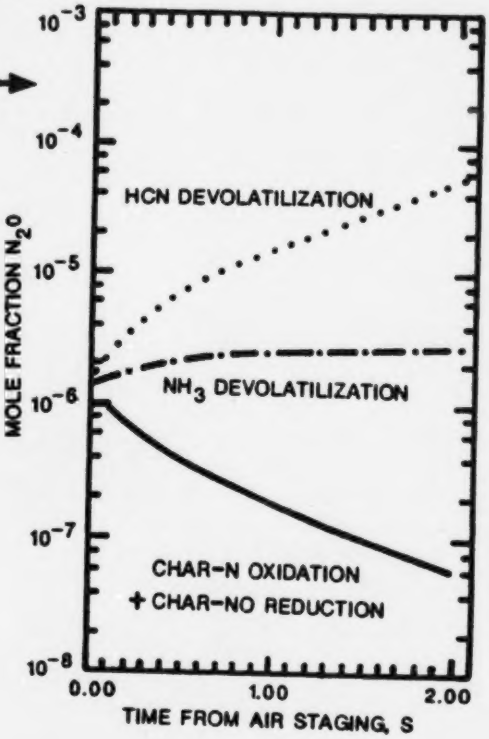

Figure 3-11. Post-flame modeling results. (Kramlich)

HOMOGENEOUS N_2O

- USE FCR–III MECHANISM

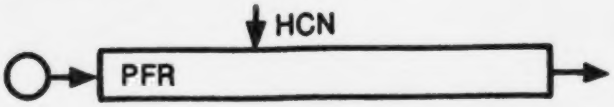

- GOAL: DOES N_2O APPEAR IF HCN IS ARTIFICALLY INTRODUCED/?

CONCLUSION

- HCN WILL CONVERT TO N_2O BETWEEN 1100 – 1400K
- NH_3 WILL NOT CONVERT

$$NCO + NO \rightarrow N_2O + CO \ (40\%)$$
$$\rightarrow N_2 + CO_2 \ (60\%)$$

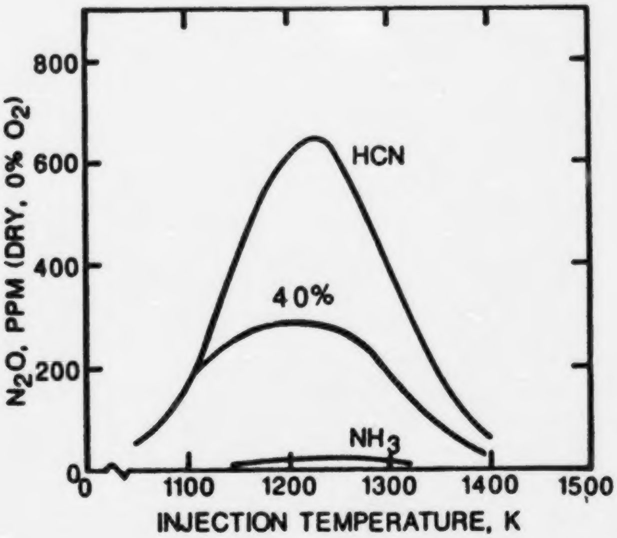

Figure 3-12. Post-flame modeling results (Artificial HCN Introduction). (Kramlich)

- OTHER CYANO SPECIES ALSO YIELD N_2O
- NH_3 DOES NOT, UNDER THESE CONDITIONS

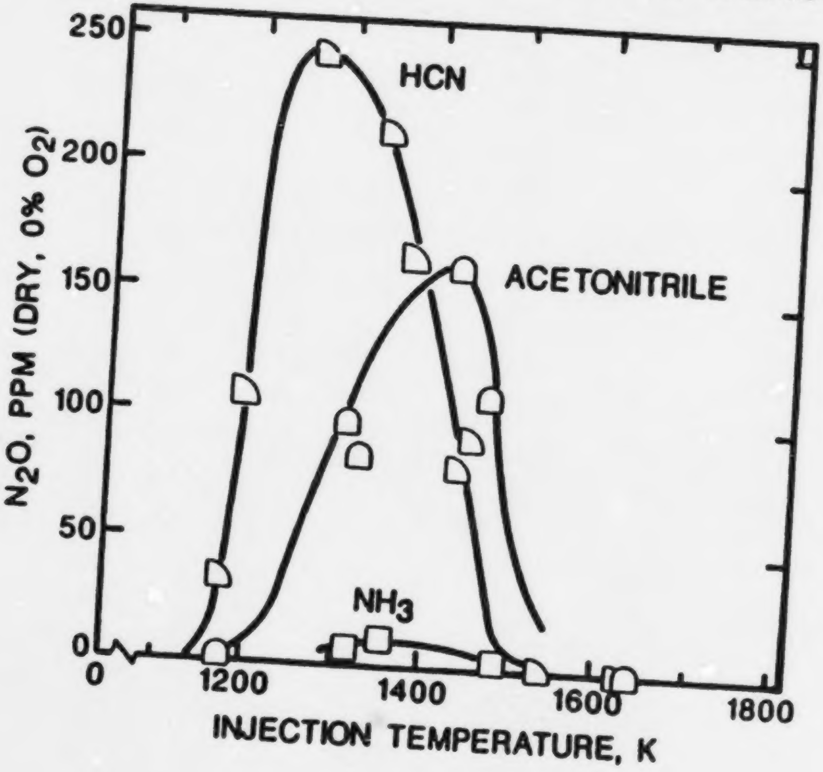

Figure 3-13. Post-flame experiment. (Kramlich)

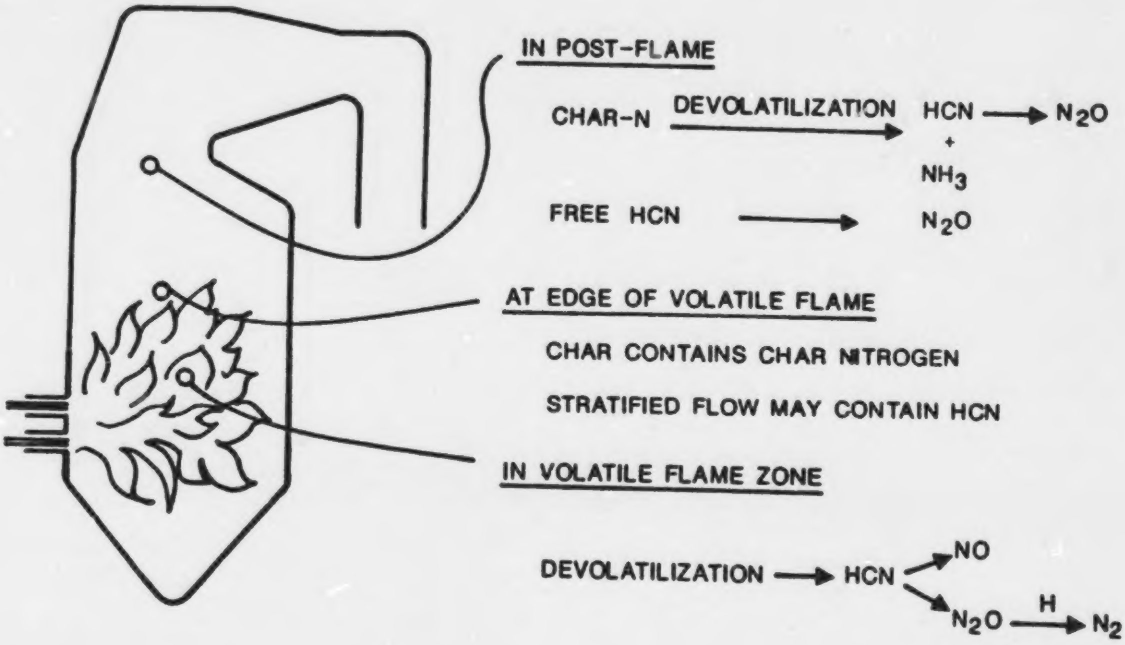
IN POST-FLAME
CHAR-N $\xrightarrow{\text{DEVOLATILIZATION}}$ HCN + NH_3
HCN → N_2O
FREE HCN → N_2O
AT EDGE OF VOLATILE FLAME
CHAR CONTAINS CHAR NITROGEN
STRATIFIED FLOW MAY CONTAIN HCN
IN VOLATILE FLAME ZONE
DEVOLATILIZATION → HCN → NO
HCN → N_2O $\xrightarrow{H}$ N_2

Figure 3-14. Mechanism overview. (Kramlich)

volatile flame in stratified flow. Some N_2O is produced in the flame zone but is rapidly destroyed to form N_2. The pertinent reactions are shown in Figure 3-15.

An enthusiastic question and answer period followed Dr. Kramlich's presentation. Dr. Zellinger asked how much HCN was injected during the tests. Dr. Kramlich replied that starting with 600 ppm NO in the post-flame environment, sufficient HCN was added so that a total of 900 ppm would be measured if all of the HCN had been converted.

Mr. M. Morgan from the International Flame Research Foundation (IFRF) commented that, although Dr. Kramlich's tests showed conditions in which HCN to N_2O formation was favored, it was not clear where NO formation was favored. He inquired whether any light could be thrown on this issue? Dr. Kramlich responded that at higher temperatures NO would be favored because at these temperatures N_2O destruction would be very efficient and because precursors to N_2O formation would be oxidized. At somewhat lower temperatures, N_2O may be favored, and at even lower temperatures HCN itself may exist.

Dr. F.C. Lockwood of Imperial College requested clarification of the meaning of "post-flame region," since his experience was with industrial equipment. Dr. Kramlich described the post-flame region as being beyond the luminous or volatile flame where the majority of the gas species have essentially reached equilibrium and the major reaction occurring is heterogeneous oxidation of char.

Mr. S.A. Sloan of Central Electric Research Laboratories was interested in the implications of NO_x control by staged combustion on N_2O emissions. Dr. Kramlich responded that, because N_2O does not tend to survive a fuel-rich environment, staged combustion may lower N_2O emissions.

Dr. H.J.A. Hasenack of Royal Dutch Shell Laboratory added that Mr. Sloan's concern in regard to staged combustion technology may be important as data suggest that N_2O formation may be possible if the fuel-rich zone becomes cool enough to fall in the 1,150-1,500 K temperature window. He warned against blindly applying NO_x control techniques to control N_2O emissions.

Dr. W.S. Lanier of the EERC emphasized that the goal of the EERC study was not to simulate a specific type of coal flame. The study was designed to identify possible mechanisms involved in N_2O emission, and the conditions used were for that purpose only.

$$\left.\begin{array}{l} HCN + O = NCO + H \\ NCO + NO = N_2O + CO \end{array}\right]$$

FORMATION

$$\left.\begin{array}{l} N_2O + H = N_2 + OH \end{array}\right]$$

REMOVAL

$$\left.\begin{array}{l} HCN + OH = HNCO + H \\ HNCO + H = NH_2 + CO \end{array}\right]$$

ALTERNATE ROUTES

Figure 3-15. Reaction Mechanisms. (Kramlich)

Dr. de Soete noted that in the model used all of the char-bound N was converted to N_2O. He asked if Dr. Kramlich believed that all char-bound nitrogen formed primarily N_2O when it reacts during char oxidation. Dr. Kramlich replied that reactions producing N_2O were favored. However, since no N_2O was seen at the end of the flame zone, this choice is irrelevant.

3.1.2 Heterogeneous Reactions (G. de Soete, IFP)

Dr. de Soete of IFP began by defining a heterogeneous reaction as one between 2 different phases, as in gas to solid. Heterogeneous reactions implying N_2O as a reactant or as a product are numerous. Three examples are:

1. Formation of N_2O from bound N during heterogeneous char oxidation.
2. Heterogeneous reduction of N_2O on char-bound C atoms during heterogeneous char oxidation.
3. Formation of N_2O during catalytic NO reduction (coupled with catalytic N_2O reduction), which may play a larger role in N_2O emissions from mobile sources.

A heterogeneous reaction rate can be expressed by:

$$V_i = k_i e_n{}^m P_y$$

where k_i is the rate constant, $e_n{}^m$ (a fraction) expresses the dependence of the covering degree, which is proportional to active sites in the solid involved in the reaction, and P_y is the dependence of partial pressure of one or more of reactant gaseous species.

Thus the study, focusing on heterogeneous reactions that imply N_2O as a reactant or product, involved 2 tasks. The first was a series of steady-state trials performed under adsorption/desorption equilibrium conditions aiming at determining of global rates of N_2O release and destruction and identifying of reaction products (establishing N, C, and O balances). The trials had to be performed using a progressive complexity of the solid reactant (graphite-char) and reactive gas composition. Specifically, the first task provided identification of the adsorption and desorption reactions composing the heterogeneous mechanisms and their reaction rates V_is. The second task involved a time-resolved study of the reactions identified in the first phase. This allowed determination of the fractions leading to determination of the rate constants, k_i's.

Dr. de Soete cautioned that although much can be learned about heterogeneous mechanisms from time-resolved or transient-state reactions, practical requirements should not be ignored. For example, exclusion of concomitant interfering gas phase could be accomplished by avoiding pyrolysis of the solid and utilizing temperature conditions for which interfering gas phase reactions may be ignored.

The formation of N_2O during NO catalytic reduction plays a major role in emissions from mobile sources using three-way catalysts. A catalyst does not normally work without a reducing agent, especially a reducing gas agent (i.e., CO or H_2). When NO is fed with CO as a reducing agent over a three-way catalyst, the fractional decrease of NO is a function of the temperature of the catalyst material. As shown in Figure 3-16 for a metal catalyst, at lower temperatures, as the concentration NO decreases because of reduction by CO, N_2O is formed and participating CO is qualitatively converted into CO_2. At higher temperatures, reduction of N_2O takes place.

Thus, passing N_2O and NO over a typical metal catalyst results in:

1. Reduction of NO at a much lower temperature than N_2O, resulting in the formation of N_2O as a function of temperature.
2. Intermediate formation of N_2O when NO is fed as a function of temperature.

It can be concluded from the above that transformation of N_2O into NO is a minor reaction. The probable reactions and rates of major reactions during heterogeneous formation and destruction of N_2O on metal catalysts are shown in Figure 3-17.

In all circumstances using graphite, N_2O will be reduced at a lower temperature than will NO, as opposed to the situation when a metal catalyst is used with a reducing agent. Since N_2O reduces at a lower temperature than NO, little N_2O is found when NO is reduced. Although reduction of NO could result in formation of N_2O, however, this reduction of NO at the temperature where N_2O can be formed occurs so fast that the N_2O cannot be seen in the gas. For graphite, this is true in both the presence and absence of oxidizing gases. The situation is the same during heterogeneous reduction of N_2O and NO

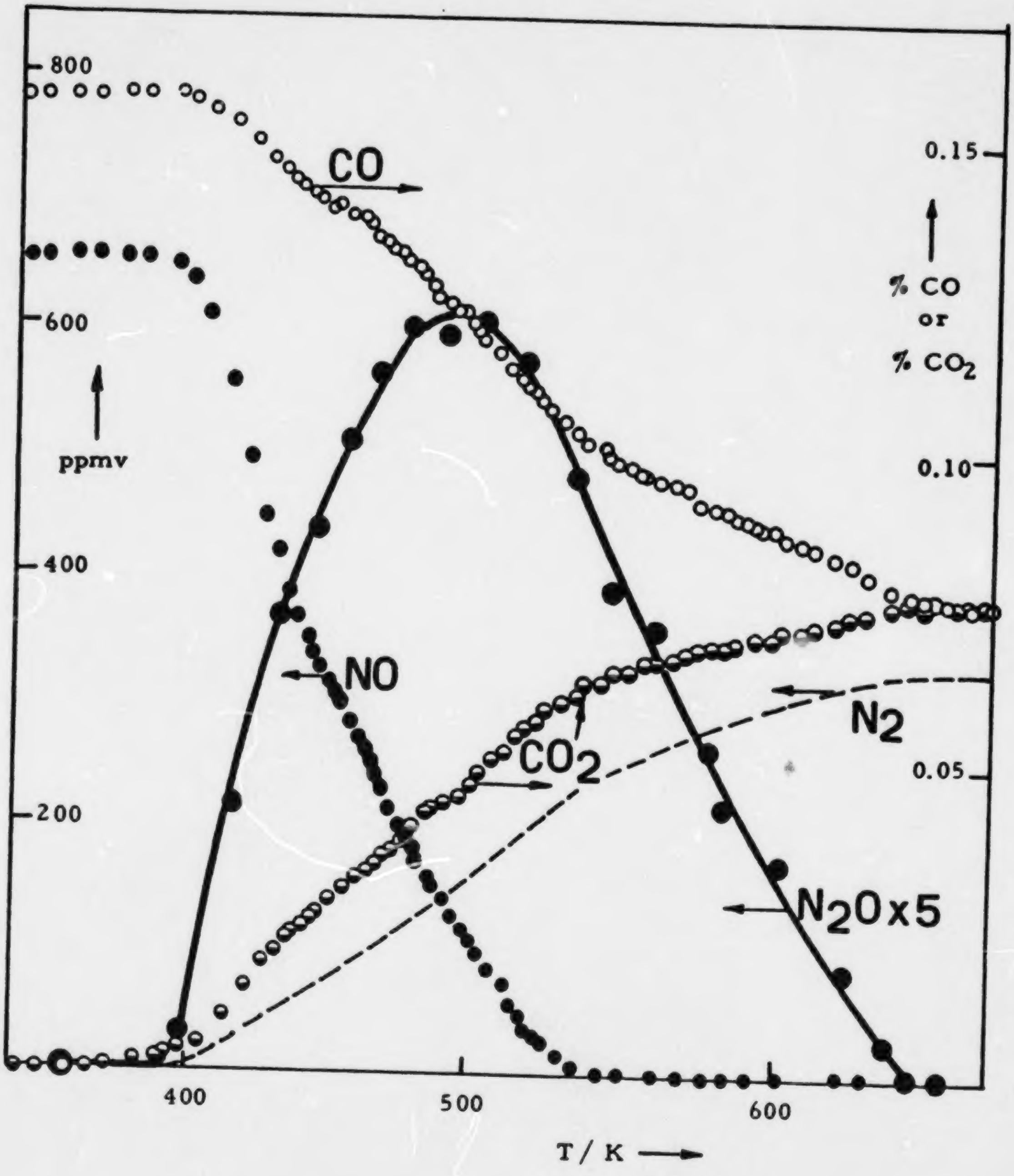

Figure 3-16. NO and CO over metal (JPB 93) catalyst. (de Soete)

MAJOR REACTIONS :

REDUCTION OF NO INTO N2	$NO + 2(-M) \xrightarrow{12} (-MO) + (-MN)$ $2(-MN) \xrightarrow{13} N2 + 2(-M)$ $NO + (-MN) \longrightarrow N2 + (-MO)$	(probable mechanism)
SCAVENGING OF OXYGEN ATOMS	$CO + (-MO) \xrightarrow{10} (CO2) + (-M)$	
N2O FORMATION	$NO + (-MN) \xrightarrow{11} (N2O) + (-M)$	(hypothetic)
REDUCTION OF N2O	$N2O + (-M) \xrightarrow{7} (N2) + (-MO)$	(hypothetic)

MINOR REACTIONS :

TRANSFORMATION OF N2O INTO NO	$N2O + (-MO) \xrightarrow{14} 2NO + (-M)$ $N2O + (-M) \xrightarrow{15} NO + (-MN)$	(?) (?)

RESULTS FROM A TYPICAL CATALYST : (Rates in $cm^3 g_{cat}^{-1} s^{-1}$)

$V_{12} = 7.7\ exp(-4840/T)P_{NO}$

$V_{11} = 0.33\ exp(-3900/T)P_{NO}$

$V_{10} = 1.63\ 10^{-1}\ exp(-3130/T)P_{CO}$

$V_{13} = 3.710^{1}\ exp(-4120/T)$

$V_7 = 5.1\ 10^5\ exp(-11130/T)P_{N2O}$

Figure 3-17. Heterogeneous formation and destruction of N_2O on metal catalyst. (de Soete)

on char-bound carbon atoms. The probable reactions and rates for heterogeneous reduction of N_2O on char-bound carbon are shown in Figure 3-18.

Shown in Figure 3-19 are the experimentally determined overall reaction rates of C oxidation and, NO, N_2O, and HCN formation as a function of temperature for Eschweiler char. The subscript e in this figure implies that these reaction rates were obtained under adsorption/desorption equilibrium rates. The figure suggests a rough proportionality between V_C, V_{NO}, and V_{N2O}.

For a Cedar Grove char, plotted in Figure 3-20 are fractions of nitrogen converting to NO and to N_2O as functions of fraction of carbon burnt. These results have been obtained for all fractions of carbon burnt and for temperatures up to 1,400 K. As a rough approximation, the fractions of N converted to NO and N_2O seem to be proportional to the fractions of carbon burnt. Thus it seems that a constant fraction of N is formed into NO and another constant fraction of N is converted into N_2O in a heterogeneous way. This is true for all char burnout fractions and at all temperatures up to 1,400 K.

Therefore, the main reaction path of N_2O formation from bound nitrogen, during char combustion, at temperatures below 1,400 K, is probably not a formation from HCN, occurring in the gas phase, but a heterogeneous reaction directly linked to char oxidation. This is suggested by reaction order with respect to oxygen of one for V_C (overall combustion rate), V_{NO} (overall NO formation rate), and V_{N2O} (overall N_2O formation rate), and similar temperature dependence of their overall rate. Trials where HCN is added to the oxidizer gas during combustion of carbonaceous materials, show that HCN is mainly converted into N_2 and NO, instead of into N_2O (Figure 3-21).

Thus based on this study, the probable mechanisms involved in formation of N_2O from bound nitrogen during heterogeneous char oxidation are shown in Figure 3-22. The parentheses in this figure imply solid bound groups. Main reaction paths for these mechanisms are shown in Figure 3-23.

Dr. J. Wendt asked for a characteristic residence time in the reactor, to which Dr. de Soete responded that it was on the order of 20-50 ms. Dr. Wendt also asked if experiments were conducted where physical characteristics of particles were changed in order to determine effects of intraparticle diffusion. Dr. de Soete answered that particle size effects were checked.

REDUCTION OF NO INTO N2	$NO + 2(-C) \xrightarrow{6} (-CO) + (-C.N)$ $2(-CN) \xrightarrow{8} N2 + 2(-C)$	
FORMATION OF N2O FROM NO	$NO + (-C.N) \xrightarrow{9} N2O + (-C)$	
REDUCTION OF N2O INTO N2	$N2O + (-C) \xrightarrow{16} N2 + (-CO)$ $N2O + (-CO) \xrightarrow{17} N2 + CO2$	
FORMATION OF NO FROM N2O	$N2O + (-CO) \xrightarrow{18} 2\ NO + (-C)$	SCAVENGING EFFECT OF N2O AND CO
ELIMINATION OF BOUND OXYGEN	$CO + (-CO) \xrightarrow{4} CO2 + (-C)$ $(-CO) \xrightarrow{2} CO$ + free carbon site $2(-CO) \xrightarrow{3} CO2 + (-C)$	
CO2 ADSORPTION	$CO2 + (-C) \xrightarrow{5} CO + (-CO)$	

TYPICAL RESULTS for CO, NO and N2O on GRAPHITE (Rates in $cm^3\ g_c^{-1}\ s^{-1}$) :

$V_6 = 5.44\ 10^1 \exp(-16060/T) P_{NO}$

$V_9 = 2.00\ 10^1 \exp(-14400/T)\ P_{NO}$

$V_{16} = 1.65\ 10^5 \exp(-19400/T)\ P_{N2O}$

$V_{17} = 3.67\ 10^3 \exp(-15450/T)\ P_{N2O}$

$V_4 = 1.21\ 10^8 \exp(-35200/T)\ P_{CO}$

$V_2 = 2.25\ 10^5 \exp(-19600/T)$

Figure 3-18. Heterogeneous reduction of N_2O on char bound carbon. (de Soete)

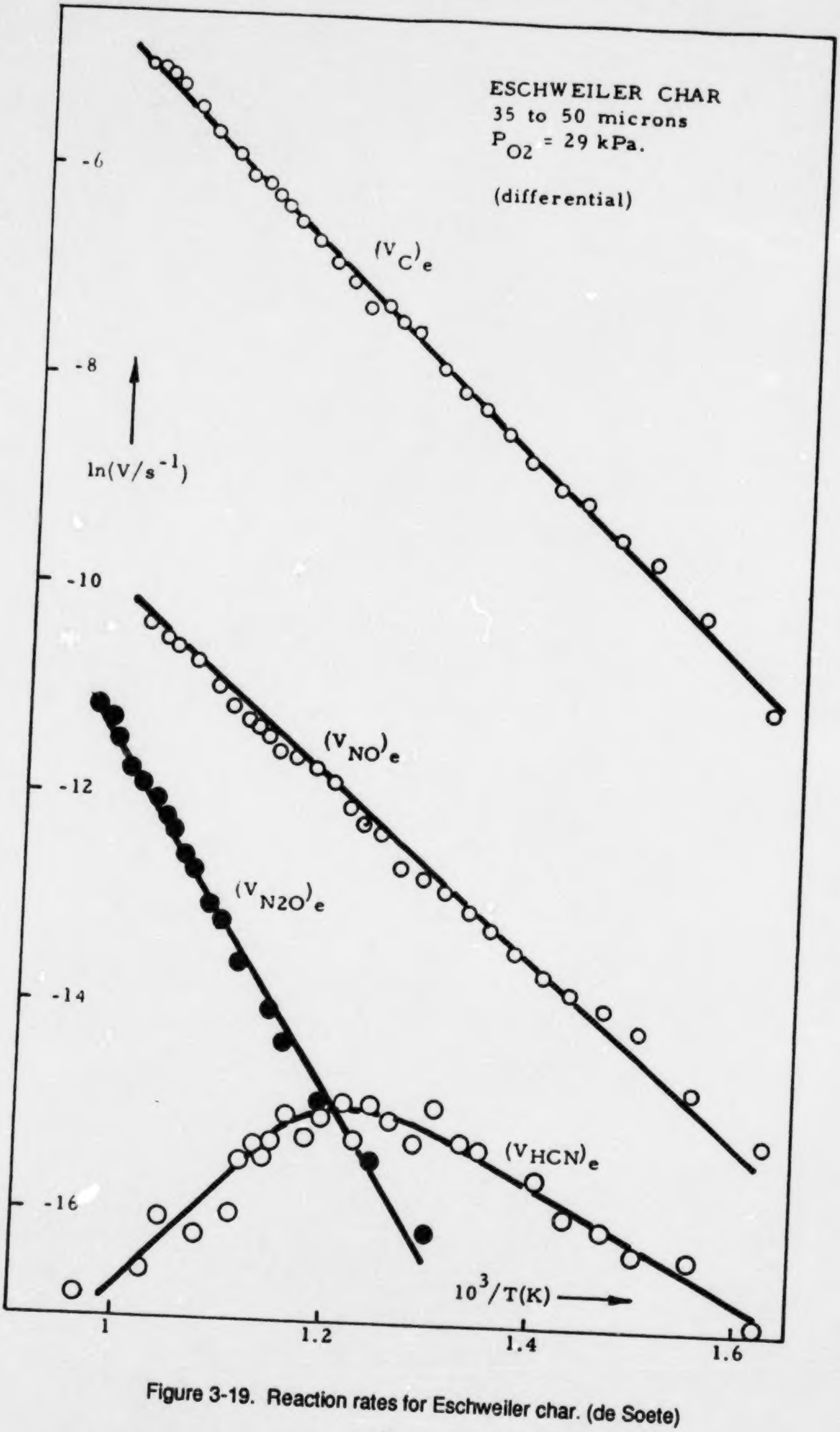

Figure 3-19. Reaction rates for Eschweiler char. (de Soete)

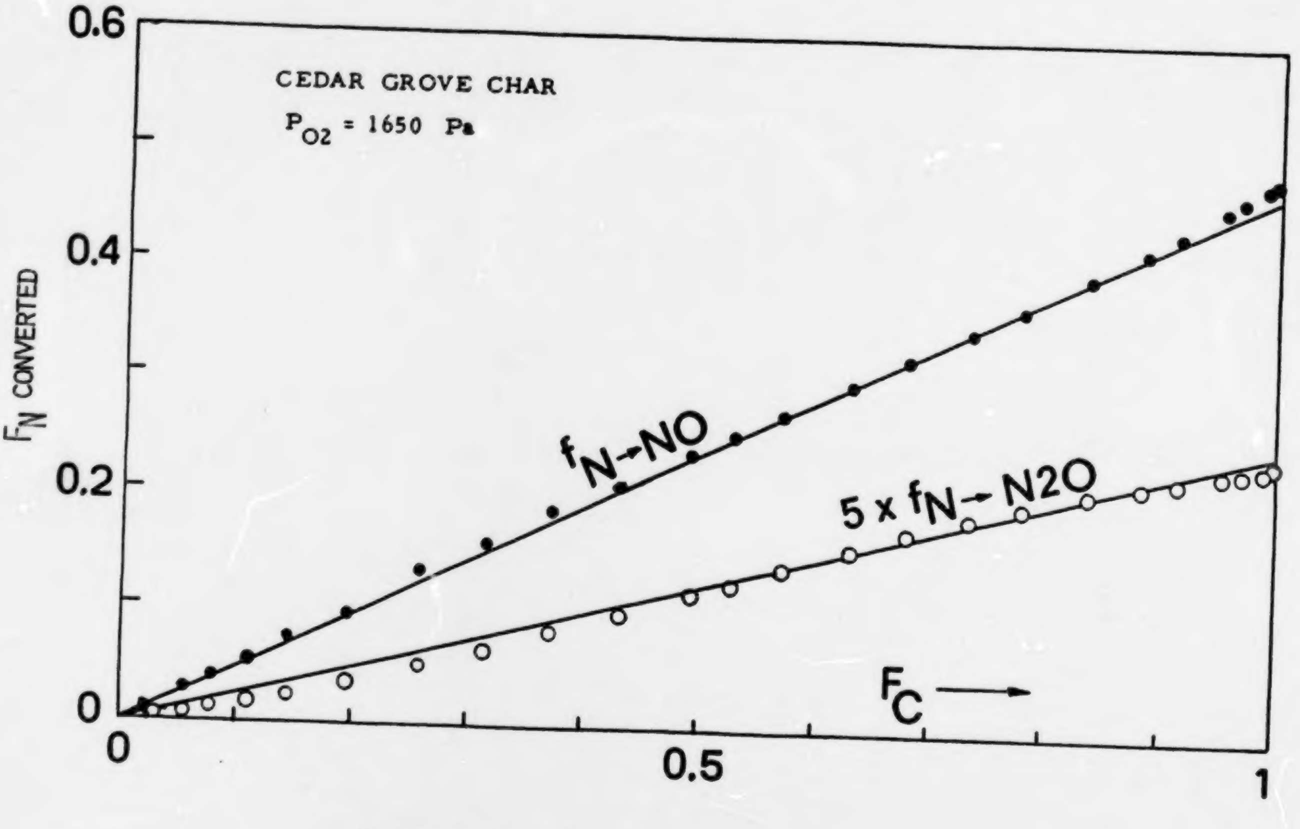

Figure 3-20. Cedar Grove char conversion of nitrogen. (de Soete)

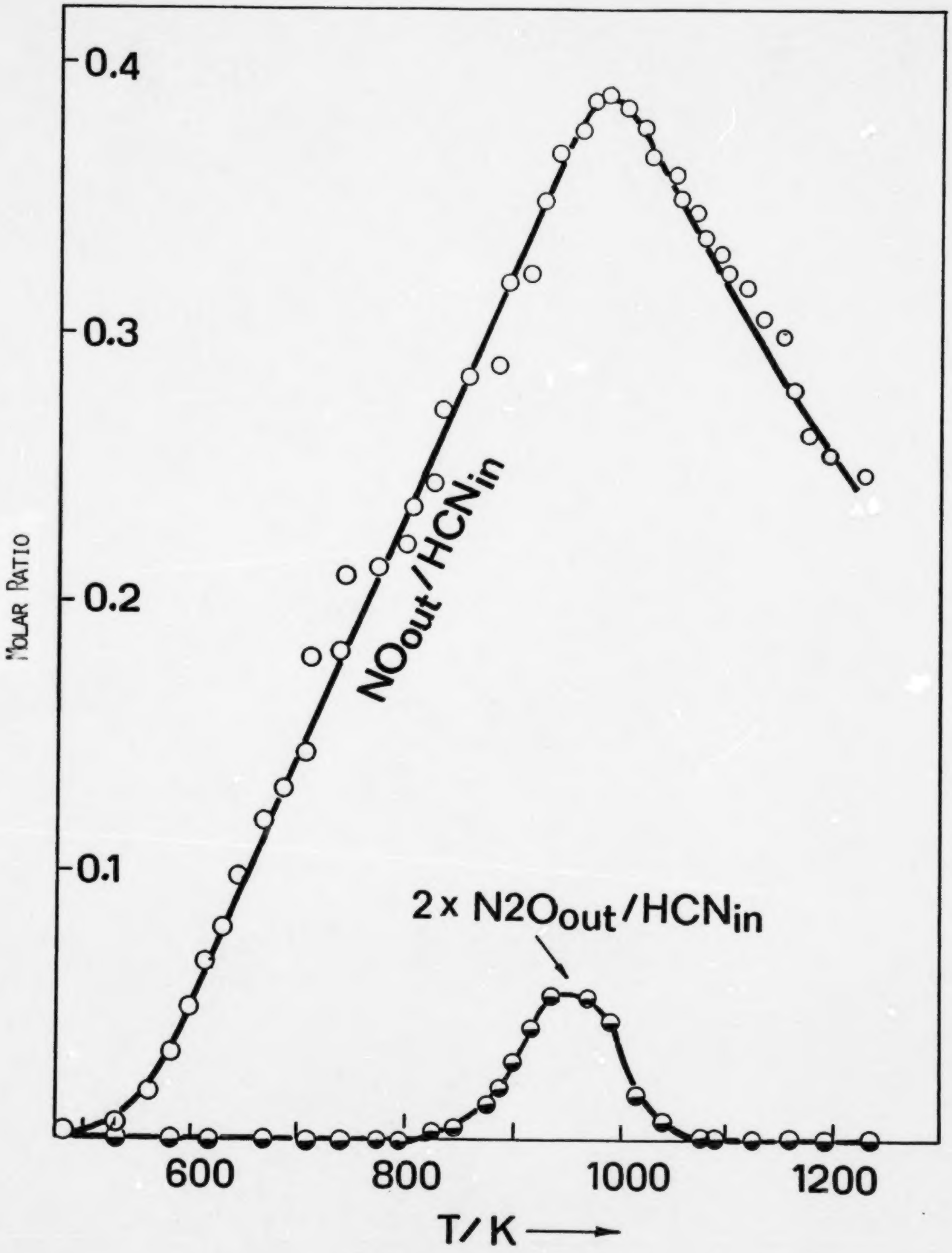

Figure 3-21. O_2 + HCN on graphite. (de Soete)

OXIDATION OF (-C) and (-H)	NITROGEN SPECIES INVOLVING REACTIONS	
CARBON REACTIONS : $O2 + 2(-C) \xrightarrow{1} 2(-CO)$ $(-CO) \xrightarrow{2} CO$ + free site $2(-CO) \xrightarrow{3} CO2 + (-C)$ + free site $CO + (-CO) \xrightarrow{4} CO2 + (-C)$ $CO2 + (-C) \xrightarrow{5} CO + (-CO)$ **HYDROGEN REACTIONS :** $2(-CH) \xrightarrow{31} H2 + 2(-C)$ $H2 + (-CO) \xrightarrow{32} H2O + (-C)$ $H2O + (-C) \xrightarrow{33} H2 + (-CO)$	**FORMATION OF NO :** $O2 + (-C) + (-CN) \xrightarrow{19} (-CO) + (-CNO)$ $(-CNO) \xrightarrow{20} NO + (-C)$ $(-CN) + (-CO) \xrightarrow{21} NO + 2(-C)$ FORMATION OF N2O : $2(-CNO) \xrightarrow{22} (-CO) + (-C) + N2O$ $NO + (-CN) \xrightarrow{23} N2O + (-C)$ $(-CNO) + (-CN) \xrightarrow{24} N2O + 2(-C)$ **HETEROGENEOUS REDUCTION OF NO AND N20** $NO + 2(-C) \xrightarrow{6} (-CO) + (-C.N)$ $2(-C.N) \xrightarrow{8} N2 + 2(-C)$ $NO + (-C.N) \xrightarrow{9} N2O + (-C)$ $N2O + (-C) \xrightarrow{16} N2 + (-CO)$ $N2O + (-CO) \xrightarrow{17} N2 + CO2$ $N2O + (-CO) \xrightarrow{18} 2NO + (-C)$ $NO + (-C) + (-CH) \longrightarrow (-CO) + (-CHN)$	**FORMATION/DESTRUCTION OF HCN :** $(-CH) + (-CN) \xrightarrow{25} HCN + (-C)$ $H2 + (-C) + (-CN) \xrightarrow{26} (-CH) + (-CHN)$ $(-CHN) \xrightarrow{27} HCN$ + free site $HCN + (-CN) \xrightarrow{28} N2 + (-CH)$ $(HCN \longrightarrow NO + \ldots?)$ **FORMATION/DESTRUCTION OF NH3 :** $H2 + (-CHN) \xrightarrow{29} NH3 + (-C)$ $NH3 + (-CO) + (-CN) \xrightarrow{30} N2 + H2O + (CH) + (-C)$ $(NH3 \longrightarrow HCN \ldots\ldots?)$ $(NH3 \longrightarrow NO \ldots\ldots?)$

Figure 3-22. Formation of N_2O from bound nitrogen during heterogeneous char oxidation. (de Soete)

N2O FORMATION from BOUND NITROGEN during CHAR combustion

(main reaction paths)

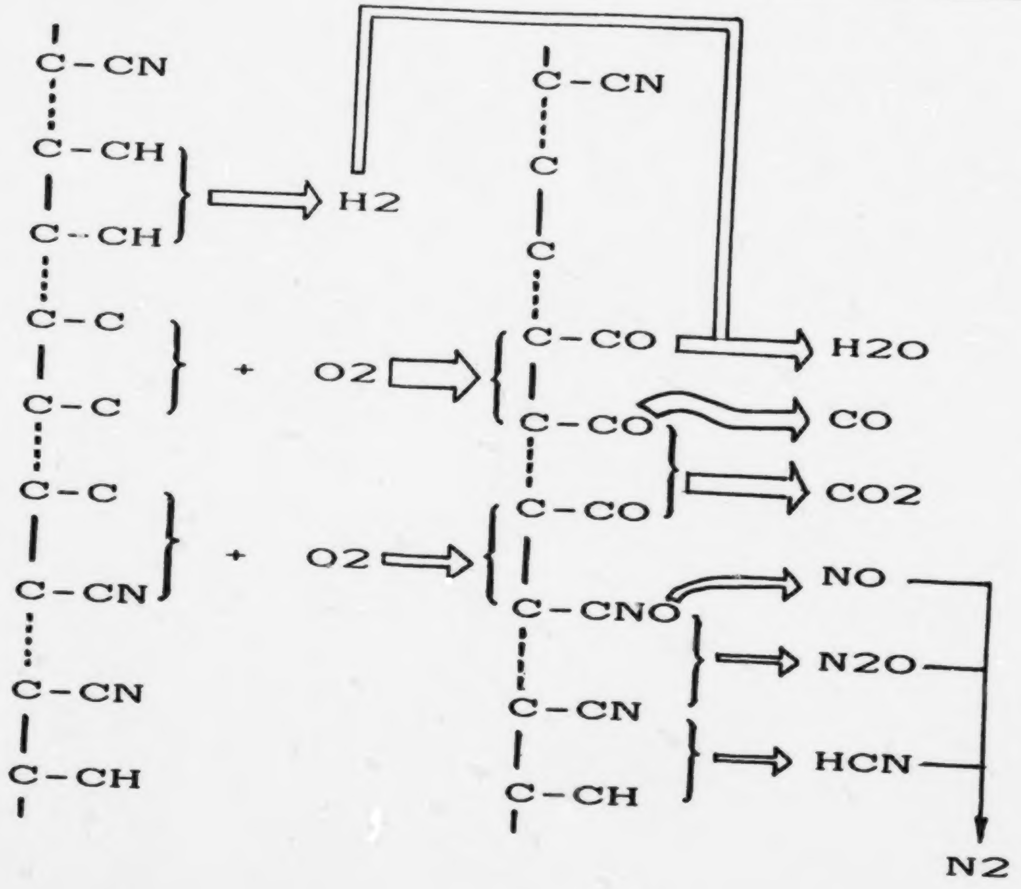
C-CN
C-CH
C-CH
H2
C-C
C-C
+
O2
C-C
C-CN
+
O2
C-CN
C-CH
C-CN
C
C
C-CO
C-CO
C-CO
C-CNO
C-CN
C-CH
H2O
CO
CO2
NO
N2O
HCN
N2

Figure 3-23. Main reaction paths of N_2O formation during char combustion. (de Soete)

Dr. S. Lanier commented that all of the reactions Dr. de Soete had studied were with O_2. He asked if any water (H_2O) were included in the stream, because a substantial amount of water is in the gases that are reacting heterogeneously with the char. Dr. de Soete responded no.

Dr. J. Kramlich asked for Dr. de Soete's speculation on how much this reaction could contribute to a coal flame situation. Dr. de Soete replied that he could not provide any quantitative speculation.

3.2 OVERALL CHEMICAL INFORMATION FROM LABORATORY COMBUSTOR EXPERIMENTS

Dr. J. Wendt of the University of Arizona was the discussion moderator of the session in which data on laboratory-scale coal combustion and integrated measurements were presented. Laboratory-scale coal combustors are larger than bench-scale facilities and have a firing capacity of 20 kW to 4 MW. The speakers in this session discussed studies involving integrated measurements taken under practical conditions where both homogeneous and heterogeneous reactions occurred. Data were collected from two types of combustors: premixed combustors, which are one-dimensional, plug-flow reactors, and turbulent diffusion-flame combustors. Dr. Wendt reminded the audience that this session would be very informal, that preliminary results would be offered, and that comments and questions were encouraged.

Dr. Wendt presented the results of DOE-funded research at the University of Arizona. The work focused on optimizing reburning configurations for NO_x control. A secondary focus of the work was on N_2O measurements. However, Dr. Wendt explained that the research was still in progress and the results were therefore preliminary.

The experimental research at the University of Arizona is being conducted on a premixed, down-fired combustor at a firing rate of 27 kW to study NO and N_2O emissions from the combustion of Beulah lignite and Utah #2 bituminous coals. N_2O was measured using an on-line GC/ECD technique where the sample gas from the combustor passed through a water quench sampling probe and a refrigeration condenser for water removal prior to analysis. Nitrous oxide levels for both coals were found to be insignificant at less than 2 ppm for stoichiometric ratios (SR) ranging from fuel rich to fuel lean. Measurements of NO and N_2O as a function of residence time at fixed fuel lean SRs, with combustion gas temperatures in the range 850-1,290 K for Beulah coal and 1,050-1,525 K for Utah coal, showed

N_2O concentrations to be less than 5 ppm and the N_2O/NO concentration ratio to be very small. Figure 3-24 illustrates that there is little N_2O formation under reburn conditions using natural gas as the secondary fuel.

Dr. Hasenack pointed out that the temperature range in the post flame region appeared to be similar to that allowing N_2O to be formed from HCN. Dr. Wendt replied that, although HCN was not measured in the tests reported here, other tests showed high levels of HCN in the rich post flame region but low levels under fuel lean conditions.

Following Dr. Wendt's presentation, Dr. W. Linak, from the Combustion Research Branch (CRB) of EPA, outlined the results of his experiments with laboratory-scale pulverized coal combustion. His work has focused on characterizing the effect of different coal types, flame shapes, and NO_x levels on N_2O emissions.

Dr. Linak presented N_2O emission data collected from a down-fired, 60,000 Btu/h laboratory-scale combustor equipped with a variable swirl burner. Samples were drawn from a post-combustion region under stack type conditions. The purpose of these experiments was to change NO emissions through changes in the overall turbulent diffusion flame type and thus to determine if a correlation between N_2O and NO emissions was valid. In an attempt to vary the NO_x concentration, burner swirl and flame shapes were altered by changing axial and radial air ratios and locations of the injector tube. A Utah bituminous coal and a Montana sub-bituminous coal were used in these experiments, the first having a higher organic content but lower moisture level than the latter. For each coal, data were collected at 3 (fuel lean) stoichiometric ratios and 2 different flame shapes—one axial and one radial. Gas samples were collected in stainless-steel containers after refrigeration drying and were analyzed for N_2O by GC/ECD. The widely scattered data, presented in Figures 3-25 and 3-26, show that N_2O emissions varied widely (10-250 ppm). There seems to be no correlation between N_2O emissions and NO_x emissions.

Earlier data (Figure 3-27), generated using on-line GC/ECD analyses and the same two coals, show very low N_2O levels <10 ppm. These data were considered suspect, however, because on-line analytical procedures had not been verified at the time the samples were measured.

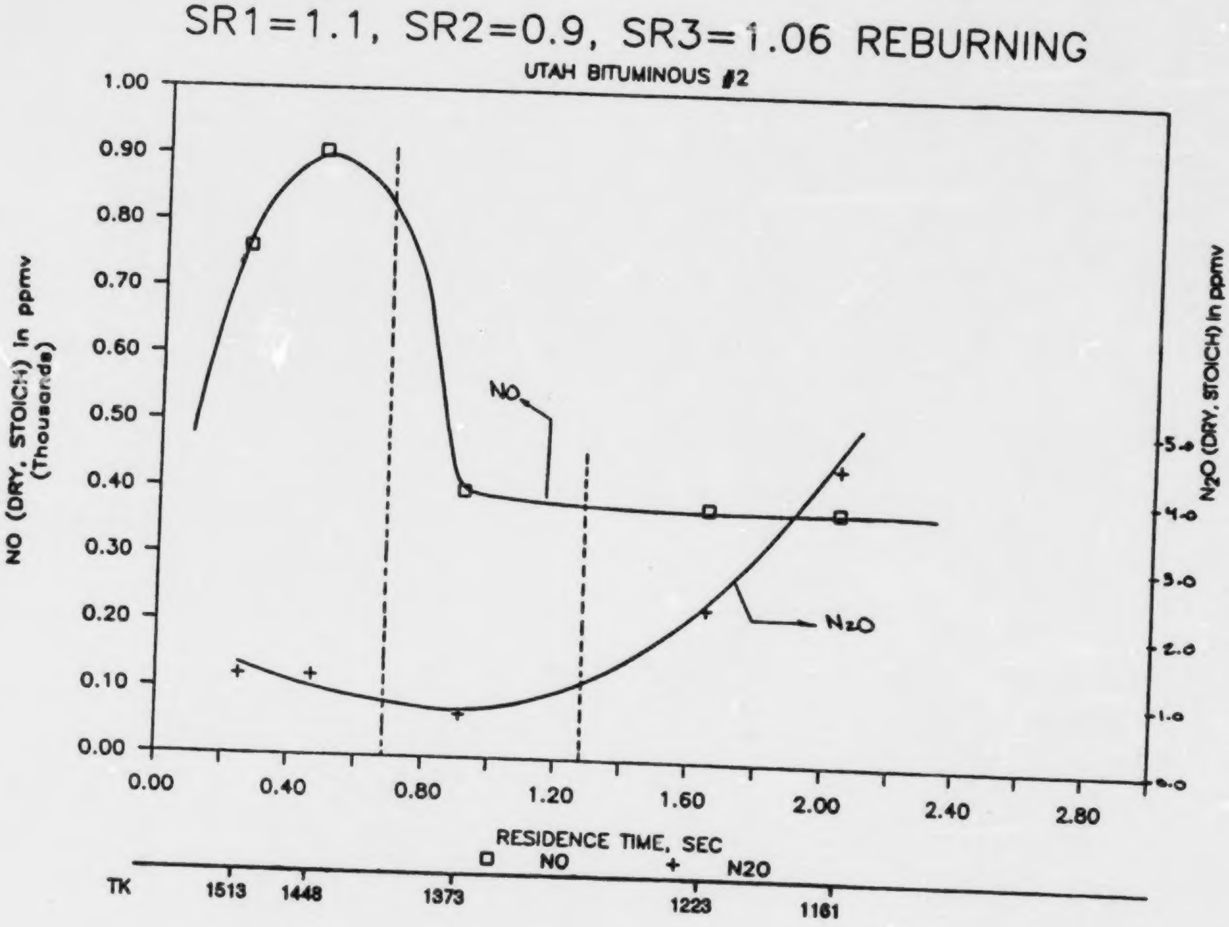

Figure 3-24. Reburn condition using natural gas. (Wendt)

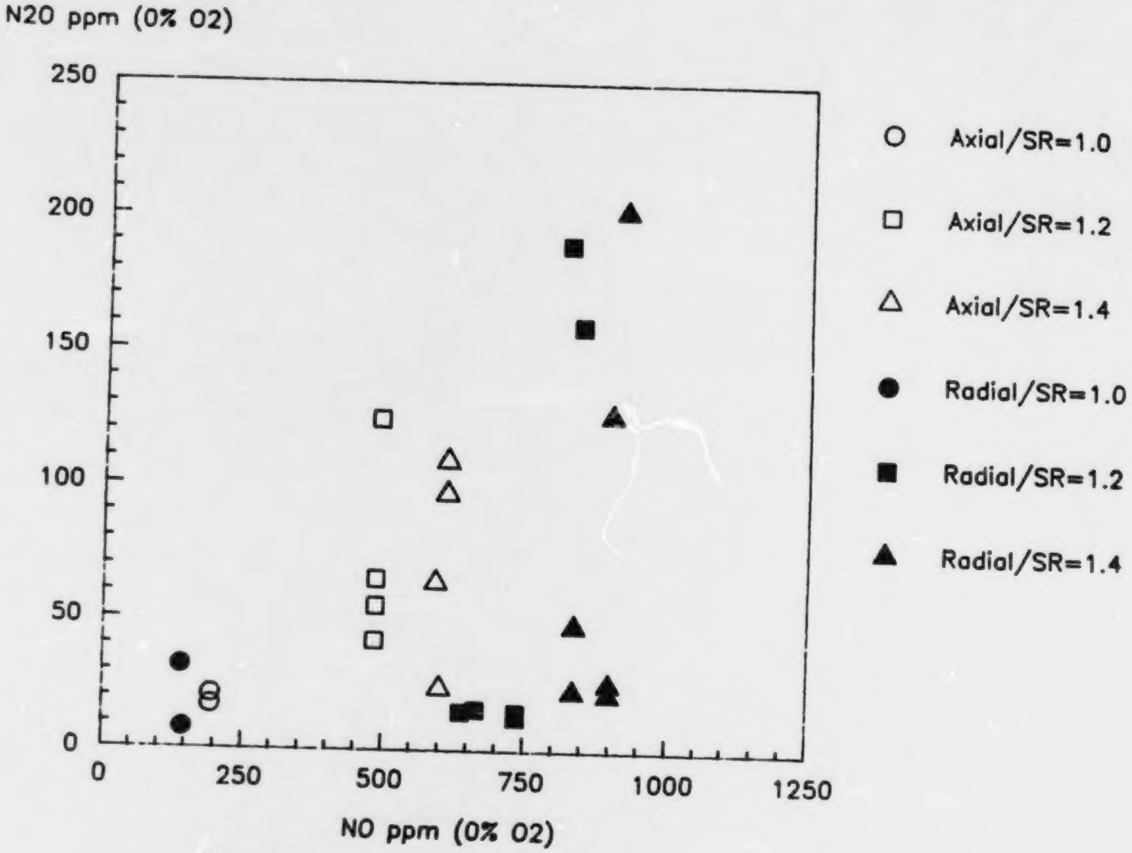

Figure 3-25. NO/N_2O for Utah bituminous (N_2O measured from sample containers). (Linak)

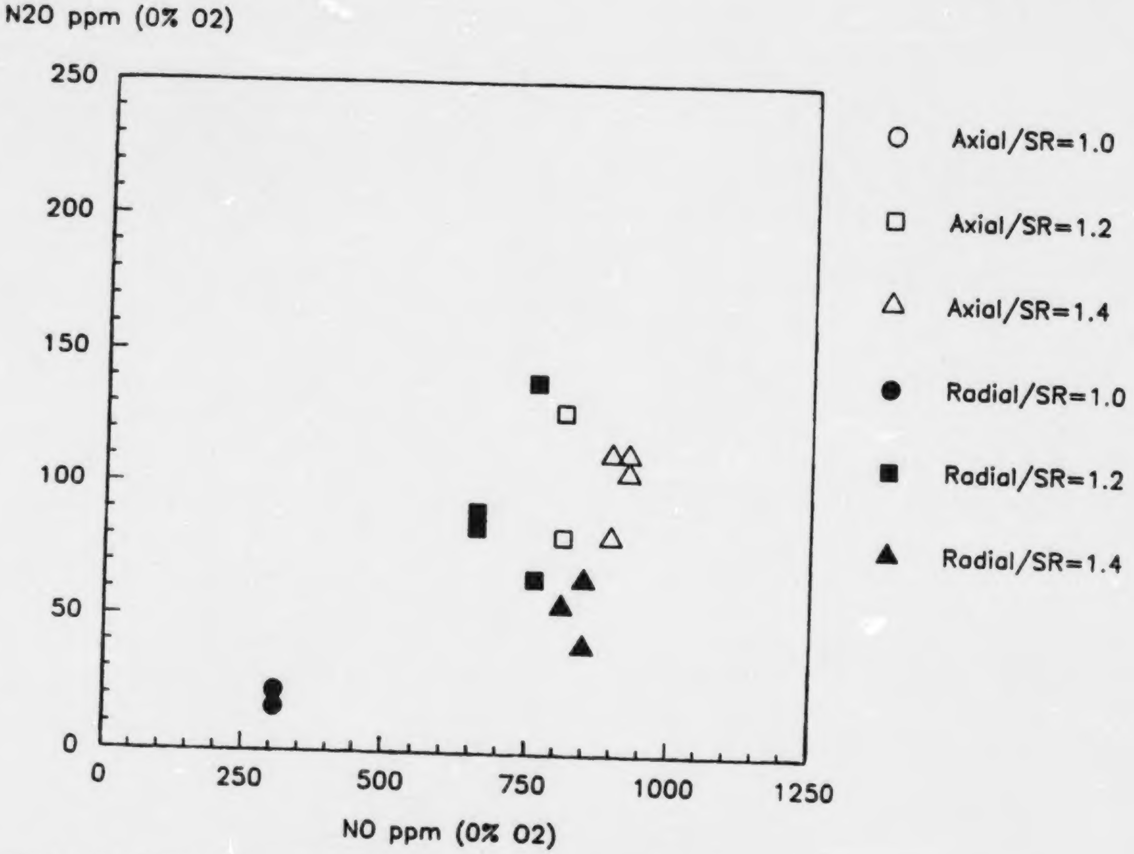

Figure 3-26. NO/N_2O for Montana sub-bituminous (N_2O measured from sample containers). (Linak)

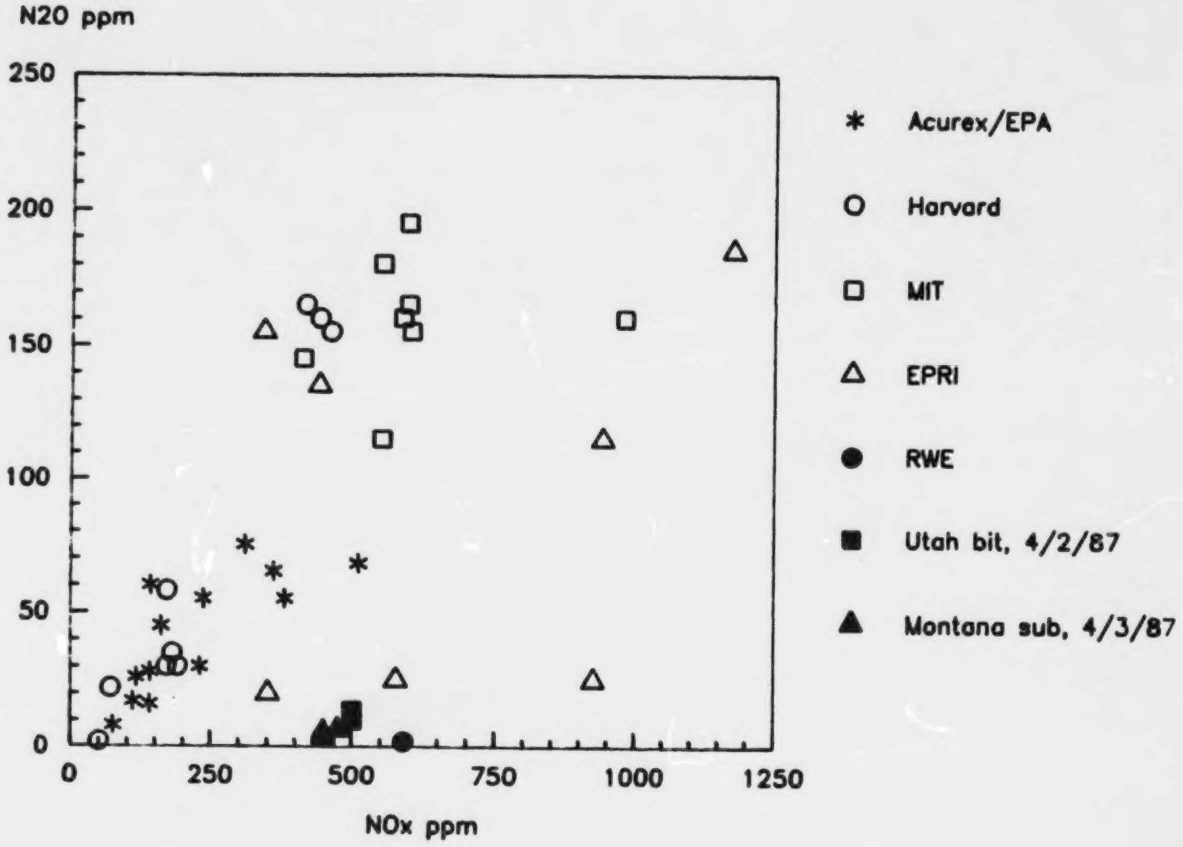

Figure 3-27. On-line data in relation to other reported data. (Linak)

Following Dr. Linak's presentation, Dr. J. Kramlich, of EERC, described his fluid bed model as a stirred reactor for bed particles releasing volatiles such as HCN, CO, and so forth, and as a plug-flow reactor for the gases moving up through the bed. Initial model results, depicted in Figure 3-28, show that NO concentration initially increased because of a leaner stoichiometry, reached a maximum of about 200 ppm, and then decreased in bed region with relatively less lean stoichiometries. The final stoichiometry was taken to be 1.25. The results also show that N_2O emissions at the end of a residence time of 0.5 s, corresponding to the beginning of freeboard part, were reasonably high (about 250 ppm).

The model predictions for variations in excess air, bed temperature, and fuel nitrogen speciation are shown in Figure 3-29. The stoichiometry in the bed was lean, so an increase in excess air did not have much effect on N_2O emissions, which are very sensitive to temperature in the range 1,000-1,200 K. NH_3 does not produce much N_2O; HCN produces reasonably high levels of N_2O; and a combination of NH_3 and HCN produces intermediate N_2O levels. All these parametric effects, explored by the model, agree with N_2O formation/destruction chemistry understood so far.

Model predictions were also made on N_2O emissions from coal and natural gas reburning. These results are shown in Figure 3-30. The first simulation was that of a gas-fired, NO-doped primary flame, which produced no N_2O. Utah bituminous coal was added downstream of the primary flame as the reburning fuel. The coal represented a minor contributor to the total reactor fuel rate (stoichiometric ratio of 0.9 and 0.8) but produced significant N_2O (45 and 85 ppm), possibly owing to HCN conversion to N_2O at relatively low post-flame temperatures according to homogeneous kinetics. The next model considered, the case of a coal primary flame with natural gas added downstream as the reburning fuel. Coal primary flame produced about 50 ppm N_2O. The addition of the natural gas, however, dropped N_2O levels almost to zero, probably because N_2O does not survive a fuel-rich zone very well. These results suggest that application of carefully picked gas reburning conditions may decrease both NO and N_2O emissions.

Dr. A. Williams of Leeds University followed Dr. Kramlich with a summary of his investigations. His experiments and measurements are shown in Table 3-1.

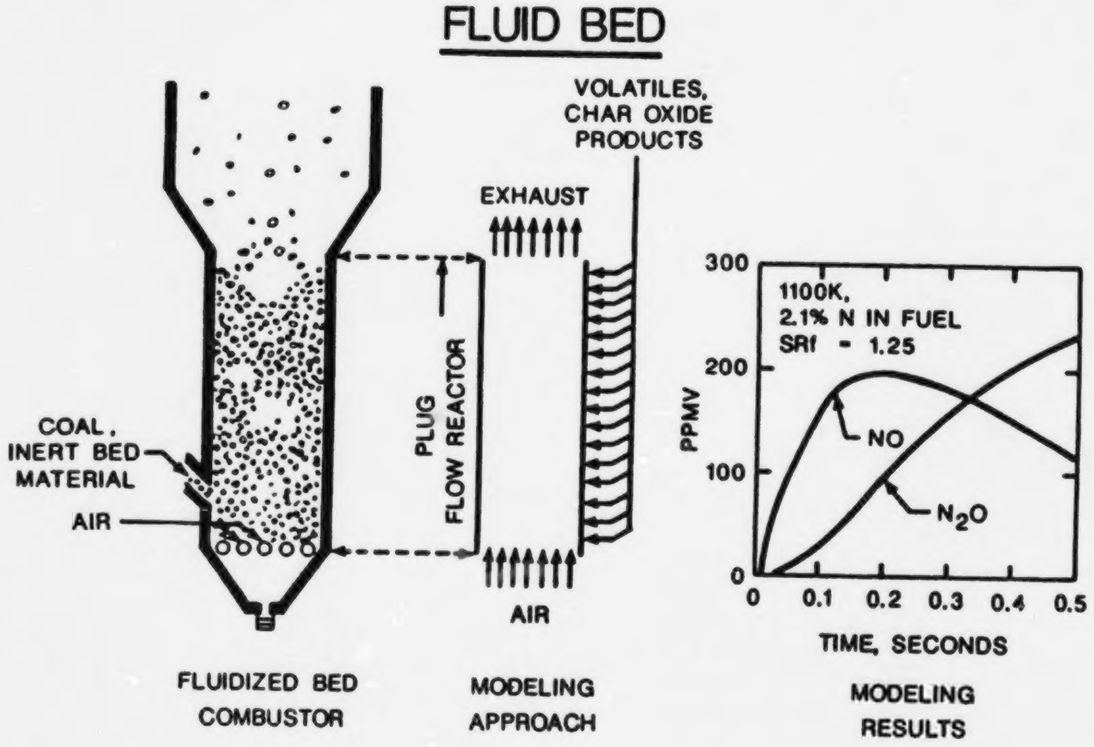
FLUID BED
VOLATILES, CHAR OXIDE PRODUCTS
EXHAUST
PLUG FLOW REACTOR
COAL, INERT BED MATERIAL
AIR
AIR
300
200
100
0
PPMV
1100K, 2.1% N IN FUEL SRf = 1.25
NO
N₂O
0
0.1
0.2
0.3
0.4
0.5
TIME, SECONDS
FLUIDIZED BED COMBUSTOR
MODELING APPROACH
MODELING RESULTS

Figure 3-28. Fluid bed modeling. (Kramlich)

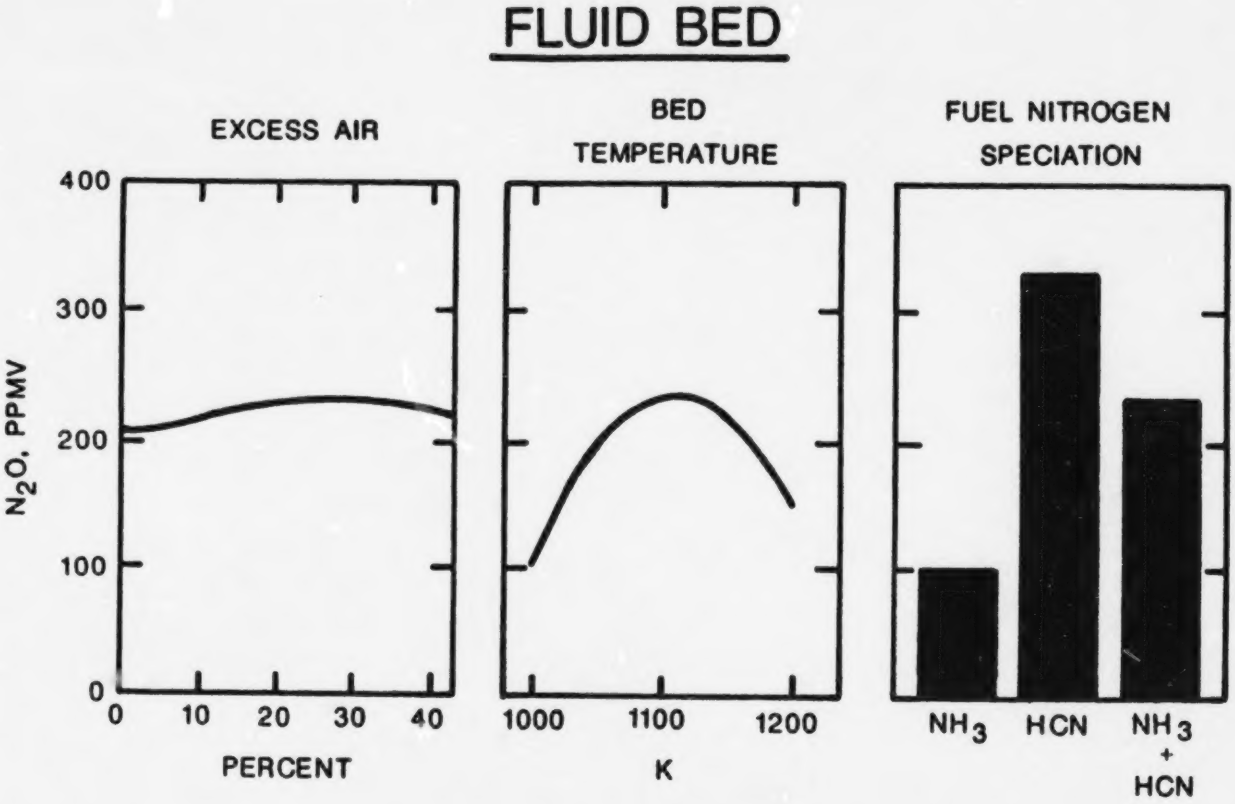

Figure 3-29. Predictions under varied conditions. (Kramlich)

REBURNING

COAL REBURNING

- GAS PRIMARY
- ALL N_2O FORMED FROM REBURNING FUEL
- COAL REBURNING FORMS SIGNIFICANT N_2O

GAS REBURNING

- COAL PRIMARY
- GAS NEARLY ELIMINATES PRIMARY N_2O

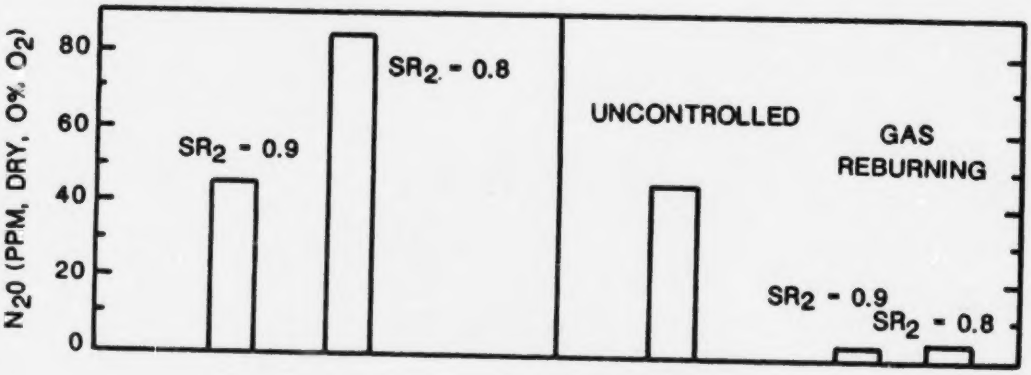

Figure 3-30. Reburning predictions. (Kramlich)

TABLE 3-1. EXPERIMENTAL MEASUREMENTS (WILLIAMS)

Combustor Type		N_2O ppm	CO_2 %	NO_x ppm	Fuel-N% in the Coal	$\frac{N_2O}{NO_x}$
A Fluidized Bed Combustion (Bed Temperature 900 °C)	Run (1)	35	7.9	450	1.2	0.078
	Run (2)	55	10.5	500	1.2	0.110
B Drop Tube Furnace (Methane Flame Supported, 1,110 °C)	Run (1)	70	10.8	450 to 500	1.3	
	Run (2)	55	7.7		1.6	
C Grate (Bed) Combustion		100	4	450	1.6	0.222
D Char Combustion (ca 1,500 °C)		200	10			0.40
E Coal Devolatilization inert		very small				

His measurements reveal that N_2O is about 10-20 percent of the total NO_x for fluidized bed and drop-tube combustion, with grate combustion producing higher levels than systems with sustained high temperature in the post-flame region.

He suggested the mechanism of N_2O formation as outlined in Figure 3-31 where coal pyrolizes to give tar + gases + char, all of which can produce N_2O.

Dr. Williams' kinetic calculations reveal that the N_2O contribution from the interaction of NH_3 + NO was only about 5 ppm. N_2O yield from tar combustion was about 10 percent of the NO produced, and N_2O yield from char combustion was also about 10 percent of the NO produced. These results suggest that at each stage of combustion, either single or staged, the N_2O is about 10 percent (or possibly higher) of the NO (+NO_2) produced, and production of N_2O is a strong function of temperature.

Dr. Williams noted that the following reaction is crucial in N_2O formation and that the NCO species can only come from HCN:

$$NCO + NO \rightarrow N_2O + CO$$

Dr. de Soete pointed out that in Dr. Williams' experiments N_2O was produced by gaseous NCO, and they did not take into account heterogeneous formation. Dr. Williams replied that this was not considered because he could not quantify any HCN on the char. Dr. de Soete stated that he had indeed found HCN in char, supporting heterogeneous formation of N_2O.

Dr. Lanier asked where the H atom comes from in the experiments with char, since the dominant N_2O destruction step involves a reaction with a H atom. Dr. Williams answered that since he was interested only in N_2O formation routes and thus high N_2O values, no hydrogen was made available for N_2O destruction.

Dr. J. Smart from the International Flame Research Foundation (IFRF) presented data on his experiments performed on a 4 MW horizontal, swirled pulverized coal fired furnace. These experiments have so far yielded only preliminary measurements. They were conducted on a burner operated with no pollution abatement and therefore yielded high NO_x emissions. The fuel was a western-Canadian

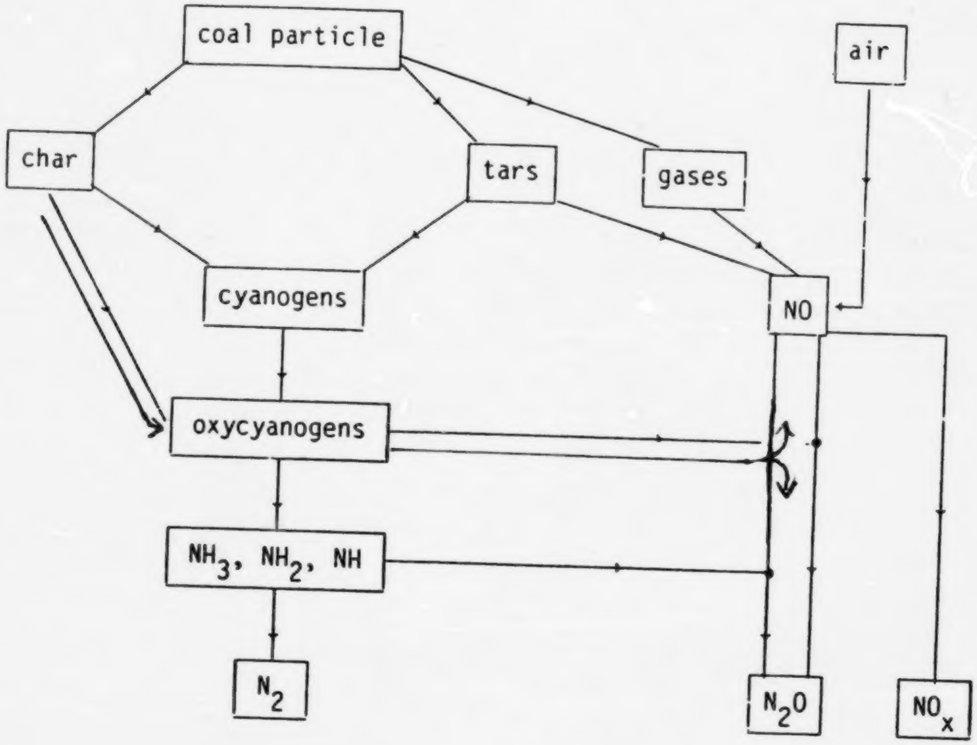
coal particle
air
char
tars
gases
cyanogens
NO
oxycyanogens
NH_3, NH_2, NH
N_2
N_2O
NO_x

Figure 3-31. NO_x and N_2O formation from coal. (Williams) bituminous coal, pulverized to a standard grind for the experiment. The species of NO, N_2O, HCN, and NH_3 were measured in the flame in 2 dimensions (axial and radial), as shown in Figure 3-32.

The preliminary results indicated that HCN and NH_3 found in the flame at the 0.1 m axial location were essentially gone by the 0.2 m location. Nitrous oxide values were low at the 0.1 m location, although at 0.2 m near peak values were achieved. N_2O and NOx levels in furnace exhaust (at about 1,070 °C) were 43 ppm and 720 ppm (at 3.6 percent O_2). The data suggest N_2O formation from fuel-bound N, but further work is needed to characterize this hypothesis.

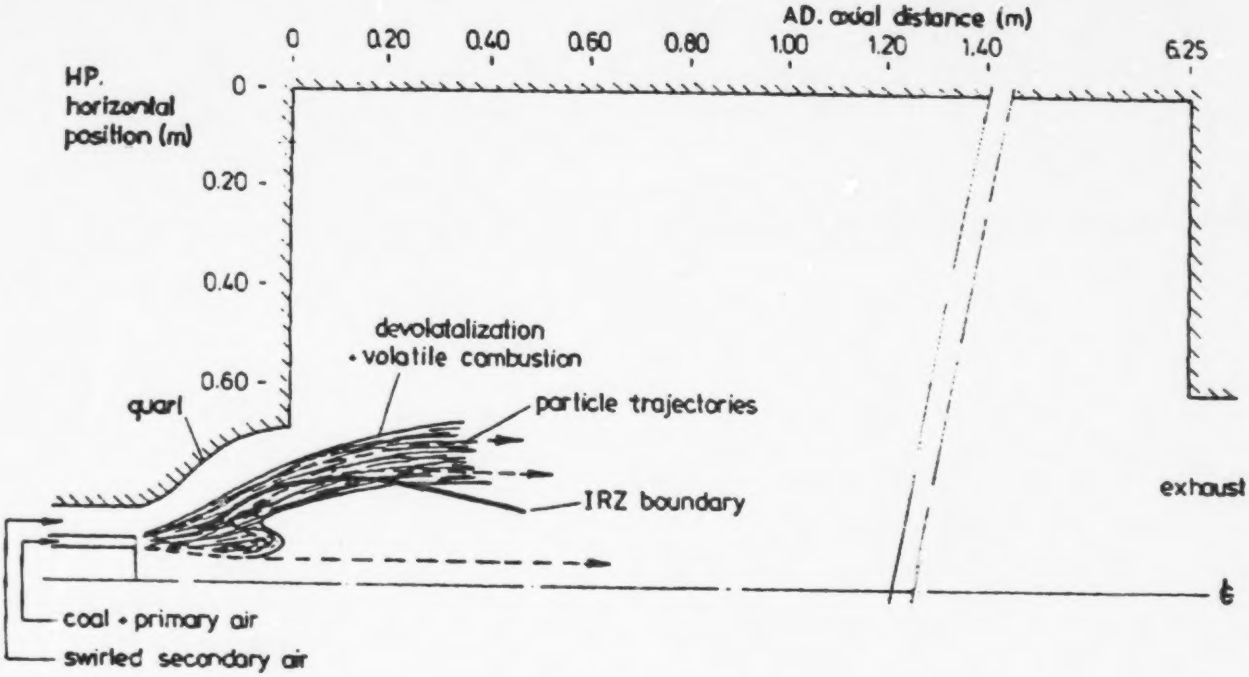
AD. axial distance (m)
0
0.20
0.40
0.60
0.80
1.00
1.20
1.40
6.25
HP. horizontal position (m)
0
0.20
0.40
0.60
devolatalization
+ volatile combustion
particle trajectories
quarl
IRZ boundary
exhaust
coal + primary air
swirled secondary air
℄

Figure 3-32. Schematic of experimental flame measurements. (Smart)

SECTION 4

SESSION 2: N_2O MEASUREMENT TECHNIQUES

Mr. J. McSorley of EPA, the discussion moderator for the second session, began by addressing the need to develop standardized sampling techniques. Given the measured increase in atmospheric N_2O levels, it can be concluded that a significant anthropogenic source exists. The relative importance of candidate sources such as agriculture, biomass burning, fossil fuel combustion, and others is unclear at this time. Therefore, a reliable, accurate method for identifying and analyzing these sources is crucial.

Mr. McSorley presented the following EPA program issues:

1. What is the global contribution of N_2O from fossil-fuel combustion versus biogenic and natural N_2O source emissions to stratospheric O_3 depletion? Furthermore, are current N_2O global emission inventories reliable with respect to N_2O combustion sources?
2. Should N_2O emissions be controlled, and if so, will the controls make a difference in stratospheric O_3 depletion?

The related technical issues are stated below:

1. What is the relative importance of N_2O emissions from fossil-fuel combustion sources (i.e., stationary combustion sources versus mobile combustion sources)?
2. What is the relative importance of N_2O emissions from natural and biogenetic sources (i.e., agriculture, biomass burning, oceans, and other sources)?

Mr. McSorley identified a crucial need for a standardized N_2O sampling and analytical protocol to verify the reliability of N_2O data gathered worldwide. A wide variance in sampling methodology is evident. Grab samples have been collected in many types of containers, including glass, stainless-steel canisters, and Tedlar bags. Sample moisture content also varies to a great degree. Furthermore, the development of an on-line real time N_2O analyzer would eliminate long analytical delays in research programs as well as the problems associated with grab sampling.

Limited methods of N_2O measurement are available. Quantification is usually done by gas chromatography using an electron capture detector (GC/ECD). The ECD has excellent detection limits, being used to measure ppb ambient N_2O levels. However, the ECD is also susceptible to many interferants found in combustion gases. The thermal conductivity detector (TCD) has also been used successfully, although detection levels are not as great as those of the ECD. A disadvantage of the GC analysis is that a true real time measurement is not possible and that a high skill level is required to perform the analysis.

4.1 OPERATING PROCEDURE FOR IN-HOUSE RESEARCH

Mr. J. Ryan of Acurex Corporation, responsible for EPA in-house analytical efforts, presented information on the development of a recommended operating procedure used for in-house combustion research. The method was derived from several different procedures designed for N_2O GC/ECD analysis. During procedure development, Mr. Ryan evaluated possible interferences contained in combustion gas samples and how they could be treated. The result was a technique for the removal of interfering H_2O and organic interferants contained in N2O samples using a P2O5/activated charcoal pre-column. The possibility of any CO2 interference was investigated by comparing N2O values when the CO2 constituent was eluted both before and after N2O using different columns. No significant difference in N2O value was observed. The possibility of detector desensitizing from oxygen exposure was not evident after repetitive introduction over a 7-h period of a standard gas mixture containing oxygen. The nonlinear property of the detector was described, demonstrating the need for a multi-point calibration in establishing accurate quantifiable limits because of the large variance in response factors.

4.2 WATER SORBENTS USED IN N_2O MEASUREMENT

Dr. de Soete then gave a brief presentation on the importance of carefully choosing H2O sorbents used in N2O sampling techniques. Many desiccants are commercially available, such as magnesium perchlorate [Mg(ClO4)2], calcium chloride (CaCl2), aquasorb (P2O5 with indicator) and silica gel (SiO2). Silica gel, however, may retain N2O (Figure 4-1); flushing with argon may release N2O, possibly affecting sample integrity.

(t = 5 minutes)

ABSORBENT	VVH(h^{-1})	N_2O_{out}/N_2O_{in}
$CaCl_2$	160	1
$M_g(ClO_4)_2$	511	1
H_2O	(341)	1
Silicagel	160	0.064

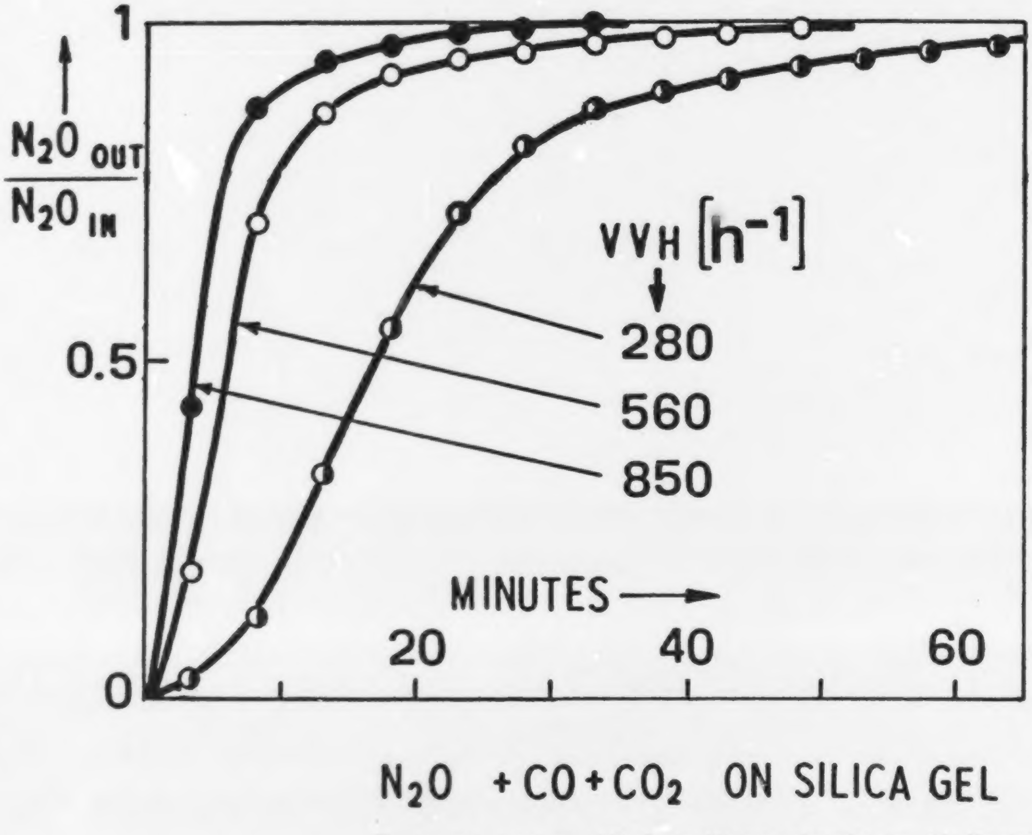

Figure 4-1. Losses of N_2O on different absorbents. (de Soete)

4.3 INTERFERENCES FROM SULFUR DIOXIDE

Dr. L. Muzio of Fossil Energy Research Corporation (FER Co.) and Dr. J. Kramlich of Energy and Environmental Research Corporation (EERC) presented startling results obtained during a collaborative study of interferences from SO_2 with respect to N_2O, in sample containers under certain conditions. While conducting natural gas tests using FER Co's combustor, high N_2O values were measured while doping with ammonia (to generate NO_x) and SO_2. N_2O samples were collected in glass flasks using an extraction system where moisture removal was not utilized prior to collection (see Figure 4-2). It was discovered that while doping with 2,500 ppm SO_2, N_2O concentrations on the order of 300 ppm were obtained, while the condition without SO_2 doping measured only about 1 ppm N_2O.

Dr. Muzio then contacted Dr. Kramlich who repeated the tests at EERC, obtaining the same results (see Figure 4-3). Similar tests were performed with a hydrogen flame in order to eliminate N_2O formation mechanisms associated with carbon chemistry. Again, similar results were observed when NO_x and SO_2 levels were duplicated. The SO_2 injection location was then varied with no significant change in results.

At this time, Drs. Muzio and Kramlich began to suspect that a reaction in the sampling system was the source of the N_2O artifact. After changing probe types, NO levels were observed while SO_2 was pulsed, under the premise that the NO was converted to N_2O by the SO_2. However, after NO levels were found to be constant, concentration was directed towards the possibility of the artifact reaction occurring in the sample container, and an attempt was made to generate N_2O in the sample flask. A synthetic mixture containing N_2, O_2, CO_2, and NO was placed in flasks, one containing deionized H_2O and no SO_2, and the other containing 1,500 ppm SO_2 and dilute sulfuric acid. Over 150 ppm N_2O was generated from the SO_2/sulfuric acid containing mixture, while virtually no N_2O was observed in the mixture lacking these two components (see Figure 4-4). Next, maintaining the same SO_2 containing mixture conditions, the pH of the liquid in the sample flasks was varied. No significant difference in N_2O generation was observed. The test was performed again without the SO_2 constituent. This time no N_2O generation was observed, isolating the importance of SO_2 in the artifact mechanism. The effects of varied SO_2 levels were then evaluated. A step change in N_2O was observed when SO_2 exceeded

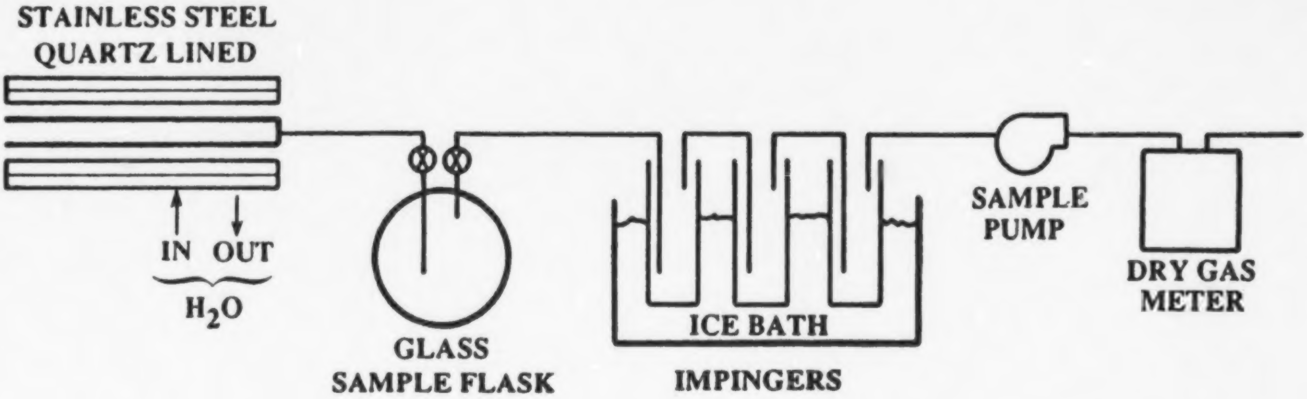
STAINLESS STEEL
QUARTZ LINED
IN
OUT
H_2O
GLASS
SAMPLE FLASK
ICE BATH
IMPINGERS
SAMPLE
PUMP
DRY GAS
METER

Figure 4-2. N_2O sampling system. (Muzio, Kramlich)

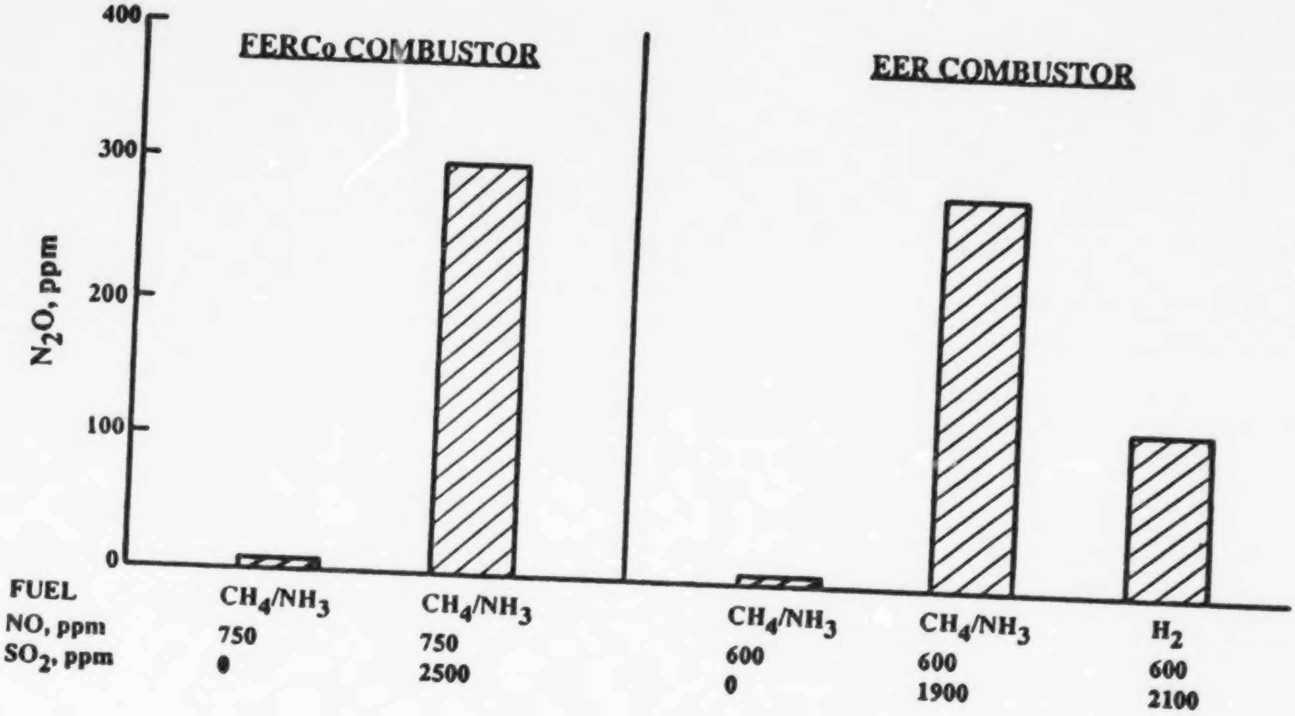

Figure 4-3. Effect of SO_2 on N_2O. (Muzio, Kramlich)

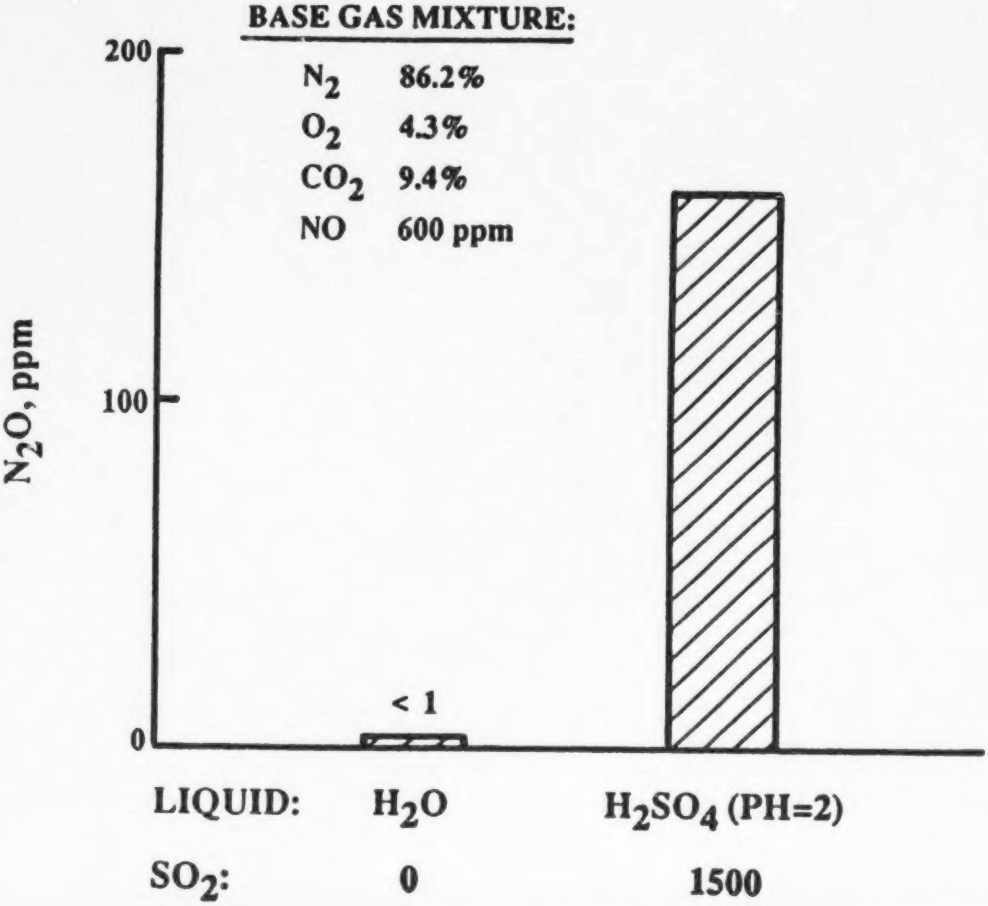

Figure 4-4 Synthetic gas mixtures in glass sample flask. (Muzio, Kramlich)

500 ppm, and it seemed to level off at over 1,500 ppm (see Figure 4-5). The effect of NO level variance was also observed in relation to N_2O generation while holding SO_2 levels constant. A ratio of N_2O to NO_x was obtained for the 2 varied NO concentrations (see Figure 4-6). The ratios are comparable to emissions reported from utility boilers. Figure 4-7 shows hypothetical chemistry obtained by a scrubber literature search that may be responsible for the N_2O artifact [9]. The reaction rates shown are consistent with the observations made to this point.

Tests were designed to determine if the removal of SO_2 or moisture could enable a sample of uncompromised integrity to be collected. The sampling system was again evaluated to determine how the components could be removed from the sample mixture. Sodium hydroxide (NaOH) and sodium carbonate (Na_2CO_3) were found to be effective in neutralizing SO_2 while having no evident effect on known N_2O levels when added to the sample container prior to collection. The conditioning of the sample prior to collection was also evaluated. Passing the sample gas through an ice-bath condenser reduced the NO/SO_2 interaction considerably, although some N_2O generation was observed. Passing the sample gas through an impinger containing a NaOH solution was successful in preventing N2O generation, but also removed CO2, another important component, from the mixture as well.

In closing, Dr. Muzio stressed the impetus of the artifact discovery in regard to current emission data bases and to the contribution from fossil-fuel combustion to the global N_2O budget. Furthermore, since this artifact reaction is evident in sample containers, is it possible for it to happen in the atmosphere as well?

4.4 CONTINUOUS INFRARED ANALYZER FOR ON-LINE N_2O MEASUREMENT

Dr. Muzio also reported on the status of research that he has been conducting with Ms. T. Montgomery of the University of California, Irvine, involving the development of an on-line N_2O analyzer. Ms. Montgomery and Dr. Muzio presented information on their investigations at the previous N_2O workshop in Boulder, Colorado [10]. The objective of the project, funded by the Electric Power Research Institute (EPRI), was to develop a continuous infrared analyzer for on-line N_2O monitoring of combustion gases. A prototype production model is being manufactured based on the results of Dr. Muzio's and Ms. Montgomery's research. The instrument operating principles are based on the ability

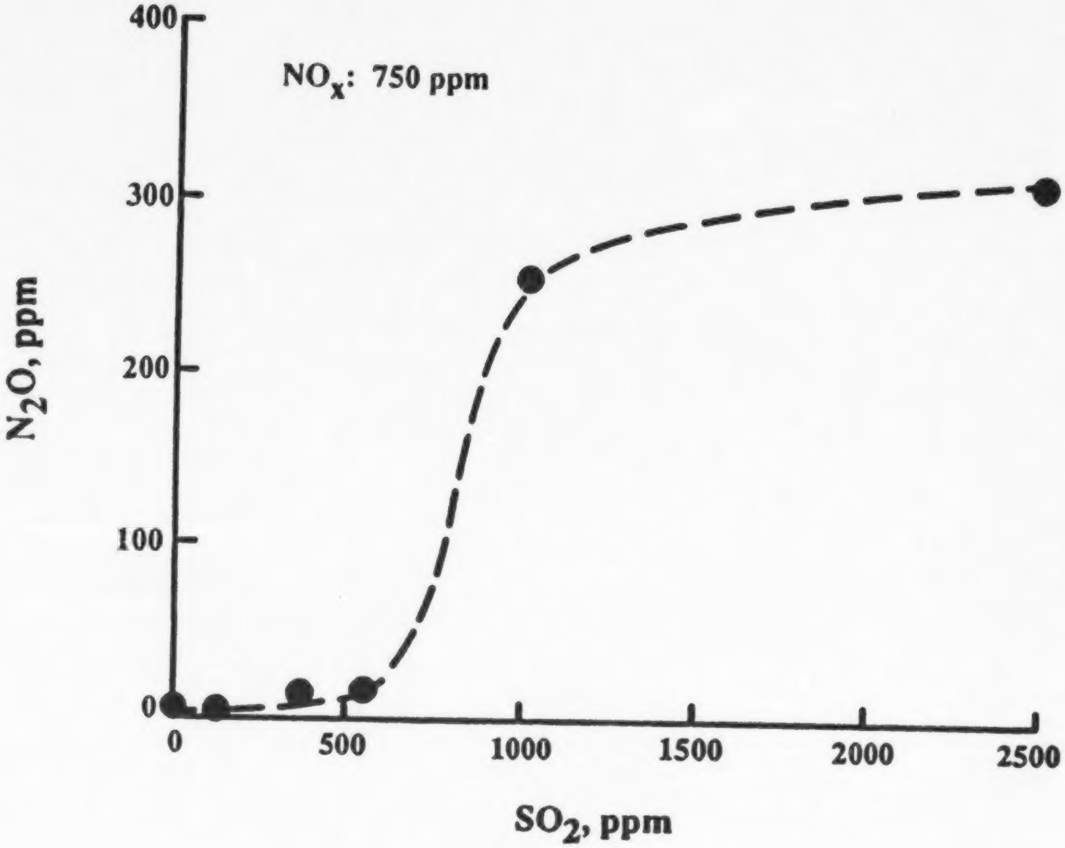

Figure 4-5. Effect of SO_2 level on N_2O. (Muzio, Kramlich)

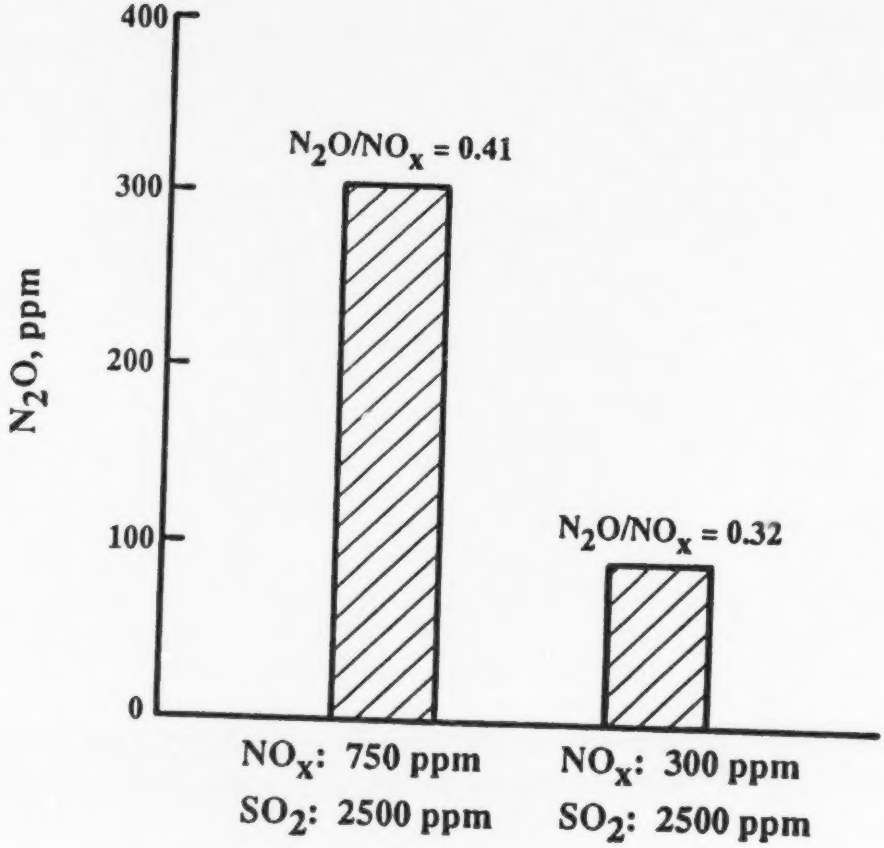

Figure 4-6. Effect of NO_x level on N_2O formation. (Muzio, Kramlich)

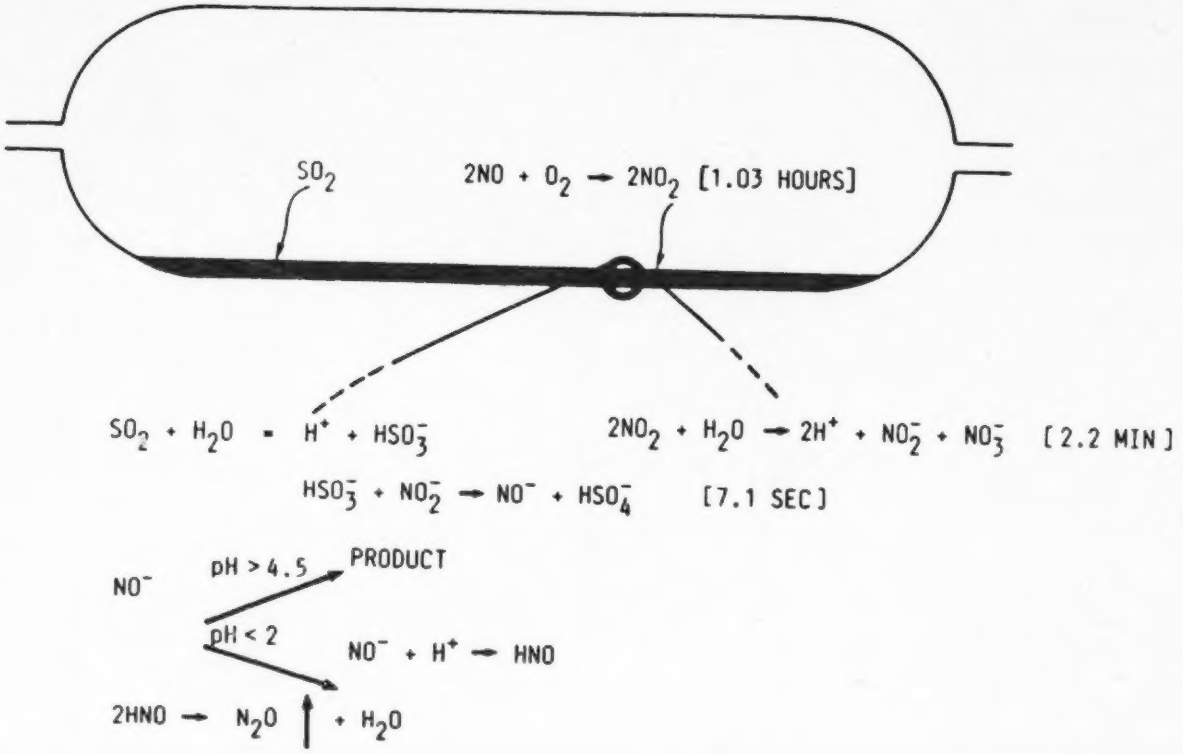
SO_2
$2NO + O_2 \rightarrow 2NO_2$ [1.03 HOURS]
$SO_2 + H_2O = H^+ + HSO_3^-$
$2NO_2 + H_2O \rightarrow 2H^+ + NO_2^- + NO_3^-$ [2.2 MIN]
$HSO_3^- + NO_2^- \rightarrow NO^- + HSO_4^-$ [7.1 SEC]
NO^-
pH > 4.5
PRODUCT
pH < 2
$NO^- + H^+ \rightarrow HNO$
$2HNO \rightarrow N_2O \uparrow + H_2O$

Figure 4-7. Hypothetical chemistry. (Muzio, Kramlich)

of N_2O to absorb infrared radiation at several wavelengths. The work focused on the 7.8 μm absorption band because of the ability to eliminate the interference of other gases present in the sample also absorbing radiation at this wavelength. The interfering gases, NO_2 and SO_2, can be easily removed by using a sodium carbonate/sodium sulfite scrubbing solution prior to introducing the gases into the analyzer. In the past year, the precision of the instrument has been improved to 5 percent without sample conditioning and to 2 percent when removing the interfering gases. The production instrument will be available for field evaluation soon.

4.5 OPTICAL INTERFEROMETRY

Mr. A. Galias of CNS presented information on the development of optical interferometric methods for measuring gases of environmental concern. The methods used involve both ultra violet (UV) and near infrared radiation absorption properties. Optical interferometry offers several advantages over conventional IR analyzers in that the Fourier transforms of the interferograms contain information on all of the wavelengths present and are not limited to 1 wavelength of detection. Therefore, more than 1 gas can be measured simultaneously. In addition, the precision in wavelengths measured is also greater, which is important in regard to isolating interferences of other gases absorbing radiation in the same wavelength region. Mr. Galais has been successful in measuring NO, NO2, and SO2 simultaneously with detection levels approaching 1 ppm. Currently, methods for measuring ammonia (NH3) and N2O are under development.

SECTION 5

SESSION 3: FULL-SCALE FIELD DATA

The third session of the workshop included a series of presentations on data collected from both mobile and stationary sources. The session included data from full-scale stationary utility facilities in the United States and Europe. The presentations provided N_2O emission values measured from different research facilities as well as industrial equipment to provide a better representation of N_2O discharge levels and to assess the role of fossil-fuel combustion on global N_2O levels. Dr. K. Hein, from RWE, was the session moderator, assisted by Dr. W. Linak of EPA during the stationary-source presentations and by Mr. A. Douaud of the IFP during the mobile-source presentations. Because of the sampling artifact discussed in the previous session, each presenter was asked to include information regarding sampling and analytical techniques used, moisture and sulfur content of the sample, and any efforts taken to remove these constituents.

5.1 FLUE GAS EXHAUST DATA FROM STATIONARY SOURCES

Most of the stationary-source data presented by European scientists provided material for an excellent comparison with data from the United States. European data represented about 70 different facilities ranging in firing capacities from 0.5-800 MW, with most facilities in the 100-600 mW range. Data from circulating and stationary fluidized bed combustors (FBCs) were included in the presentations. Data from coal combustors made up a significant portion of the presentations, although emission data from peat, distillate oil, wood, refuse, and natural gas combustion were also discussed.

5.1.1 N_2O Emission Data From Test Rigs and Full Scale Units

Dr. Hein and Dr. L. Raible, both of RWE, presented data covering emission values from test rigs and full-scale facilities. Table 5-1 contains data from a PFBC test rig. The high N2O values are consistent with other data on fluidized bed combustors. Table 5-2 contains data obtained from several test- and pilot-scale SCR facilities. Different catalysts were compared for NOx reduction and N2O

TABLE 5-1. N_2O DATA: PFBC TEST RIG (HEIN)

probe/ date	power MWth	p bar	bed temperature °C	O_2 %	CO vpm	NO vpm	N_2O vpm
1/23.3.88	0,75	6	835	6,3	82	173	95
2/24.3.88	0,56	6	835	8,83	141	203	193
3/24.3.88	0,59	6	850	9,16	159	211	168
4/29.3.88	0,71	7	850	8,83	107	203	95
5/31.3.88	0,34	3	845	7,29	512	255	115

Coal:			
	9 % H_2O	77,2 % C	(waf)
	8,44 % ash	4,6 % H	(waf)
	29 % volatiles	6,79 % O	(waf)
		1,32 % N	(waf)

TABLE 5-2. N_2O DATA: SCR TEST/PILOT-SCALE (HEIN)

Test unit	catalyst type	NO_x mg/m^3 before/behind SCR	T °C	N_2O vpm before SCR	N_2O vpm behind SCR
RWE high dust SCR	TiO_2 (Jap.)	600/200	350	1 - 2	0,31 - 0,44
	molecular sieve				< 0,65
	Fe/Cr-oxide				1
BASF high dust SCR	TiO_2 (Jap.)	1050/158	380	4,4	0,8
low dust SCR	TiO_2 (Jap.)	1113/167	365	13	2,14

emissions. Table 5-3 contains data collected from full-scale units using various NOx reduction methods while firing on a European brown coal. The N2O levels presented were relatively low in relation to U.S. reported data from similar facilities. To demonstrate this, the N2O values were added to a graph presented at the Boulder, Colorado workshop. This graph, containing the RWE data, is reproduced in Figure 5-1.

The sampling system, collected the gas in both glass and stainless-steel vessels. Moisture was removed with a refrigeration condenser prior to sample collection. The sulfur content of the brown coal was estimated to be 0.8-0.9 percent. The N_2O analysis was done by both GC/ECD and TCD.

Dr. J. Jacobs of VGB presented data collected at two combustion test rigs operated by Dr. H. Kremer at Bochum University-Rohr. On-line N_2O measurements were made on a 50 KW_{th} pulverized coal combustor and a 100 KW_{th} fluidized bed combustor. The on-line measurements were made using an IR analyzer utilizing a dual wavelength (7.8 µm/8.168 µm) absorption technique. The maximum values of N_2O observed from the coal dust flame were 30 ppm at 2,000 ppm N_2O. The fluidized bed combustor yielded peak values of 100 ppm N_2O.

5.1.2 German Power Plants

Dr. H. Koeser of L&C Steinmuller presented data from several large German power plants (see Table 5-4). The data also show relatively low N_2O emissions. The samples were collected while the utilities were operated under normal conditions. Moisture was removed from the gas stream using a refrigeration condenser. The samples were analyzed by GC/ECD and GC/TCD at Steinmuller.

5.1.3 Italian Power Plants

Dr. R. Tarli of Ente Nazionale Energia Elettrica (ENEL) presented data that probably best represented N_2O emission values from industrial facilities. His stack gas samples were analyzed by an on-line GC/ECD method, which produced a near real-time value. Data were collected from both fuel oil and coal combustion facilities, as shown in Tables 5-5 and 5-6, respectively. Virtually no N_2O was detected from burning a high sulfur (3 percent), #6 fuel oil, while 5 ppm was the maximum value obtained from burning an African low sulfur (0.6 percent) bituminous coal.

TABLE 5-3. N_2O DATA: BROWN COAL FULL-SCALE RWE (HEIN)

Probe/ date	Unit/ power MWel	with/without combustion modification	% N in coal raw (waf)	O_2 %	CO mg/m^3_N (dry 6% O_2)	NO as NO_2 mg/m^3_N (dry,6% O_2).	vpm	N_2O vpm ECD	HC
1/25.4.88	"1"/300	with CM	0,38 (1,05)	2,6	210	170	102	11,1	
2/25.4.88	"1"/300	with CM	0,38 (1,05)	2,6	210	170	102	6	5
3/28.4.88	"1"/300	with CM	0,37 (0,99)	2,2	210	195	120	5,5	4
4/28.4.88	"1"/300	with CM	0,37 (0,99)	2,2	210	195	120	5,2-6,5	5
5/28.4.88	"1"/300	with CM	0,37 (0,99)	2,2	210	195	120		4
6/28.4.88	"1"/300	with CM	0,37 (0,99)	2,2	210	195	120		<
7/06.5.88	"2"/300	with CM	0,41 (1,05)	2,7	150	170	102	1,6-2,1	<
8/06.5.88	"3"/300	without CM	0,41 (1,05)	5,7	9	645	322	5,1-8	5,

(Fig. 12 from: EPA/NOAA/NASA/USDA N_2O-Workshop; Sept. 87, Boulder, Colorado)

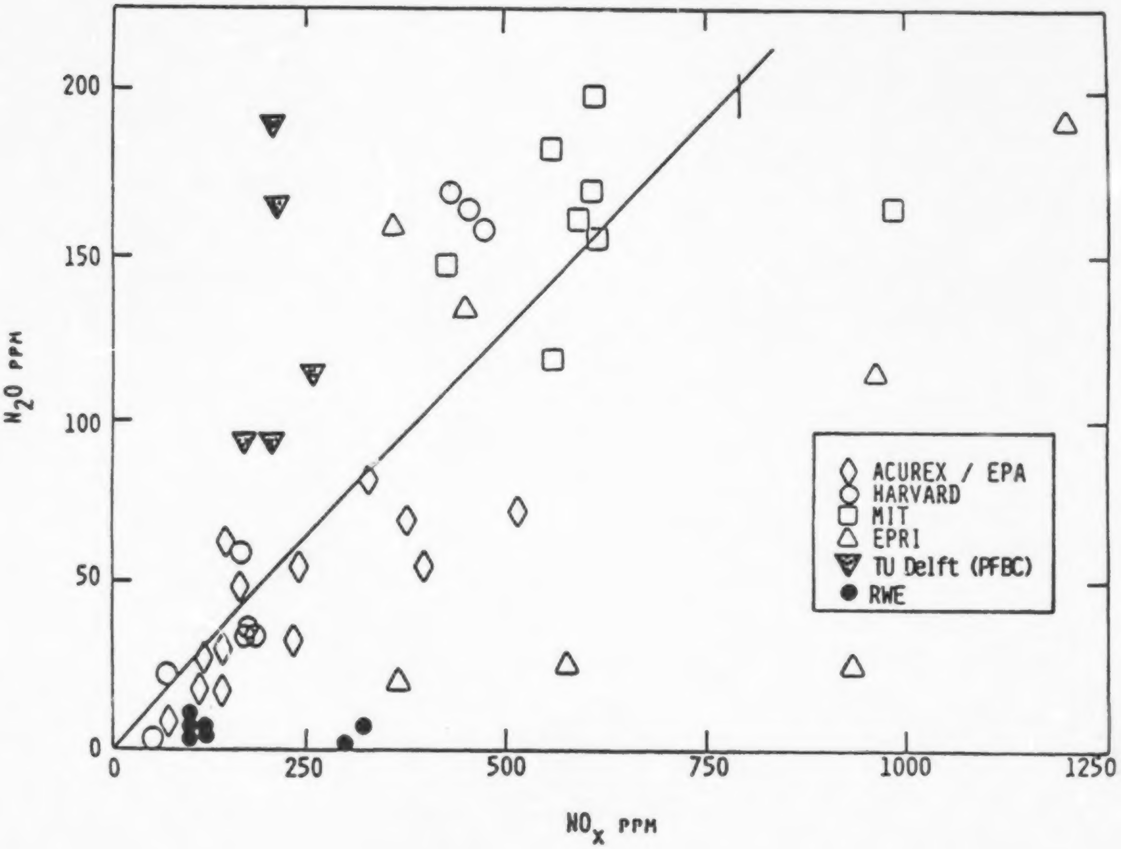

Figure 5-1. Comparison with previous results. (Hein)

TABLE 5-4. N_2O EMISSIONS FROM GERMAN POWER PLANTS (KOESER)

firing equipment	size MW_{el}	fuel	NO_x vpm	flue gas O_2 Vol-%	N_2O vpm
wet-bottom boiler	510	german bituminous coal	863	4.6	26.7 ± 3.8
dry-bottom boiler	465	german bituminous coal	196 46	2.9 2.9	25 18 after SCR
dry-bottom boiler	84	imported bituminous coal	307 75	7.8 8.1	3.9 2 after SCR
grate	42 t/h	municipal refuse	101	10	4.7 ± 1.1

TABLE 5-5. DATA FROM FACILITY BURNING #6 FUEL OIL (TARLI)

UNIT "A"

Nominal rating:	320 MW(e)
Boiler type:	Once-through (U.P.), subcritical
Burner configuration:	Opposite firing
Burner type:	Cell burners
Fuel:	#6 oil (3% S)

Unit Load (MWe)	O_2 at ECO (%)	Flue Gas Recirculation Fans Damper Opening (%)		Concentration (ppm)		
				NO_x	NO	N_2O
310	0.8	100	100	355	335	N.D.
280	1.1	100	100	295	280	N.D.
200	1.6	100	100	235	225	N.D.
310	0.8	0	5	480	460	1
250	1.3	0	25	335	320	1
160	2.5	0	65	220	200	N.D.

TABLE 5-6. DATA FROM FACILITY BURNING COAL (TARLI)

UNIT "B"

Nominal rating:	171 MW(e)
Boiler type:	Drum boiler, natural circulation
Burner configuration:	Corner firing
Number of burner elevation:	6
Fuel:	Bitiminous coal (from South Africa)

Unit Load (MWe)	O_2 at ECO (%)	Concentration ppm	
		NO_x	N_2O
130	4	N.A.	5.1 ± 0.2
165	4	386 ± 5	3.3 ± 0.4
165	4	386 ± 5	2.1 ± 0.2
165-115	4	N.A.	2.5 ± 0.1

5.1.4 Emissions of N_2O From British Power Stations

Dr. A. Sloan of Central Electricity Research Laboratories (CERL), presented data collected from 2 power plants in England. Dr. Sloan was interested in verifying the existence of a N_2O/NO_x ratio relationship. Table 5-7 contains data from the Eggborough and Fiddler's Ferry power plants. While expecting to see a ratio on the order of 20 percent, ratios of less than 5 percent were obtained. The N_2O data obtained at the Eggborough power station were collected with a sample system using a refrigeration condenser for moisture removal. The samples were collected in polyvinylidenechloride bags and analyzed within 24 h by GC/ECD. At Fiddler's Ferry, a more extensive N_2O measurement effort was performed. Both wet and dry grab samples as well as an on-line IR analyzer were employed. Figure 5-2 shows the set up for N_2O sample collection and measurement. The data presented in Table 5-8 show good agreement between both the wet and dry grab samples and the IR measurements. The grab samples were analyzed on site by GC/ECD within an hour of collection. SO_2 emission levels at both power plants were estimated to be 1,200 ppm.

5.1.5 Emission Data from Swedish Stationary Combustion Sources

Mrs. K. Dahlberg of the Swedish Environmental Research Institute (SERI) presented data from a wide variety of combustors and fuels used in Sweden. Table 5-9 lists the type of combustion unit and the fuel used in 17 different power plants. Table 5-10 lists the N_2O emission values from each unit. The N_2O levels of the FBCs were high relative to the other methods of combustion presented. Grab samples were collected in 15 L polyethylene coated aluminum bags and analyzed by GC/ECD. Silica gel was used as a desiccant. Tests were performed both with and without the use of silica gel with no significant variance in N_2O values obtained.

Mr. S. Andersson of Gotaverken Energy Systems, an FBC manufacturer, presented data collected with the assistance of Mrs. K. Dahlberg of SERI on their FBC units (see Table 5-11). The N_2O values presented were considerably lower than those obtained by Dahlberg at similar facilities. It was hypothesized that the use of fuel lower in nitrogen content may account for this, since the samples were collected and analyzed the same way.

TABLE 5-7. SUMMARY OF N_2O AND TOTAL NO_x EMISSIONS (SLOAN)

Station	Unit	Load (MW_e)	No. of Samples	Dry at 3% O_2 dry		Ratio $N_2O:NO_x$ as %
				N_2O (ppm)	$NO + NO_2$* ppm	
Eggborough	4	455	4	32 ± 2.0	700**	4.6
Eggborough	1	300	4	26 ± 3.3	-	-
Fiddler's Ferry	1(Low NOx)	485 ± 15	20	2.4 ± 1.3	270 ± 25	0.8 ± 0.5
Fiddler's Ferry	3	475 ± 25	16	4.5 ± 2.6	385 ± 30	1.1 ± 0.6

* Assumed $NO_2 = 0.05$ NO.

** Typical of previous flue gas monitoring.

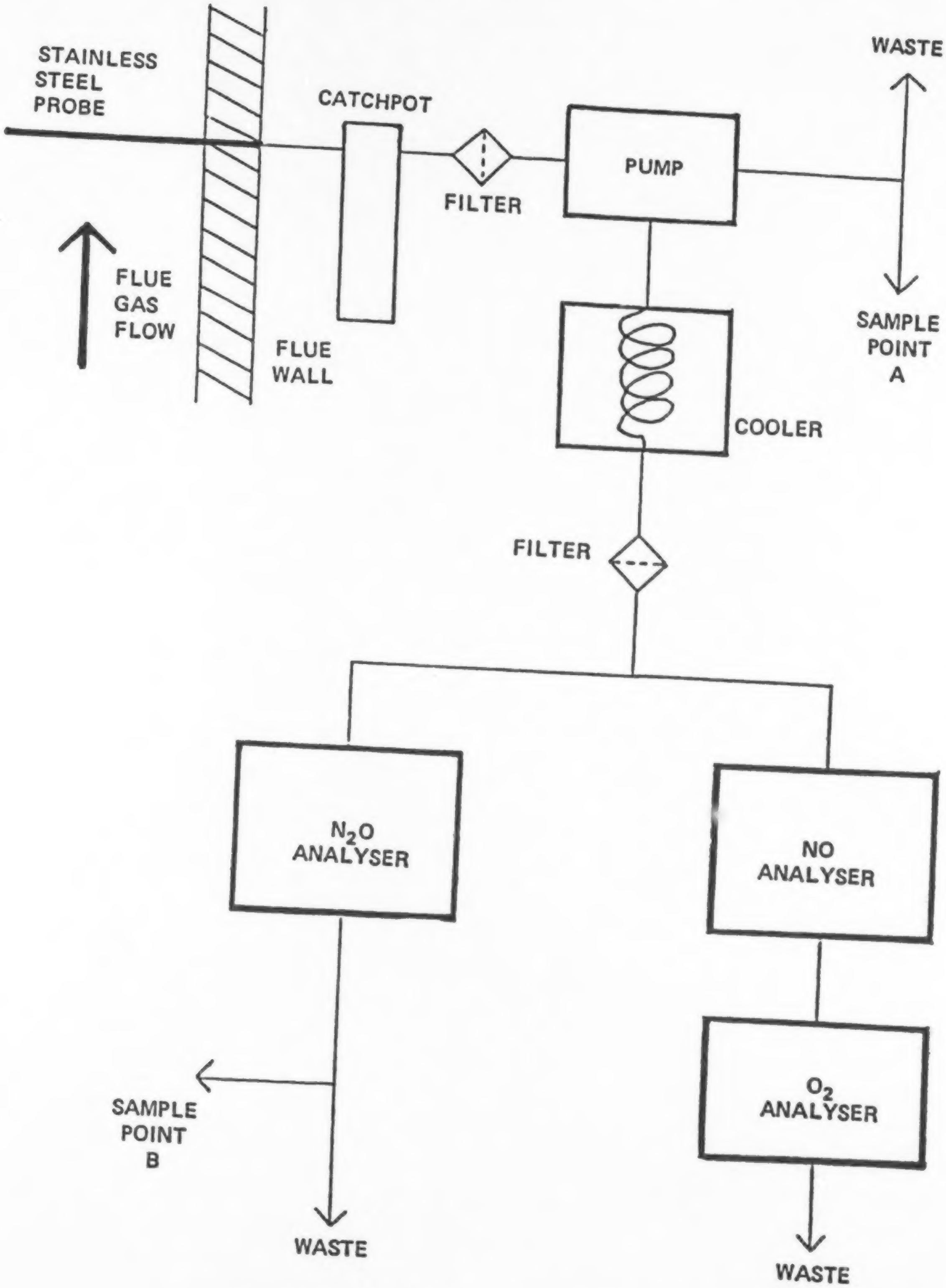
STAINLESS STEEL PROBE
CATCHPOT
FILTER
PUMP
WASTE
SAMPLE POINT A
FLUE GAS FLOW
FLUE WALL
COOLER
FILTER
N_2O ANALYSER
NO ANALYSER
O_2 ANALYSER
SAMPLE POINT B
WASTE
WASTE

Figure 5-2. Extractive flue gas sampling system. (Sloan)

TABLE 5-8. MEASUREMENT OF N_2O UNDER VARIED CONDITIONS (SLOAN)

Run No.	Date	Load (MW_e)	O_2 dry (%)	NO dry (ppm)	N_2O dry		N_2O dry at 3% O_2 d.	
					IR (ppm)	GC (ppm)	IR (ppm)	GC (ppm)
F1A	9.12.87	450	7.2	260	2.0	5.8	2.6	7.6
F1B	"	450	7.6	230	2.4	3.7	3.2	5.0
F2A	"	490	6.4	210	2.3	1.1	[illegible]	1.4
F2B	"	490	6.4	210	2.3	2.2	2.8	2.7
F3A	"	490	6.3	210	2.2	1.6	2.7	2.0
F3B	"	490	6.5	210	2.4	2.2	3.0	2.7
F4A	"	490	6.8	225	2.2	0.6	2.8	0.8
F4B	"	490	6.8	225	2.2	2.1	2.8	2.7
F5A	"	490	6.7	225	1.6	1.1	2.0	1.4
F5B	"	490	6.7	225	1.6	1.5	2.0	1.9
F6A	"	490	6.8	235	1.7	1.8	2.1	2.3
F6B	"	490	6.8	210	1.7	0.6	2.1	0.8
F7A	"	490	6.5	215	2.4	1.0	3.0	1.2
F7B	"	490	6.5	210	2.4	0.7	3.0	0.9
F8A	"	490	6.7	210	1.6	0.6	2.0	0.8
F9A	10.12.87	480	6.5	195	-	1.0	-	1.2
F9B	"	480	6.5	195	-	1.4	-	1.7
F10A	"	480	6.4	195	-	2.9	-	3.6
F10B	"	480	6.4	195	-	1.6	-	2.0
F11A	11.12.87	490	6.5	220	-	3.4	-	4.2

TABLE 5-9. COMBUSTION METHODS AND FUELS IN SWEDISH COMBUSTORS (DAHLBERG)

Plant No.	Fuel	Combustion unit		
01.	Oil	Small furnace for house heating	- 30	kW
02.	"	Top-mounted pressurized air burner	12	MW
03.	"	Top-mounted with 2 rotary burners	50	MW
04.	"	Tangentially placed angle burners	~ 70	MW
K5.	Pulverized coal	Front-wall mounted burners	90	MW
K6.	"	Tangentially mounted burners	125	MW
K7.	Coal	Chain-grate, with a steam boiler producing	40	ton/h
K8.	"	Bubbling fluidized bed	16	MW
K9.	"	Circulating fluidized bed	50	MW
F10.	Wood chips	Stationary inclined grate furnace	5.8	MW
F11.	" "	Converted boiler with pre-oven	30	MW
V12.	Firewood	Tile stove		
T13.	Peat	Moving grate furnace	5.5	MW
T14.	"	Circulating fluidized bed	42	MW
G15.	Natural gas	Front-wall mounted burners	150	MW
G16.	" "	Small furnace for house heating		
L17.	Black Liquor	Recovery furnace		

TABLE 5-10. EMISSIONS FROM VARIOUS COMBUSTORS (DAHLBERG)

Plant No.	N_2O ppmv	N_2O mg/MJ	CO_2 %	% of maximum loading
01.	3	2	8.8	
	0.6	0.5	7.8	
	3	2	9.6	
	2	2	10.0	
02.	28	17	12.4	
	17	11	11.7	
03.	40	20	15.1	100
	3	4	9.0	70
	4	2	14.6	60
04.	23	12	14.5	
	38	20	14.5	
K5.	21[1/]	20	7.7	
	5	4	11.8	
	3	2	11.5	
	60	49	11.0	
K6.	7	5	14.5	
	3	3	10.4	
K7.	1	0.8	11.0	80
	8	7	10.0	90
	2	2	9.8	90
	5	4	11.0	95
K8.	137	90	14.3	
K9.	88	57	14.5	70
	79	51	14.4	90
	128	88	13.7	60
	165	-	-	-
	106	-	-	80
F10.	5	5	10.5	70
	3	2	12.2	85
	4	4	9.5	80
F11.	5	4	12.7	75
	5	5	11.5	80
	8	6	14.0	75
V12.	0.9	1	4.0	
	1	2	4.4	
	10	14	4.0	
	3	5	2.0	
T13.	18	15	12.5	
	10	6	15.5	
	9	6	14.0	
T14.	52	34	15.1	
G15.	2	2	8.0	50
	2	2	8.4	75
G16.	9	8	8.0	
	3	3	8.0	
	23	22	7.0	
C17.	2	2	12.0	
	0.3	0.3	9.2	
	2	2	10.2	

[1/] The sample was stored 3 days before analysis

TABLE 5-11. FBC EMISSIONS (ANDERSSON)

Boiler type (design load)	Load	Fuel	N_2O	CO_2	N_2O at 10 % CO_2
CFB (20 MW)	18 MW	RDF	12 ppm 10	11,0 % 11,7	11 ppm
CFB (50 MW)	51 MW	Wood waste	19 ppm 14	14,5 % 13,8	13 ppm 10
CFB (20 MW)	18 MW	Peat	10 ppm 6	- -	- -
CFB (40 MW)	26 MW	Peat	75 ppm 76	12,1 % 12,0	62 ppm 63
	33 MW	Coal	56 ppm 49	13,0 % -	43 ppm
	34 MW	Coal + 8 % Peat	69 ppm 62	12,4 % 13,7	56 ppm 45

5.1.6 Excess Air Variation in a Circulating FBC

Mrs. L. Fuller of Studsvik Energy presented data collected on 2 different coals burned in a 40 MW_{th} circulating FBC in which excess air was varied (see Table 5-12). A trend toward higher N_2O emission was observed with a higher stoichiometric ratio. Grab samples were collected in 2 L Tedlar bags and analyzed by GC/ECD. Moisture removal was accomplished using silica gel. Ms. Fuller remarked that the samples were analyzed on the same day and 24 h after collection with little difference in final values. Tests were also conducted to compare samples collected with and without silica gel to ensure sample integrity.

5.1.7 N_2O Emissions From Power Plants in Finland

Dr. G. Hellen of EKONO discussed data collected from 20 power plants in Finland using different types of combustion techniques and fuels (see Tables 15-13 through 15-15). Again, high N_2O values were found in FBCs, with considerably lower values found in other types of combustion facilities. Figure 5-3 presents a graphic representation of the N_2O and NO_x values from all plants and fuels. There did not seem to be an obvious relationship between N_2O and NO_x emissions. Dr. Hellen also described his work in assessing the sampling and analytical equipment used. Samples were collected in polyethylene lined aluminum bags using silica gel for moisture removal and analyzed by GC/MS. A test was performed demonstrating that the use of silica gel resulted in no losses of N_2O. In addition, a stability study was conducted on an actual stack gas sample. The sample was repeatedly analyzed over a 2-wk period with no significant change in concentration observed.

5.1.8 Data from Dutch Power Stations

Dr. H. Spoelstra of KEMA presented data he collected while inventorying N_2O emissions from Dutch power stations. Table 15-16 represents data collected from facilities burning natural gas as well as coal, revealing relatively low N_2O emissions. Table 15-17 contains data obtained from a catalytic NO_x reduction facility. N_2O samples were collected both before and after the titanium base catalyst. Lower N_2O concentrations were observed at the exit of the catalyst. No FBCs were sampled. Samples were collected in teflon lined stainless-steel containers downstream of 2 ice-bath condensers and analyzed by GC/ECD.

TABLE 5-12. EXCESS AIR VARIATION DATA (FULLER)

	Test no.1	Test no.2
COAL:	KUTZNEZ	AUSTRALIAN
% volatiles (dry)	37.1	36.9
% nitrogen	2.2	1.7
% sulphur	0.37	0.58
Load (MW_{th})	27	30
Limestone addition (kg/h)	50	175

Test no.	$\%O_2$	Bed temp. C	Flue gas temp. C	$CO+H_2$ ppm	SO_2 ppm
1	3.2	870	125	41	146
	5.0	848	129	40	94
	7.3	826	133	48	79
2	3.5	848	127	34	164
	5.3	840	132	34	164
	5.3	852	132	35	166
	7.2	845	137	34	153

Comparison of the two CFB tests.

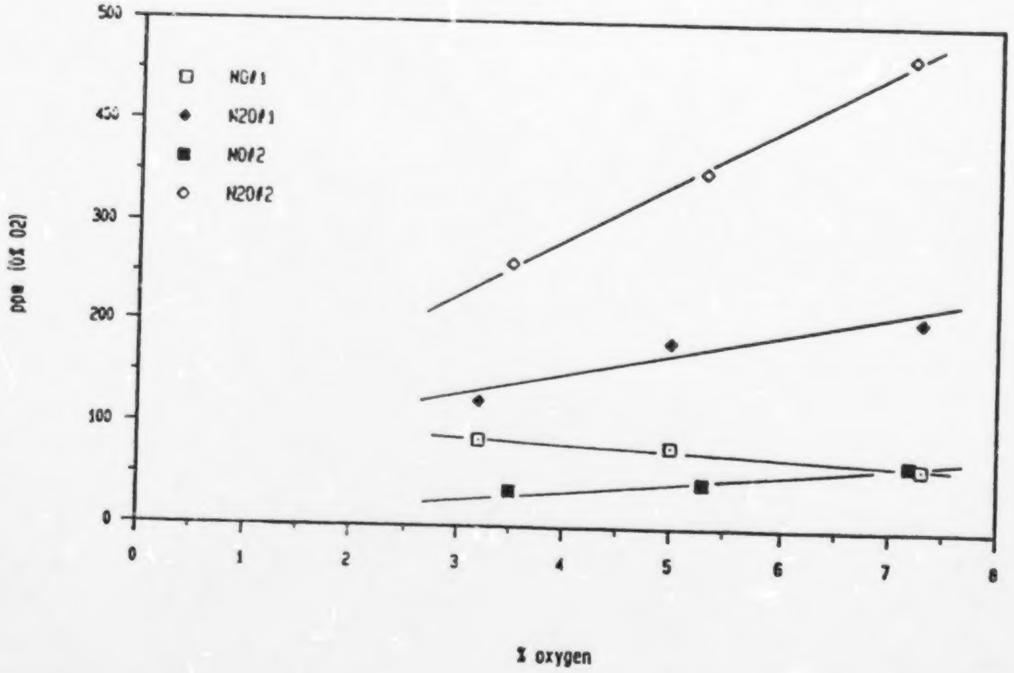

TABLE 5-13. N_2O FIELD TEST DATA FROM VARIOUS COMBUSTION PLANT SOURCES USING AN FBC (HELLEN)

Plant	Combustion technique	Fuel type	Fuel nitrogen content	Fuel coal content	Nominal power	Load	N2O-conc.	Emission factor N2O	NOx-conc.	Emission factor NOx	N2O/NOx (volume)
no			weight-% dry	weight-% dry	MWt	%	ppmv,dry	mgN2O/MJ (input)	ppmv,dry	mgNO2/MJ (input)	%
1	Circ. Fluidised Bed(CFB)	Coal	1.9	68	80	85	96	58	130	80	74
2	"	"	1.3	75	30	70	80	49	100	60	80
3	"	Milled peat(1/2) Wood(1/2)	1.3	53	60	100	7	5	170	130	4
4	Stat. Fluid. Bed(SFB)	Milled peat(2/3) +oil(1/3)	1.6	61	18	100	16	11	200	140	8
5	"	Milled peat	1.8	55	15	75	43	30	220	160	20
6	"	Coal	1.25	76.1	35	100	23	17	130	100	18

TABLE 5-14. N_2O FIELD TEST DATA FROM VARIOUS COMBUSTION PLANT SOURCES USING A CONVENTIONAL BURNER (HELLEN)

Plant	Combustion technique	Fuel type	Fuel nitrogen content	Fuel coal content	Nominal power	Load	N2O-conc.	Emission factor N2O	NOx-conc.	Emission factor NOx	N2O/NOx (volume)
no			weight-% dry	weight-% dry	MWt	%	ppmv,dry	mg N2O/MJ (input)	ppmv,dry	mg NO2/MJ (input)	%
1	Burner	Pulverized peat	1.8	55	160	100	20	17	270	240	7
2	"	P.p.(3/4) N.gas(1/4)	1.7	57	200	85	29	20	240	180	12
3	"	Pulverized peat	1.42	53.7	5.3	100	18	11	440	290	4
3	"		1.42	53.7	5.3	74	21	13	330	220	6
4	Burner	Pulverized coal	1.6	72	450	100	11	7	630	430	2
4	"		1.6	72	450	60	3	2	500	340	1
5	"	"	1.9	68	240	100	27	18	620	430	4
6	Burner	Heavy oil	0.5	86	3.2	95	39	23	240	150	16
7	"	"	0.5	86	3.2	100	73	46	230	150	32
8	Burner	Natural gas	0.05	98.9	400	86	1	1	450	280	0

TABLE 5-15. N_2O FIELD TEST DATA FROM VARIOUS COMBUSTION PLANT SOURCES USING GRATE COMBUSTION (HELLEN)

Plant	Combus-tion tech-nique	Fuel type	Fuel nitrogen content	Fuel coal content	Nominal power	Load	N2O-conc.	Emission factor N2O	NOx-conc.	Emission factor NOx	N2O/NOx (volume)
no			weight-% dry	weight-% dry	MWt	%	ppmv,dry	mg N2O/MJ (input)	ppmv,dry	mg NO2/MJ (input)	%
1	Grate	Milled peat	1.8	55	15	90	17	13	280	220	6
2	Grate	Pressed peat	1.8	55	5	80	6	5	270	220	2
3	Grate	Wood chips	0.7	50	14	60	1	1	80	80	1
4	"	"	0.7	50	27	56	1	1	90	80	1
5	Grate	Coal	1.6	72	35	66	20	18	150	140	13
6	Grate	Coal(1/2) Wood(1/2)	1.1	59	50	100	34	26	180	140	19

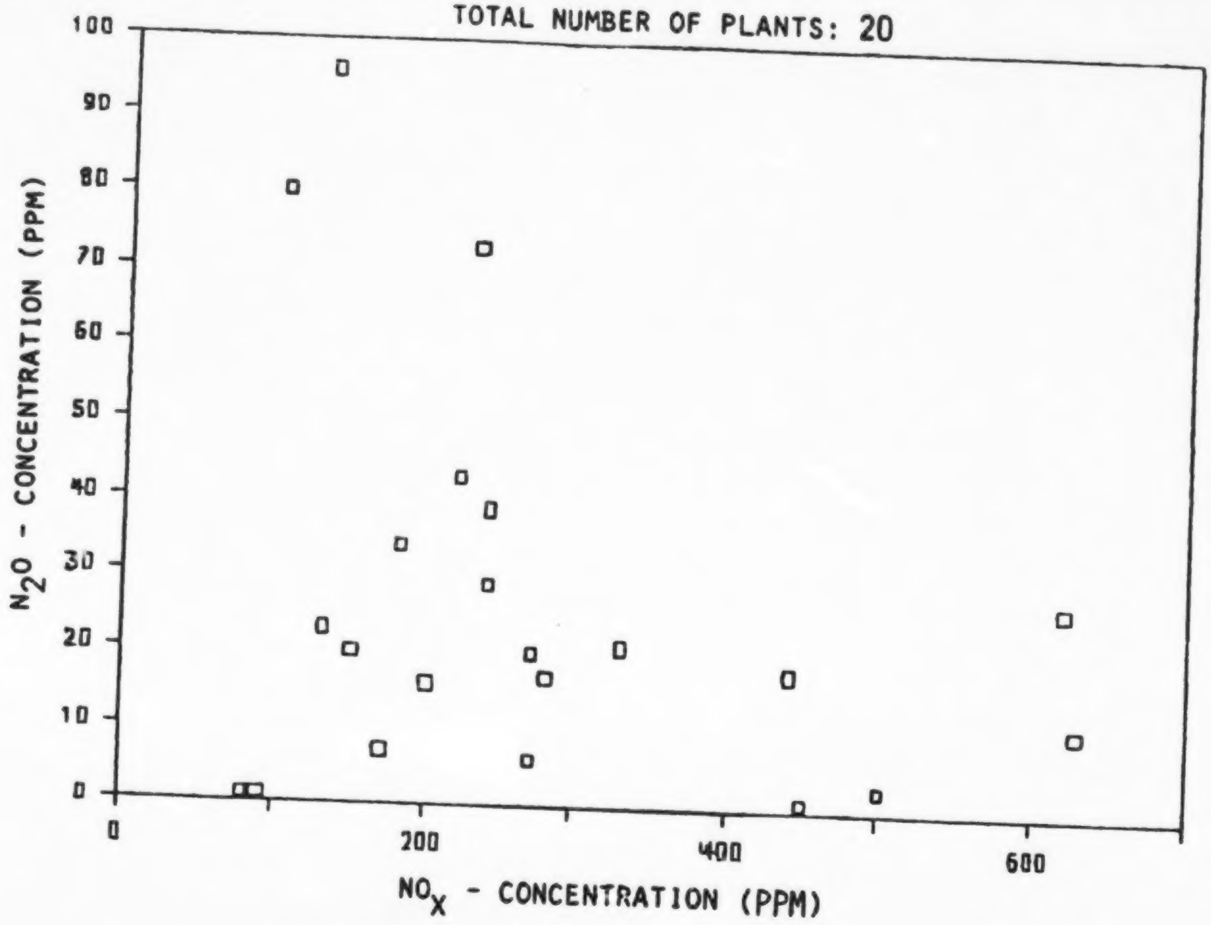

Figure 5-3. N_2O and NO_X concentrations from all plants and combined combustion techniques. (Hellen)

TABLE 5-16. N_2O CONCENTRATIONS IN STACK GAS FROM ELECTRICITY POWER STATIONS (SPOELSTRA)

Gas

Max cap MW	Cap MW	Range ppm (3% O_2, day)	No. of Samples	NO_x Conc. ppm
100	100	<1	4	215
100	100	≤1	4	190
100	70	~1	4	215

Power Coal

Max cap MW	Cap MW	Range ppm (3% O_2, day)	No. of Samples	NO_x Conc. ppm
120	120	10	1	
		20-25	2	
180	108	3	1	
	144	10	1	
	180	10-15	3	
400	400	.9	1	(350)
600	600	<1	2	(550)
600	600	5-8	6	(400)

( ) = estimated

TABLE 5-17. CATALYTIC DeNO$_X$ (SCR) (SPOELSTRA)

	Power Coal Range of N_2O Concentration (3% O_2, dry)			
CAP MW	IN ppm	No. of Samples	Out ppm	No. of Samples
120	20-25	2	6	2
	10	1	3	4

5.1.9 Data From U.S. Power Plants

Mr. S. Wilson of Southern Company Services presented N_2O data collected for the EPA. Mr. Wilson was asked by the EPA to collect samples in order to assist in evaluating the GC analytical system being developed through J. McSorley's in-house program. Samples were collected from conventional utility boilers with various firing configurations. Figure 5-4 illustrates the relatively high N_2O concentrations obtained from these coal-fired facilities. Figure 5-5 is a graphic representation of his data plotted along with results presented at the Boulder workshop. A detailed description of the sampling and analytical background revealed that almost no moisture removal was attempted prior to collection. The sample canisters contained condensed combustion water, and analysis was performed as late as 2-wk after collection. Because of the proposed sampling artifact and the use of coal with high sulfur content, conditions seemed conducive to sample container N_2O generation. These sampling and analysis factors cause the integrity of these data to be highly suspect.

Dr. Muzio presented data that he had collected over the last few years for EPRI where during sample collection, very little had been done to remove moisture or SO_2. Figure 5-6 shows these data along with a single point under the same firing conditions where both the SO_2 and moisture have been removed from the sample. Where earlier over 100 ppm N_2O had been reported, replicating this condition reveals an N_2O concentration of approximately 3 ppm.

5.2 EXHAUST DATA FROM MOBILE SOURCES

Only 2 presentations addressed N_2O emissions from mobile sources.

5.2.1 Comparison of Vehicles With and With Out Catalytic Converters

Mrs. A. Lindskog of SERI described her research on automobile 3-way catalytic NO_x converters. The concentration of N_2O in automobile exhaust was measured during the Swedish driving cycle. The tests included catalyst and non-catalyst vehicles under cold-start and warm-start conditions. Table 5-18 indicates that the N_2O emissions from a catalyst vehicle are 4-5 times greater than that of a non-catalyst vehicle, depending on start conditions. Table 5-19 presents N_2O concentrations both before and after

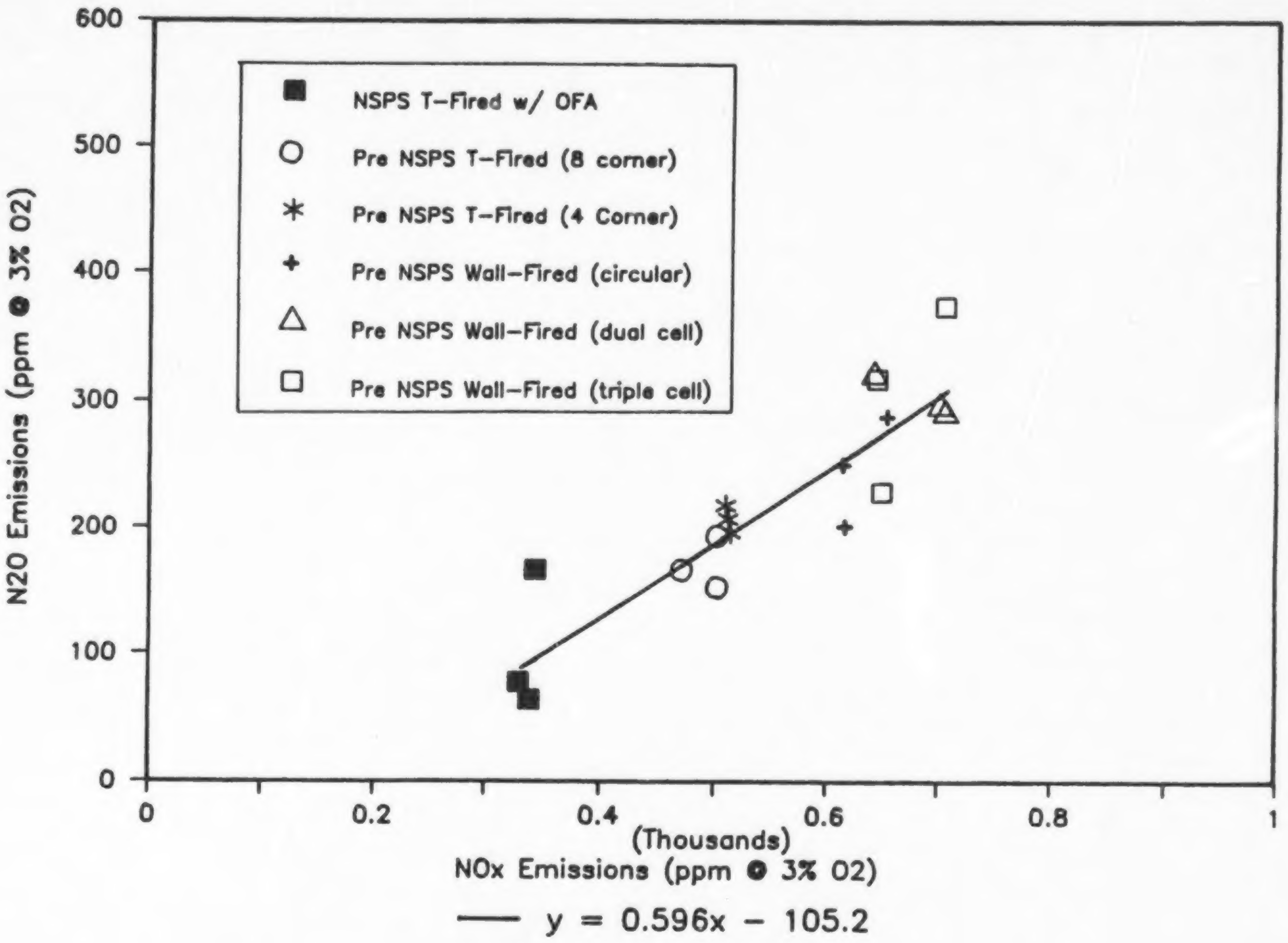

Figure 5-4. N_2O versus NO_x emissions. (Wilson)

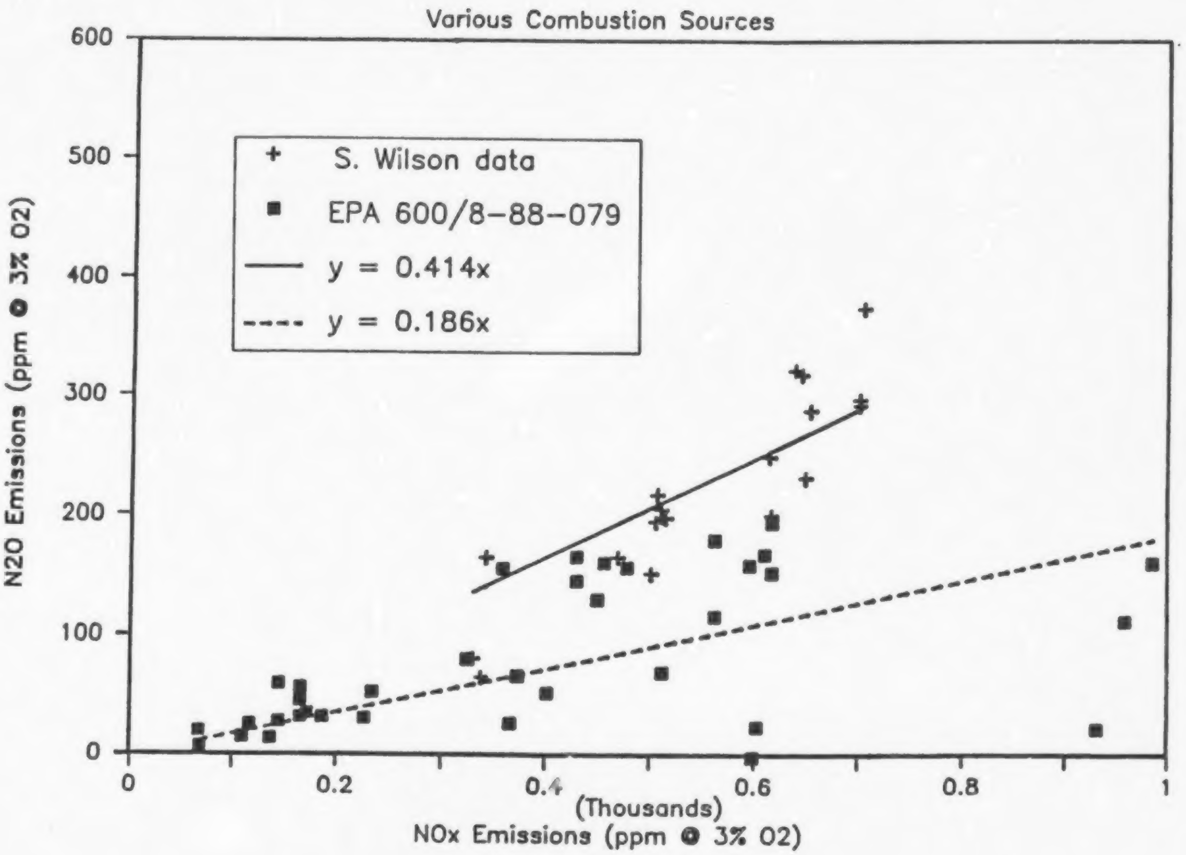

Figure 5-5. N_2O versus NO_x emissions, compared with Boulder Workshop data. (Wilson)

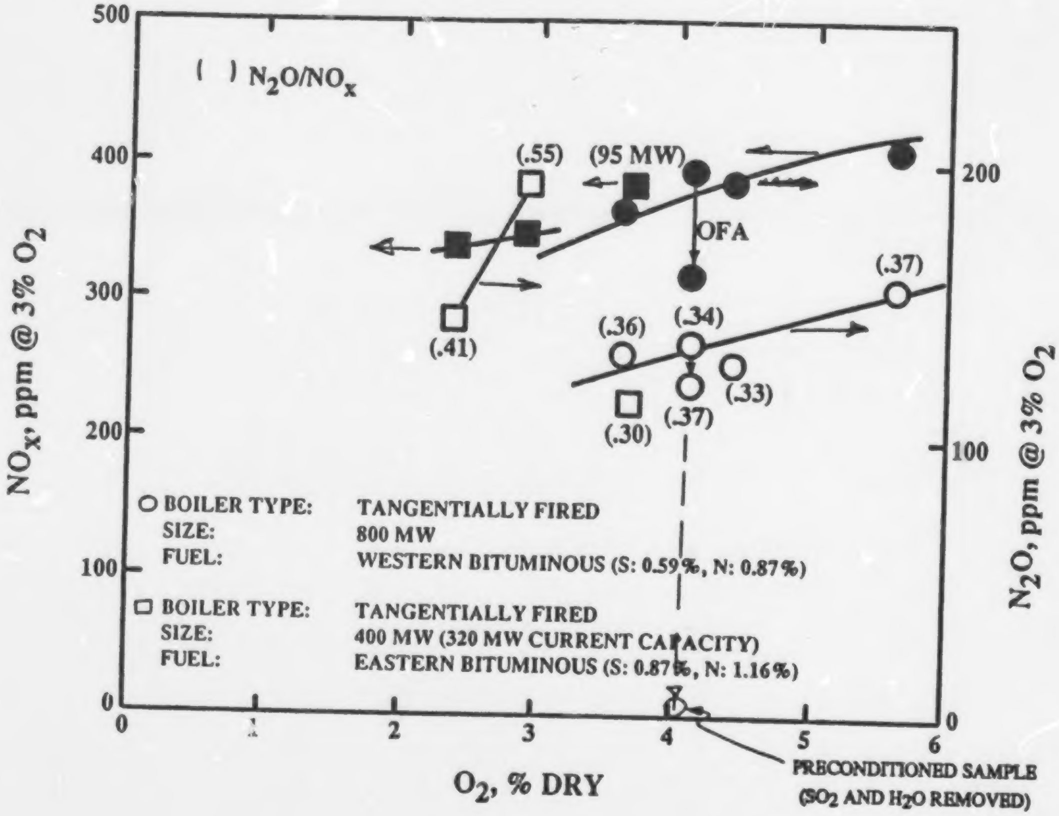

Figure 5-6. EPRI N_2O measurements with repeat condition. (Muzio)

TABLE 5-18. CATALYST VEHICLE VERSUS CARBURETOR VEHICLE (LINDSKOG)

	CATALYST VEHICLE				CARBURETTOR VEHICLE			
	COLD START		WARM START		COLD START		WARM START	
TEST NO	NO_x	N_2O	NO_x	N_2O	NO_x	N_2O	NO_x	N_2O
1	0.275	0.13	0.063	0.031	1.191	0.096	1.343	0.094
2	0.282	0.41	0.075	0.62	1.163	0.044	1.321	0.044
3*	0.267	0.61	0.114	0.30	1.125	0.061	1.313	(0.57)
4	0.289	0.14	0.064	0.070	1.078	0.031	1.246	0.062
MEAN:		0.32		0.25		0.058		0.067

TABLE 5-19. CATALYST VEHICLE DATA (LINDSKOG)

CONCENTRATION OF N_2O IN THE EXHAUST PIPE, BEFORE AND AFTER THE CATALYST (PPMV)					
TEST NO	COLD START		WARM START		
	BEFORE	AFTER	BEFORE	AFTER	
1	19	39	26	11	
2	25	45	33	25	
3	19	50	24	42	
4	18	29	30	27	

THE VEHICLE WAS NOT PREPARED AHEAD OF THE TEST.

the catalyst under the 2 start conditions. In regard to the N_2O generation artifact, Mrs. Lindskog encountered a situation where the N_2O concentration increased in one of her samples, but she could not explain a possible cause.

5.2.2 Comparison of N_2O Emissions from City and Suburban Driving

Mr. M. Prigent of IFP presented data, shown in Figures 5-7 and 5-8, reflecting research conducted at the institute. The data compare N_2O emissions proportional to catalyst temperature produced by simulated city and suburban driving on gasoline engine vehicles. City driving, with lower exhaust temperatures, generated higher N_2O values than suburban driving. The city, or European driving style, was contrasted with the driving style prevalent in the United States, in which higher exhaust temperatures are generated and lower N_2O values are observed. Tests were also conducted using diesel engine vehicles, obtaining results generally similar to those of the gasoline engine vehicles.

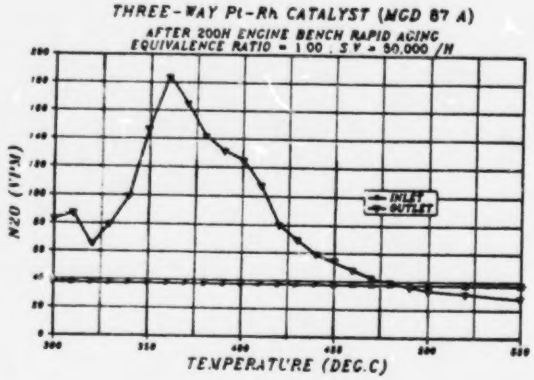

Steady state N_2O concentration in engine exhaust as a function of catalyst inlet temperature at $\phi = 1.00$

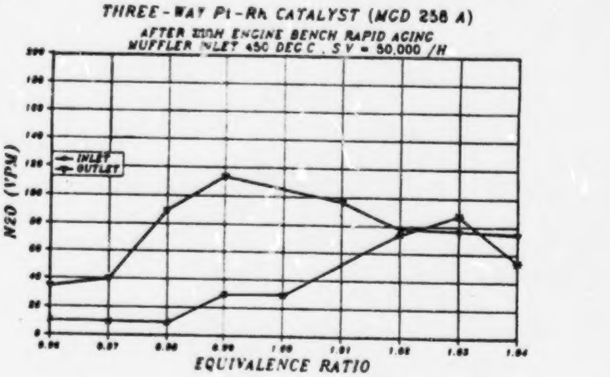

Steady state N_2O concentration in engine exhaust as a function of equivalence ratio; inlet catalyst T = 450°C

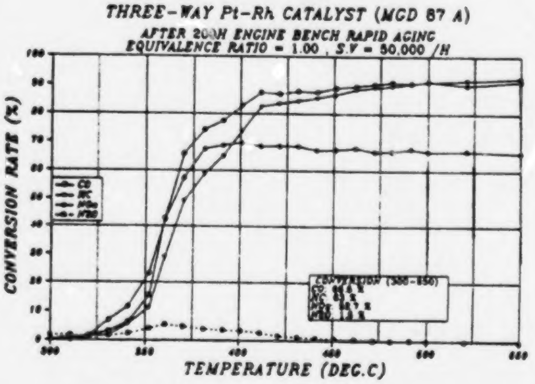

CO, HC and NO gross conversion and NO into N_2O conversion as a function of catalyst inlet T at $\phi = 1.00$

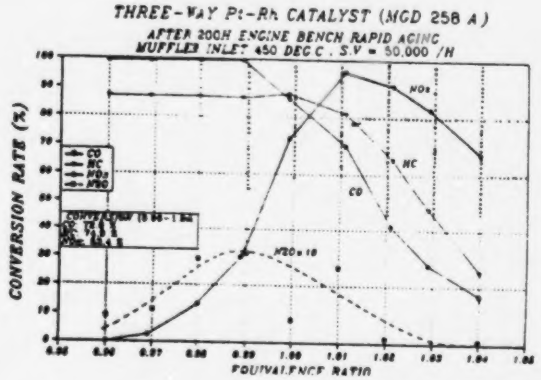

CO, HC and NO gross conversion and NO into N_2O conversion as a function of equivalence ratio; inlet catalyst T=450°C

Figure 5-7. City versus suburban driving. (Prigent)

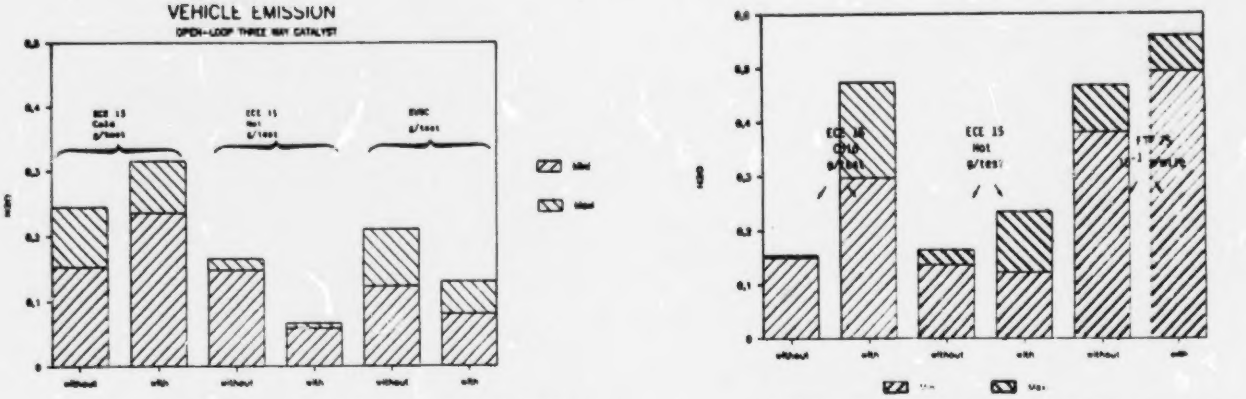

Gasoline vehicle, 1.91 engine, carburettor, with or without open-loop 3-way Pt-Rh catalyst

Gasoline vehicle, 2.21 engine, EFI+O_2 sensor, with without closed loop 3-way Pt-Rh catalyst

rpm	Load	NO_x VPM	N_2O VPM	N_2O/NO_x %
3000	4/4	392	44.1	11.25
3500	4/4	415	35.5	8.55
4000	4/4	360	16.4	4.55
3000	3/4	330	13.5	4.09

Diesel engine, 1.91, steady state NOx and N_2O concentrations in exhaust gas

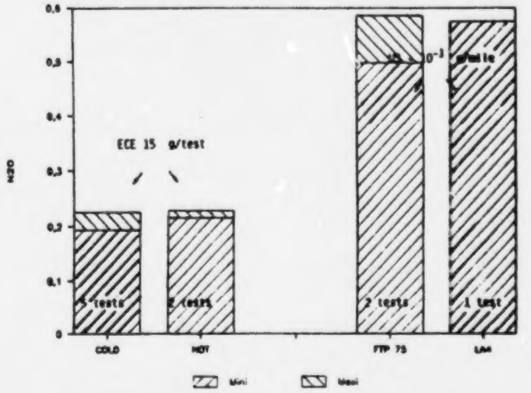

Diesel vehicle, 1.91 engine, N_2O global emissions on ECE and FTP driving cycles

Figure 5-8. Gasoline versus diesel vehicles. (Prigent)

SECTION 6

SESSION 4: GENERAL DISCUSSION TO ARRIVE AT PRACTICAL CONCLUSIONS

The remainder of the workshop was designated for open discussion of material presented during the past 2 days and for reaching practical conclusions on the direction of future research efforts. Dr. S. Lanier of EERC, the session moderator, began by presenting 2 key questions representing EPA's concerns:

1. What is the direct global contribution of N_2O from fossil-fuel combustion versus other sources, and are present global N_2O inventories reliable?
2. Should N_2O emissions be controlled, and will controls make a difference?

The information derived from the previous two N_2O workshops resulted in a series of significant issues that received additional research. These workshops concluded:

1. The need to understand the N_2O formation and destruction mechanism.
2. The need to standardize sampling measurements of N_2O from flue gases and the need to develop an on-line analyzer.
3. The need to develop a global N_2O combustion emission data base.
4. The need to address the effect of possible controls.

In an attempt to define the relationship between combustor sources and the annual increase in measured N_2O levels, Dr. Lanier presented a unique method of back-calculating the average influx of N_2O and the relative contribution of fossil-fuel combustion. Dr. Lanier pointed out that current data suggest a 0.2-0.3 percent increase in N_2O annually or about 0.69 ppb/yr. Dr. Hasenack was not satisfied that Dr. Lanier's figures show a true increase and questioned their statistical significance. Dr. Levine responded that the 0.2-0.3 percent increase in 12 different sites over an 8-yr period was valid and was statistically supported by the investigators who reported the figures.

Dr. Lanier accounted for his previous statement by saying that with the current atmospheric burden and global sinks an estimated 5.5 x 10^6 metric tons of N_2O as nitrogen (N) are added to the atmosphere annually. His method of back-calculating was sufficiently accurate that the AP42 atmospheric model was not essential. If coal combustion is the major source of anthropogenic N_2O, then given a global coal consumption of 2.4 x 10^9 metric tons per year, petroleum equivalent, an average emission of 132 ppm N_2O would account for the observed increase in atmospheric N_2O concentrations. Dr. Lanier noted that if direct N_2O emissions of coal-fired combustors exceeded 100 ppm, then these combustors would be a dominant source of N_2O. However, if N_2O levels are less than 20 ppm, then coal combustors are probably not a dominant source. Therefore, the validity of the data could establish whether or not coal-fired utility boilers are significant contributors to the N_2O increase.

Finally, mobile source N_2O emissions were discussed. Dr. Lanier proposed that with an average emission rate of 100 mg/mi and an estimated 1.6 x 10^{12} mi of driving in the United States each year, American drivers contribute 1.5 x 10^5 metric tons of N_2O to the total influx. If the United States accounts for 48 percent of worldwide gasoline consumption, then the calculated total N_2O emissions worldwide would be 3.1 x 10^5 metric tons, indicating that mobile sources are probably not a significant source of N_2O.

Dr. Lanier offered the following conclusions to the participants for discussion:

1. A critical need exists to develop and validate sampling and analysis procedures.
2. The GC/ECD method of analysis appears adequate, but the development of a continuous emission monitor for N_2O is encouraged.
3. Following validation, repeat sampling of utility boiler and fuel classes, which have previously indicated high N_2O emissions, is urgently needed.
4. Prediction of global N_2O increases based on AP42 NO_x factors is not scientifically justifiable.
5. Mobile sources are a minor contributor to the N_2O emissions.
6. European data indicate that direct N_2O emissions from coal-fired boilers are a minor contributor of N_2O.

7. Continued evaluation of N_2O emissions from fluidized beds is encouraged.
8. Other combustion sources, such as a petroleum catalytic crackers should be evaluated.
9. No clear consensus exists as to how NO_x combustion modifications will affect emissions.

A vigorous discussion period followed Dr. Lanier's conclusions, showing general agreement with them. Dr. Hasenack, however, was not convinced that NO cannot be converted to N_2O in the atmosphere, and he recommended adding to the list a call for research to explore the question. The group generally agreed and added that contribution from other combustion sources should also be evaluated, biomass burning in particular.

The conference participants agreed most strongly that a suitable and valid sampling protocol should be developed. Dr. de Soete solicited European volunteers to assist in investigating the sampling protocol. IFP and EPA had already committed additional research to that area. Dr. Smart and Mr. Morgan offered their services and suggested a collaboration with EPA, since strong ties were already present between EPA and their organizations. Dr. de Soete and Mr. McSorley were suggested as designated contacts to facilitate information exchange on sampling protocols.

Dr. Hein summarized the final conclusions reached from the discussion as follows:

1. New information on N_2O formation and destruction mechanisms in stack gas samples precludes earlier coal- and oil-fired boiler data.
2. Assuming that the European data are valid, the direct emission of N_2O from coal-fired boilers is a minor contributor to observed global increases in N_2O.
3. Sampling, handling, and measurement techniques must be thoroughly studied to assess NO conversion to N_2O in sample containers characterizing catalytic effects.
4. Repeat and extended measurements of NO_x and N_2O emissions from different combustion equipment types, fuel, etc., are needed, with special attention to FBC units as high emitters of N_2O.
5. All other combustion sources, including biomass burning, should be included in the evaluation of global N_2O emissions.

In closing the workshop, Mr. P. Eyzat, director of the IFP, expressed his concern over the long-term global effects of N_2O emissions and the crucial need for collaboration among nations. He stated that although more information is needed, it is safe to assume that mobile sources have a minor role in global increases in N_2O. Mr. Eyzat also expressed concern over the dilemma that low NO_x emission systems may have high N_2O emissions, citing three-way catalytic mufflers and FBCs as examples. How should the problem of the N_2O increase be ranked in the priorities of combustion system research and development? More research and funding are needed from all nations.

SECTION 7

SUMMARY AND CONCLUSIONS

Information presented at this workshop suggests that N_2O emissions have a significant effect on both stratospheric O_3 depletion and global climate change. Studies indicate an annual increase in N_2O in the atmosphere of 0.2-0.3 percent, and isolating the source of the increase is essential to prevent further worldwide climate change. There is still some question as to whether the combustion of fossil fuels is directly responsible for the increase. More research is needed to find reliable and accurate techniques for establishing a data base of N_2O emissions from combustion.

The mechanisms and conditions involved in N_2O combustion formation and destruction are not well characterized. Nitrous oxide formation is possible in post-flame, temperature-dependent, gas phase reactions. Material presented at the workshop suggests that volatile HCN exposed to temperatures between 1,150 K and 1,500 K can be converted to N_2O. The possibility of this is supported by models and experiments. Heterogeneous N_2O formation mechanisms are also possible, but the amount of N_2O they produce is less than observed high stack emissions. The use of catalysts for NO_x reduction methodologies have not been well characterized for N_2O formation. The production of N_2O is temperature dependant and does not seem to be significant in these reactions.

Most of the information presented at the workshop was related to N_2O measurement techniques. Dr. Muzio's presentation on N_2O generation in sample containers questions the validity and accuracy of much of the reported data. A verifiable sampling technique is essential to assess the role of fossil-fuel combustion in rising concentrations of atmospheric N_2O. Dr. Muzio pointed out that NO_x, SO_2, and H_2O are involved in the N_2O artifact scenario. The removal of either of these components could halt the generation of N_2O. However, considerable research is still needed in this area, because these mechanisms may also occur in the atmosphere. Should this be the case, positive identification of the reaction mechanism is crucial, which opens an entirely new avenue of research. Although sampling questions still exist, the analytical methodologies employed in quantifying grab samples are adequate. The development of an on-line continuous N_2O monitor would be invaluable in combustion research.

Substantial data were presented on the N_2O direct-emission levels from various European stationary utilities employing several different types of combustion techniques. Fuels other than coal were included in these presentations. Considerably lower N_2O emissions were realized in relation to United States data. In the presentations, methods of sampling were also described. Much of the European data include extensive moisture removal in sampling. A refrigeration condenser was used, and desiccants were employed. Several presentations included on-line measurements, which showed very low N_2O concentration levels on non-FBC combustors. Table 7-1 represents a compilation of N_2O emissions data presented over the course of the workshop. The data presented on FBCs showed significantly higher levels of N_2O emissions, which supports predictions of computer modeling. The emission of N_2O from mobile sources appears to be very dependent on driving styles. The conversion of NO_x to N_2O is directly related to catalyst temperature, which is proportional to driving speed or rotations per minute. Lower temperature catalysts produce higher N_2O emissions.

A general discussion period completed the 2-day workshop, put in perspective the information presented, and enabled participants to set priorities for research and goals. Standardization of a practical and accurate sampling protocol was deemed most essential. There is no way to assess N_2O emissions from fossil-fuel combustion unless an accurate measurement technique is available. Once a suitable sampling protocol has been installed, the retesting of utility boilers, catalytic crackers, and other combustion sources should be performed. The combustion of fuels other than coal and heavy distillates should be considered, particularly biomass burning, where limited sampling efforts have shown significant emissions. A general consensus was reached that direct emissions of N_2O from the combustion of fossil fuels is possibly not the major source of N_2O in the atmosphere, but more research should be conducted to support this conclusion.

TABLE 7-1. N_2O EMISSIONS DATA SUMMARY

COUNTRY	GROUP	COMBUSTOR TYPE	SIZE MW	LOAD MW	FUEL USED	SAMPLE COLLECTION METHOD	MOISTURE REMOVAL METHOD	ANALYTICAL METHOD	N2O PPM	NOX PPM	SO2 PPM
ENGLAND	CERL	WALL FIRED	450	455	PULVERIZED COAL	PVC BAG	CONDENSER	GC/ECD	32	~700	~1200
		WALL FIRED	450	300	■	PVC BAG	■	GC/ECD	26	—	~1200
		TANG. FIRED	500	475	■	PVC BAG/(ON-LINE)	■	GC/ECD/(IR)	2.4	270	~1200
		TANG. FIRED	500	485	PULVERIZED COAL	PVC BAG/(ON-LINE)	CONDENSER	GC/ECD/(IR)	4.5	385	~1200
FINLAND	EKONO	CIRC FL BED	80	85%	COAL	P.E. LINED	SILICA GEL	GC/MS	96	130	—
		■	30	70%	COAL	ALUMINUM BAGS	■	■	80	100	—
		CIRC FL BED	60	100%	MILLED PEAT/WOOD	■	■	■	7	170	—
		STAT FL BED	18	100%	MILLED PEAT/OIL	■	■	■	16	200	—
		■	15	75%	MILLED PEAT	■	■	■	43	220	—
		STAT FL BED	35	100%	COAL	■	■	■	23	130	—
		CONV BURNER	160	100%	PULVERIZED PEAT	■	■	■	20	270	—
		■	200	85%	PULV PEAT/NAT GAS	■	■	■	29	240	—
		■	5.3	100%	PULVERIZED PEAT	■	■	■	18	440	—
		■	5.3	74%	PULVERIZED PEAT	■	■	■	21	330	—
		■	450	100%	PULVERIZED COAL	■	■	■	11	630	—
		■	450	60%	PULVERIZED COAL	■	■	■	3	500	—
		■	240	100%	PULVERIZED COAL	■	■	■	27	620	—
		■	3.2	95%	HEAVY OIL	■	■	■	39	240	—
		■	3.2	100%	HEAVY OIL	■	■	■	73	230	—
		CONV BURNER	400	86%	NATURAL GAS	■	■	■	1	450	—
		GRATE	15	90%	MILLED PEAT	■	■	■	17	280	—
		■	5	80%	PRESSED PEAT	■	■	■	6	270	—
		■	14	60%	WOOD CHIPS	■	■	■	1	80	—
		■	27	56%	WOOD CHIPS	■	■	■	1	90	—
		■	35	66%	COAL	P.E. LINED	■	■	20	150	—
		GRATE	50	100%	COAL/WOOD	ALUMINUM BAGS	SILICA GEL	GC/MS	34	180	—

(continued)

TABLE 7-1. N_2O EMISSIONS DATA SUMMARY (continued)

COUNTRY	GROUP	COMBUSTOR TYPE	SIZE MW	LOAD MW	FUEL USED	SAMPLE COLLECTION METHOD	MOISTURE REMOVAL METHOD	ANALYTICAL METHOD	N2O PPM	NOX PPM	SO2 PPM
ITALY	ENEL	OPPOSITE FIRING	320	310	#6 FUEL OIL (3% S)	ON-LINE	CONDENSER	GC/ECD	ND	355	—
		ONCE THROUGH	"	280	"	"	"	"	ND	295	—
		"	"	200	"	"	"	"	ND	235	—
		"	"	310	"	"	"	"	1	480	—
		OPPOSITE FIRING	"	250	"	"	"	"	1	335	—
		ONCE THROUGH	320	160	#6 FUEL OIL (3% S)	"	"	"	ND	220	—
		CORNER FIRED	171	130	BITUM. COAL (.6% S)	"	"	"	5.1	—	—
		DRUM BOILER	"	165	"	"	"	"	3.3	386	—
		CORNER FIRED	"	165	"	"	"	"	2.1	386	—
		DRUM BOILER	171	165-115	BITUM. COAL (.6% S)	ON-LINE	CONDENSER	GC/ECD	2.5	—	—
NETHERLANDS	KEMA	—	100	100	NAT GAS	TEF LINED SS BOMB	CONDENSER	GC/ECD	~1	215	—
		—	100	100	"	"	"	"	~1	190	—
		—	100	70	NAT GAS	"	"	"	~1	215	—
		—	120	120	COAL	"	"	"	10	—	—
		—	120	120	"	"	"	"	20-25	—	—
		—	180	108	"	"	"	"	3	—	—
		—	180	144	"	"	"	"	10	—	—
		—	180	180	"	"	"	"	10-15	—	—
		—	400	400	"	"	"	"	<1	350	—
		—	600	600	"	"	"	"	<1	550	—
		—	600	600	"	"	"	"	5-8	400	—
		SCR	120	120	COAL	TEF LINED SS BOMB	CONDENSER	GC/ECD	3-6	—	—

(continued)

TABLE 7-1. N_2O EMISSIONS DATA SUMMARY (continued)

COUNTRY	GROUP	COMBUSTOR TYPE	SIZE MW	LOAD MW	FUEL USED	SAMPLE COLLECTION METHOD	MOISTURE REMOVAL METHOD	ANALYTICAL METHOD	N2O PPM	NOX PPM	SO2 PPM
SWEDEN	SERI	TOP FIRED	12	—	OIL	P.E. LINED	SILICA GEL	GC/ECD	17,28	—	—
		TOP FIRED ROTARY	50	100%	"	ALUMINUM BAGS	"	"	40	—	—
		TOP FIRED ROTARY	50	70%	"	"	"	"	3	—	—
		TOP FIRED ROTARY	50	60%	"	"	"	"	4	—	—
		TANG FIRED	70	—	OIL	"	"	"	23,38	—	—
		TANG FIRED	125	—	PULV COAL	"	"	"	3,7	—	—
		WALL FIRED	90	—	PULV COAL	"	"	"	3-60	—	—
		BUBBLING FBC	16	—	COAL	"	"	"	137	—	—
		CIRC FBC	50	60%	"	"	"	"	128	—	—
		"	"	70%	"	"	"	"	88	—	—
		"	"	80%	"	"	"	"	106	—	—
		"	"	90%	"	"	"	"	79	—	—
		CIRC FBC	50	—	COAL	"	"	"	165	—	—
		STAT GRATE	5.8	70%	WOOD CHIPS	"	"	"	5	—	—
		STAT GRATE	"	80%	"	"	"	"	4	—	—
		STAT GRATE	5.8	85%	"	"	"	"	3	—	—
		PRE-OVEN	30	75%	"	"	"	"	5,8	—	—
		PRE-OVEN	30	80%	WOOD CHIPS	"	"	"	5	—	—
		MOVING GRATE	5.5	—	PEAT	"	"	"	9-18	—	—
		CIRC FBC	42	—	PEAT	"	"	"	52	—	—
		WALL FIRED	150	50%	NAT GAS	"	"	"	2	—	—
		WALL FIRED	150	75%	NAT GAS	P.E. LINED	"	"	2	—	—
		RECOVERY FURN	—	—	BLACK LIQUOR	ALUMINUM BAGS	SILICA GEL	GC/ECD	~1-2	—	—
	GES	CIRC FBC	20	18	RESIDUAL DIST FUEL	P.E. LINED	SILICA GEL	GC/ECD	10,12	—	—
		"	20	18	PEAT	ALUMINUM BAGS	"	"	6,10	—	—
		"	40	26	PEAT	"	"	"	76	—	—
		"	"	33	COAL	"	"	"	49,56	—	—
		"	40	34	COAL/PEAT	P.E. LINED	"	"	62,69	—	—
		CIRC FBC	50	51	WOOD WASTE	ALUMINUM BAGS	SILICA GEL	GC/ECD	14,19	—	—

(continued)

TABLE 7-1. N_2O EMISSIONS DATA SUMMARY (concluded)

COUNTRY	GROUP	COMBUSTOR TYPE	SIZE MW	LOAD MW	FUEL USED	SAMPLE COLLECTION METHOD	MOISTURE REMOVAL METHOD	ANALYTICAL METHOD	N2O PPM	NOX PPM	SO2 PPM
	S.E.	CIRC FBC	40	27	COAL (.4% S)	TEDLAR BAGS	SILICA GEL	GC/ECD	123-209	61-87	79-146
		CIRC FBC	40	30	COAL (.6% S)	TEDLAR BAGS	SILICA GEL	GC/ECD	233-444	36-64	153-166
W. GERMANY	RWE	PRESS FBC	—	0.34	COAL	SS AND GLASS BOMBS	CONDENSER	GC/TCD	115	255	—
		*	—	0.56		*	*	*	193	203	—
		*	—	0.59		*	*	*	168	211	—
		*	—	0.71		*	*	*	95	203	—
		PRESS FBC	—	0.75		*	*	*	95	173	—
		—	300	—	BROWN COAL (~.9% S)	*	*	*	5-11	102-120	—
		—	300	—		*	*	*	~2	102	—
		—	300	—		SS AND GLASS BOMBS	CONDENSER	GC/TCD	5-8	322	—
	L&C S	WET BOTTOM	—	510	BITUM COAL	SS AND GLASS BOMBS	CONDENSER	GC/TCD	27	863	—
		DRY BOTTOM	—	465	BITUM COAL	*	*	*	25	196	—
		DRY BOTTOM	—	84	BITUM COAL	*	*	*	4	307	—
		GRATE	—	42(t/h)	MUNICIPAL REFUSE	SS AND GLASS BOMBS	CONDENSER	GC/TCD	5	101	—
	VGB	COAL COMBUSTOR	—	0.05	COAL DUST	ON-LINE	—	IR	30	2000	—
		FBC	—	0.1	PULV COAL	ON-LINE	—	IR	100	—	—
USA	SCS	WALL, TANG. FIRED	—	—	PULV COAL	SS AND GLASS BOMBS	—	GC/ECD	100-400	300-500	—
	FERCO/	TANG FIRED	800	800	PULV COAL	GLASS BOMB	—	GC/ECD	130	—	—
	EPRI	TANG FIRED	800	800	PULV COAL	GLASS BOMB	*	GC/ECD	3	—	—
	EPA	DOWN FIRED	0.029	0.017	PULV BIT COAL	SS BOMB	CONDENSER	GC/ECD	10-220	150-900	—
		DOWN FIRED	0.029	0.017	PULV BIT COAL	ON-LINE	CONDENSER	GC/ECD	< 10	600	—
	UA/DOE	DOWN FIRED	0.029	0.027	PULV COAL	GLASS BOMB	CONDENSER #	GC/ECD	< 5	400-900	—

NOTE: * BOTH MOISTURE AND SO2 WERE REMOVED PRIOR TO SAMPLE COLLECTION
A WATER QUENCH PROBE WAS USED AT POINT OF SAMPLING

SECTION 8

REFERENCES

1. 1958-1983 Data From C.D. Keeling, Scripps Institution of Oceanography. 1984 Data From GMCC/NOAA (Preliminary).
2. M.A. Khalil and R.A. Rasmussen: Tellus 35B, (1983).
3. D.R. Blake and F.S. Rowland, Science, 239, 1988.
4. G.I. Pearman, Etheridge, D., De Silva F., and Fraser, P.J. Nature, 320 (1986).
5. M. Kavanaugh, Atmospheric Environment 21, 463-468 (1987).
6. M.B. McElroy and S.C. Wofsy: Tropical Forests and World Atmospheres, 1985.
7. W. Seiler and R. Conrad: Geophysiology and Amazonia, 1987.
8. Ch. Brühl, P.J. Crutzen, Climate Dynamics 2, 173-203 (1988).
9. Chang, S.G. et al. in Flue Gas Desulfurization, edited by J.L. Hudson and G.T. Rochelle, ACS Symposium Series 188 American Chemical Society, Washington, DC, pp 127-152. 1982.
10. Kramlich, J.C. et al., EPA/NOAA/NASA/VSDA N_2O Workshop Volume I: "Measurmenet Studies and Combustion Sources," September 15-17, 1987, Bould[illegible], Colorado. EPA-600/8-88-079 (NTIS No. PB88-214911), 1988.

APPENDIX A

EUROPEAN WORKSHOP ON N_2O EMISSIONS

Organized by EPA and IFP
Institut Francais du Petrole (Building "le Sequoia")
June 1-2, 1988

AGENDA

Wednesday June 1, 1988

8:00 a.m		Registration of Participants
8:30 a.m		Welcome Address (G. de Soete, IFP)
		OPENING SESSION
8:45 a.m.	1.0	Stratospheric Ozone Depletion and Global Climate Change (S. Seidel, EPA)
9:30 a.m.	2.0	OECD Perspective (P. Stolpman, OECD) Discussion
10:00 a.m.	3.0	Impacts of N_2O and Other Trace Gases on Stratospheric Ozone (J. Levine, NASA)
11:45 a.m.	4.0	Modeling the Effects of N_2O and Other Trace Gases on Climate and Ozone Distribution (C. Brühl, Max Planck Institut) Discussion
12:00 p.m.		SESSION 1: MECHANISMS OF N_2O FORMATION AND DESTRUCTION DURING COMBUSTION
	1.0	Basic Kinetics (Discussion moderator, N. Brown, Lawrence Berkeley Lab)
		1.1 Gas Phase Kinetics (J. Kramlich, EERC)
1:00 p.m.		Lunch (Third Floor)
2:00 p.m.		1.2 Heterogeneous Reactions (G. de Soete, IFP)
		Discussion
3:00 p.m.		Break
3:45 p.m.	2.0	Overall Chemical Information from Laboratory Combustor Experiments (Discussion moderator, J. Wendt, University of Arizona) Data Presented by: W. Linak, EPA (15 min) J. Kramlich, EERC (10 min) A. Williams, Leeds University (20 min) J. Smart, IFRF (15 min)

SESSION 2: N_2O MEASUREMENT TECHNIQUES
(Discussion Moderator: J. McSorley, EPA)

8:30 a.m.	1.0	Problems (J. McSorley, EPA)
		The Need to Develop Standardized Sampling and Analysis Methods
		Ambient Methods
		Source Methods
		Gas Chromatography with ECD (J. Ryan, Acurex Corporation)
		Interferences from Sulfur Dioxide
9:15 a.m.	2.0	Continuous On-line Infrared Methods (L. Muzio, EPA)
	3.0	Optical Interferometry: A Potential Method for N_2O Analysis (A. Galais, CNS)
10:15 a.m.		Coffee (Cafeteria, Ground Floor)

SESSION 3: FULL-SCALE FIELD DATA
(Discussion Moderator: K. Hein, RWE)

10:30 a.m.	1.0	Flue Gas Exhaust Data from Stationary Sources (W. Linak, EPA)
		Data Presented by:
		K. Hein, RWE (10 min)
		H. Koeser, Steinmuller (5 min)
		R. R. Tarli, ENEL (15 min)
		J. Philippe, CERChar (15 min)
		A. Sloan, CEGB (10 min)
		K. Dahlberg, SERI (15 min)
		A. Feugier, IFP (10 min)
		L. Fuller, Studsvik Energy (10 min)
		G. Hellen, EKONO (30 min)
		H. Ten Brink, ENC (5 min)
		H. Spoelstra, CHEMA (10 min)
		S. Wilson, SCS (10 min)
		Discussion
1:00 p.m.		Lunch (Third Floor)
2:00 p.m.	2.0	Exhaust Data from Mobile Sources (A. Douaud, IFP)
		Data presented by:
		A. Lindskog, SERI (15 min)
		M. Prigent, IFP (20 min)

3:00 p.m.

SESSION 4: GENERAL DISCUSSION TO ARRIVE AT PRACTICAL CONCLUSIONS
(Discussion Moderator: S. Lanier, EERC)

1.0	Conclusions
	Relative N_2O Fluxes
	Scatter and Uncertainties of the Data
	Delineation of Information Gaps
	Reemphasis on Importance of Standardized Sampling and Analysis Methods
2.0	Satisfaction with N_2O Source Sampling and Analysis Methods?

3.0 Needs for Further Data Collection
  Gaps
  Priorities
4.0 Preparation of Written Record of Conclusions

5:15 p.m. CLOSING ADDRESS (P. Eyzat, IFP)

APPENDIX B

EUROPEAN WORKSHOP ON N_2O EMISSIONS
Co-Sponsored by EPA AND IFP
Institut Francais du Petrole

LIST OF PARTICIPANTS

Mr. J. Anderson
ASEA PFBC
S-61200 Finspong, Sweden

Mr. Sven Andersson
Gotaverken Energy Systems
P.O. Box 8734
40275 Goteborg, Sweden

Dr. Aldo Baldacchi
Ente Nazionale Energia Elettrica
Dpt SAS
Via A. Pisano 120
I-56100 Pisa, Italy

Mr. Niklas Berge
Studsvik Energy
Studsvik
61182 Nykoping, Sweden

Dr. Richard Borio
Combustion Engineering
1000 Prospect Hill Road
P.O. Box 500
Windsor, Connecticut 06095

Mr. H.M. Ten Brink
Netherlands Energy Research Foundation
P.O. Box 1
1755 ZG Petten, Netherlands

Dr. Nancy Brown
HI Cyclotron Road, Bldg 29C - Room 100
c/o Lawrence Berkeley Laboratories
Berkeley, California 94720

Dr. Christoph Brühl
Max Planck Institut fur Chemie
P.O. Box 3060
D-6500 Mainz, West Germany (RFA)

Madame Michele Chevrier
Regie Nationale des Usines Renault
Direction des Etudes - DLA
8-10 Avenue Emile Zola
92109 Boulogne Billancourt, France

Mrs. K. Dahlberg
Swedish Environmental Research Institute
S-40258 Goteborg, Sweden

Mr. Andre Douaud
Institut Francais du Petrole
BP 311
92506 Rueil-Malmaison, France

Dr. Robert Epprrley
Fuel Tech. Europe
28A Cadogan Square
London SW1 XOJH, England

Mr. Pierre Eyzat
Institut Francais du Petrole
BP 311
92506 Rueil-Malmaison, France

Mrs. Lisa Fuller
Studsvik Energy
S-61182 NYKOPING, Sweden

Dr. Dian Gaffen
NOAA
USA

Mr. R.E. Hall
U.S. Environmental Protection Agency
Combustion Research Branch (MD-65)
Research Triangle Park, North Carolina 27711

Dr. H.J.A. Hasenack
Royal Dutch Shell Laboratory
Badhuisweg 3
1031 CM Amsterdam, The Netherlands

Prof. K Hein
RWE, Betriebsverwaltung Fortuna
Postfach 1461
5010 Bergheim 4, West Germany (RFA)

Dr. Goran Hellen
EKONO Oy
P.O. Box 27
SF-00131 Helsinki, Finland

Dr. Alain Henriet
Peugeot S.A.
Etudes et Recherches
Direction Technique, Lab. de Chemie
Centre Technique Citroen
78140 Velizy Villacoublay, France

M. Tore Hulggard
Instituttet for Kemitenknik
Danmarks Tekniske Hojskole
Bygning 229
2800 Lyngby, Denmark

Dr. J. Jacobs
Combustion Department
VGB Technische Vereinigung der
Grosskraftwerksbetreiber
Klinkestrasse 27-31
4300 Essen 1, West Germany (RFA)

Mr. Sven A. Jansson
ASEA PFBC
S-61200 Finspong, Sweden

Prof. Karl Knoblauch
Berbau-Forschung BmbH
Franz-Fisher-Weg 61
4300 Essen 13, West Germany (RFA)

Dr. Heinz Koeser
L & C Steinmueller GmbH
Fabrikstrasse 1
5270 Gummersbach, West Germany (RFA)

Dr. Hans-Jurgen Krabbe
Vereinigte Elektrizitratswerke
Westfalen AG, Postfach 105056
Rheinlanddamm 24
4600 Dortmund 1, West Germany (RFA)

Dr. John Kramlich
Energy and Environmental Research Company
18 Mason
Irvine, California 92718

Dr. W.S. Lanier
Energy and Environmental Research Company
3622 Lyckan Parkway, Suite 5006
Durham, North Carolina 27707

Mr. Dominique Laurent
ELF, Centre de Recherche Solaize
BP 22
69360 Saint Symphorien d'Ozon, France

Dr. Joel Levine
NASA
Langley Research Center
Hampton, Virginia 23665

Dr. W. P. Linak
U.S. Environmental Protection Agency
Combustion Research Branch (MD-65)
Research Triangle Park, North Carolina 27711

Prof. Oliver Lindkvist
Chalmers University of Technology
Department of Inorganic Chemistry
41296 Goteborg, Sweden

Mr. Jan Lindquist
Ambassade de Suede
Dpt Technique
17 Rue Barbet de Jouy
75007 Paris, France

Mrs. Anne Lindskog
Swedish Environmental Research Institut
P.O. Box 47086
S-40258 Goteborg, Sweden

Dr. F.C. Lockwood
Mechanical Engineering Department
Imperial College
Exhibition Road
London, SW7 2BX, England

Mr. Joseph McSorley
U.S. Environmental Protection Agency
Combustion Research Branch (MD-65)
Research Triangle Park, North Carolina 27711

Dr. Mark Morgan
International Flame Research Foundation
c/o Hoogovens BV, P.O. Box 1000
1970 CA, Ijmuiden, The Netherlands

Dr. Larry Muzio
Fossil Energy Research
23342 Unit C
South Point
Laguna Hills, California 92653

Dr. Heine Nielsen
Petrokraft AB
Box S2090
40025 Gothenburg, Sweden

Mr. Jean-Luc Phillipe
CERChar
Rue Aime Dubost, BP 19
62670 Mazingarbe, France

Mr. Michel Prigent
Institut Francais de Petrole
BP 311
Rueil-Malmaison, France

Prof Daniel Puechberty
U.A. CNRS 230
Coria, BP 118
76130 Mont Saint Aignan, France

Dr. Ludwig Raible
RWE Betriebsverwaltung Fortuna
Postfach 1461
5010 Bergheim 4, West Germany

Mr. Jeffrey V. Ryan
Acurex Corporation
Research Triangle Park, North Carolina 27709

Mrs. Kelley Ryan
Acurex Corporation
Research Triangle Park, North Carolina 27709

Mr. S. Seidel
U.S. Environmental Protection Agency
ANR-445
Office of Air and Radiation 40L
M Street, SW
Washington, DC 20460

Dr. Sam A. Sloan
Central Electric Research Laboratories
Kelvin Avenue
Leatherhead, Surrey KT22 7SE
England

Dr. John P. Smart
International Flame Research Foundation
c/o Hoogoven, P.O. Box 10000
1970 CA, Ijmuiden, The Netherlands

Dr. Gerard de Soete
Institut Francais du Petrole
BP 311
92506 Rueil-Malmaison, France

Dr. Paul Stolpman
Head of Pollution Control Division
OCDE
15 Bd de l'Admiral Bruix
15016 Paris, France

Dr. Roberto R. Tarli
Ente Nazionale Energia Elettrica
Dpt SAS
Via A. Pisano 120
I-56100 Pisa, Italy

Mr. Jean-Noel Thuillard
Section Pollution et Carburants
Centre Technique Renault
Rue Cochet
91510 Le Lardy, France

Prof. Jost L.O. Wendt
University of Arizona
Geology Building, Room 142
North Campus Drive
Tuscon, Arizona 85721

Prof. Alan Williams
Department of Fuel and Energy
Leeds University
Leeds LS2 9JT, England

Dr. Steven Wilson
Southern Company Services
800 Shades Creek Park
P.O. Box 2625
Birmingham, AL 35202

Dipl. Ing. Gunter Zellinger
Oesterreichische Draukraftwerke AG
Hauptverwaltung/BM
Kohldorfestrasse 88
A-9020 Klagenfurt, Austria